



Chair of Reservoir Engineering

Master's Thesis



Walid Hamad

December 2019

*To my parents and my family.*

**AFFIDAVIT**

I declare on oath that I wrote this thesis independently, did not use other than the specified sources and aids, and did not otherwise use any unauthorized aids.

I declare that I have read, understood, and complied with the guidelines of the senate of the Montanuniversität Leoben for "Good Scientific Practice".

Furthermore, I declare that the electronic and printed version of the submitted thesis are identical, both, formally and with regard to content.

Date 03.12.2019



Signature Author  
Walid, Hamad

## Acknowledgements

I would like to thank Mr. Prof. Holger Ott for his unlimited support and guidance, and Ms. Dip-Ing Kata Kurgyis.

A great thank to the team of OMV TECH Center & Lab Gänserndorf, especially Mrs. Linda Kirchberger (Head of TECH Center & Lab bei OMV), Mr. Christian Einzinger (Department Manager Petrophysics & Reservoir Technologies (Laboratory) bei OMV), and Mr. Thomas Gumpenberger (Petrophysicist).

Finally, I would like to thank Mrs. and Mr. Ransmayer, Mrs. and Mr. Scherrer, GiG, all of my colleagues, and my friends for their support, especially Mr. Loay Alkafry and Mr. Jesse El-Aayi (E&P Engineering and Technology Manager at IPS).

## Abstract

Low salinity water injection (LSWI) became lately one of the most desirable enhanced oil recovery (EOR) and improved oil recovery (IOR) methods since it is considered a low cost, flexible method and environmentally friendly. The increased interest in this method encouraged the researchers to conduct different tests and experiments in different lithologies to explain the mechanism(s) behind it, and then many field pilots to study the compatibility and profitability of LSWI method. Up to now, it is difficult to build a concrete statement about the LSWI mechanism and hence in which reservoir it is applicable.

The present thesis tries to study the behavior of LSW spontaneous imbibition (LSW SI) in sandstone outcrops plugs, Bentheim sandstone, using Amott test. The work contains plugs preparing, starting from drilling and preserving them until the restoration process starts. The restoration stage aims to establish a favorable reservoir wettability condition, a mixed wet or weak water-wet state. The restoration process contains the cleaning process, drying process, saturating the plugs with connate water, with different concentrations and compositions, drain them with crude oil, and aging them at ambient pressure and reservoir temperature. The plugs were divided into four groups; each of them was aged for a certain time.

After the end of the preparation period, the test was conducted by placing the plugs in Amott cells and immersing them with imbibed water with different concentrations and compositions. The result was obtained regularly by reading the cumulative oil production. Different scenarios were planned for the test among them using one composition/one concentration during the test or changing the water salinity and/or composition during the test.

The results were analyzed by studying the cumulative oil production behavior and by linking this behavior with the different variable parameters to add worth statements and discoveries to the previous conclusions that have been drawn by other researchers and to help further workers in this field to improve their works and findings.

Results showed an increase in oil wetness with time. Although no clay minerals were detected in the plugs, the hematite film is responsible for this alteration. Moreover, a small increment of the recovery factor (RF) due to imbibing low salinity water was detected. The main mechanism behind this increment is believed to be the Expansion of the Double Layer (EDL). However, other mechanisms are also possible to have a contribution to this increment. The capillary diffusion coefficient ( $D_c$ ) showed higher values in the case of LSW SI than it is in case of high

salinity water spontaneous imbibition (HSW SI). This difference hypothesizes the higher values of the capillary forces in the second case than in the first case, and hence the higher residual oil saturation ( $S_{or}$ ). EDL theory is also in agreement with the increase of the Dc values and reduces the capillary forces, which causes increase of RF.

Finally, this works expected to open a space for further and future works in the field of LSWI studies, for example, studying LSWI behavior with the of micromodels equipped with synthetic lithology and observing this behavior under microscopy and other imaging methods to provide more reliable conclusions about this problem.

## Zusammenfassung

Die Wassereinspritzung mit niedrigem Salzgehalt (LSWI) wurde in letzter Zeit zu einer der begehrtesten Methoden zur verbesserten Ölrückgewinnung (EOR und IOR), da sie als kostengünstiges, flexibles und umweltfreundliches Verfahren gilt. Das zunehmende Interesse an dieser Methode ermutigte die Forscher, verschiedene Tests und Experimente in verschiedenen Lithologien durchzuführen, um die Mechanismen dahinter zu erklären, und dann viele Feldpiloten, um die Kompatibilität und Rentabilität der LSWI-Methode zu untersuchen. Bisher ist es schwierig, eine konkrete Aussage über den LSWI-Mechanismus und damit über dessen Einsatzgebiet zu treffen.

Die vorliegende Arbeit versucht, das Verhalten der LSW-spontane Imbibition (LSW SI) in Sandsteinfelsen Stecker, Bentheim-Sandstein, unter Verwendung des Amott-Tests zu untersuchen. Die Arbeit beinhaltet die Vorbereitung der Stecker, beginnend mit dem Bohren und deren Konservierung bis zum Beginn des Restaurierungsprozesses. Die Wiederherstellungsstufe zielt darauf ab, einen günstigen Zustand der Benetzbarkeit des Reservoirs, eine Mischbenetzbarkeit oder schwachen Wasserbenetzbarkeit, herzustellen. Der Restaurierungsprozess umfasst den Reinigungsprozess, den Trocknungsprozess, das Sättigen der Stopfen mit Solen in verschiedenen Konzentrationen und Zusammensetzungen, das Ablassen mit Rohöl und das Altern bei Umgebungsdruck und Reservoirtemperatur. Die Stecker wurden in vier Gruppen eingeteilt; Jeder von ihnen war für eine bestimmte Zeit gealtert.

Nach dem Ende der Vorbereitungszeit wurde der Test durchgeführt, indem die Stopfen in Amott-Zellen gegeben und mit aufgesaugtem Wasser mit verschiedenen Konzentrationen und Zusammensetzungen eingetaucht wurden. Das Ergebnis wurde regelmäßig durch Ablesen der kumulierten Ölproduktion erhalten. Für den Test wurden verschiedene Szenarien geplant, wobei eine Zusammensetzung / eine Konzentration während des Tests verwendet wurde oder der Salzgehalt und / oder die Zusammensetzung des Wassers während des Tests geändert wurden.

Die Ergebnisse wurden analysiert, indem das kumulative Ölproduktionsverhalten untersucht und dieses Verhalten mit den verschiedenen variablen Parametern verknüpft wurde, um wertvolle Aussagen und Entdeckungen zu den vorherigen Schlussfolgerungen, die von anderen Forschern gezogen wurden, hinzuzufügen und um weiteren Arbeitnehmern auf diesem Gebiet zu helfen, sich zu verbessern ihre Werke und Schlussfolgerungen.

Die Ergebnisse zeigten eine Zunahme der Ölfeuchtigkeit mit der Zeit. Obwohl in den Stecker keine Tonminerale nachgewiesen wurden, ist der Hämatitfilm für diese Veränderung verantwortlich. Darüber hinaus wurde ein geringer Anstieg des Erholungsfaktor (RF) aufgrund des Aufsaugens von Wasser mit niedrigem Salzgehalt festgestellt. Es wird angenommen, dass der Hauptmechanismus hinter diesem Inkrement die Expansion der Doppelschicht (EDL) ist. Es ist jedoch auch möglich, dass andere Mechaniker an dieser Erhöhung teilnehmen. Die Kapillardiffusionskonstante ( $D_c$ ) zeigte bei LSW SI höhere Werte als bei HSW SI (High Salinity Water Spontaneous Imbibition). Diese Differenz hypothetisiert die höheren Werte der Kapillarkräfte im zweiten Fall als im ersten Fall und damit die höhere Restölsättigung ( $S_{or}$ ). Die EDL-Theorie stimmt auch mit der Erhöhung der DC-Werte und der Verringerung der Kapillarkräfte überein, die eine Erhöhung der RF verursachen.

Schließlich sollen diese Arbeiten einen Raum für weitere und zukünftige Arbeiten im Bereich der LSWI-Studien eröffnen, beispielsweise die Untersuchung des LSWI-Verhaltens mit Mikromodellen, die mit synthetischer Lithologie ausgestattet sind, und die Beobachtung dieses Verhaltens unter dem Mikroskop und anderen bildgebenden Verfahren, um verlässlichere Schlussfolgerungen zu ziehen dieses Problem.

## Table of Contents

Declaration.....	<b>Error! Bookmark not defined.</b>
Erklärung .....	<b>Error! Bookmark not defined.</b>
Acknowledgements.....	iii
Abstract.....	v
Zusammenfassung.....	vii
Table of Contents.....	ix
List of Figures .....	xi
List of Tables .....	xiii
Nomenclature.....	xv
Abbreviations.....	xvii
Chapter 1: Introduction.....	19
1.1 Background and Context.....	19
1.2 Scope and Objectives.....	20
1.3 Overview of Thesis .....	20
1.4 Achievements.....	20
Chapter 2: Literature Review .....	25
2.1 Low Salinity Water Effect .....	25
2.2 Oil Recovery by SI.....	34
Chapter 3: Experiment preparation, setup, and conduction .....	41
3.1 Samples characterization .....	41
3.2 Restoration .....	50
3.3 Amott SI Test.....	61
Chapter 4: Results and Discussion.....	65
4.1 Restoration Process .....	65
4.2 Aging time effect .....	68
4.3 Low salinity effect .....	69
4.4 Water wet state by H1 and L1, and aging time .....	72
4.5 Curvature .....	73
4.6 Imbibition.....	75
4.7 Issues related to the results .....	86
Chapter 5: Conclusion.....	88
5.1 Summary .....	88
Chapter 6: References.....	90



## List of Figures

Figure 1: The program of the experiment .....	22
Figure 2: A sketch represents micro-dispersion formation .....	32
Figure 3: Boundary conditions and pressure gradient for (A) counter-current flow, (B) mixed flow, and (C) co-current flow (after (Morrow and Mason 2001)) .....	37
Figure 4: Saturation profiles for (A) co-current, (B) counter-current, and (C) mixed imbibition (after Bourbiaux & Kalaydjian (1990)) .....	38
Figure 5: Boundary conditions for core samples summarized by (Morrow and Mason 2001) .....	39
Figure 6: Core plug drilled from outcrop Bentheim Sandstone .....	42
Figure 7: Bentheim Sandstone XRD analysis .....	44
Figure 8: Bentheim thin section under optical microscopy .....	45
Figure 9: Geological features in the Bentheim Sandstone – studied under polarized and non-polarized lenses .....	46
Figure 10: Unpolarized thin-section images of Bentheim sandstones .....	47
Figure 11: Permeability-Porosity relationship .....	48
Figure 12: Pore size distribution of Bentheim Sandstone .....	49
Figure 13: Saturation platform sketch .....	54
Figure 14: Wettability index as a function of the initial water saturation for different aging times, temperatures, and injected pore volumes. (after Jia, Buckley, & Morrow (1991)) .....	58
Figure 15: Amott cell .....	62
Figure 16: Air/brine/rock system contact angle of (A) B8-8TH-H1 and (B) B7-8TH-L1 systems .....	62
Figure 17: Temperature variation during the experiment period .....	63
Figure 18: Produced oil during the experiment for all of the systems .....	67
Figure 19: RF of three plugs with different aging time with respect of other parameters .....	68
Figure 20: Recovery factor for high salinity SI case and Low salinity SI case. ....	69
Figure 21: The compensation between brine composition and salinity and the time to determine the final wettability state .....	72
Figure 22: H1/8TH/glass contact angle changes during the experiment .....	74
Figure 23: Droplets size changes of the system B8-H1-8TH-H1 .....	74
Figure 24: Droplets distribution on the plug's wall during the time for the system B8-H1-8TH-H1 .....	76
Figure 25: Droplets distribution at the surface of the system B4-H1-8TH-H1 .....	78
Figure 26: Schematic water profile during the SI experiment .....	79
Figure 27: Flow regime dominance during the experiment .....	80
Figure 28: The relationship between the produced oil and the time to the power $\nu$ .....	80
Figure 29: History matching of the produced oil of the system B3-H1-8TH-H1 .....	81
Figure 30: The relationship between Diffusion Capillary Coefficient and the water saturation .....	84
Figure 31: The relationship between Diffusion Capillary Coefficient and the normalized water saturation .....	84
Figure 32: Normalized $V_o$ as a function of $tD$ .....	85



## List of Tables

Table 1: Samples' geometry .....	42
Table 2: Measured porosity values for the Bentheim Sandstone plugs .....	47
Table 3: Gas and brine permeability of Bentheim Sandstone plugs used in our experiments .	48
Table 4: Grains and Bulk densities .....	49
Table 5: The two brines characteristics.....	56
Table 6: Plugs' state after renaturation with brine and crude oil.....	57
Table 7: 8TH Crude Oil characteristics .....	59
Table 8: Aging groups, times, and conditions .....	60
Table 9: A summary of the different tests set up .....	64
Table 10: A comparison between three systems with different aging times with respect of the other parameters.....	69
Table 11: Droplets relative density and size on the plugs sidewalls.....	76
Table 12: Relative values of the product $\sigma \cos(\theta)$ of the different systems compared to the reference system B8-H1-8TH-H1 .....	86



## Nomenclature

$K$	Brine Permeability
$D_c$	Capillary diffusion coefficient
$k_r$	Relative permeability
$N_c$	Capillary Number
$P$	Pressure
$P_c$	Capillary Pressure
$T$	Temperature
$t$	Time
$V_o$	Oil Volume
$\sigma$	Interfacial Tension
$\Phi$	Porosity
$S_{wc}$	Connate Water Saturation
$R_w$	Water resistivity
$S_w$	Water Saturation
$S_o$	Oil Saturation
$S_{or}$	Residual Oil Saturation
$S_{wi}$	Initial Water Saturation
$\mu_o$	Oil viscosity
$t_D$	Dimensionless time
$L_c$	The characterization length

Many other Nomenclature, that are used in the equations and models, will be explained and clarified after these equations and models.



## Abbreviations

AN	Acid Number	PUTS	Polished uncovered thin section
BL	Buckley-Leverett	PUTS	Polished uncovered thin section
BT	Break Through	PV	Pore Volume
CEC	Cation Exchange Capacity	RCA	Routine Core Analysis
CF	Core Flood(ing)	RF	Recovery Factor
CO	Crude oil	SCAL	Special Core Analysis
COBR	Crude Oil/Brine/Rock	SD	Spontaneous Displacement
CT	Computed tomography	SEM	scanning electron microscope
CTIS	The critical value of total ionic strength	SI	Spontaneous Imbibition
DOM	The dissolved organic matter	STOIP	Stock-tank oil initially in place
DSB	Dielectric surface behaviors	SWCTT	Single well chemical tracer test
$E_D$	Displacement Efficiency	SWW	Strong Water Wet
EDL	Electrical double layer	TAN	Total Acid Number
EOR	Enhanced Oil Recovery	TBN	Total Base Number
$E_s$	Sweep Efficiency	TDS	Total Dissolved Solids
$E_v$	Vertical Efficiency	TFT	Thin film transition
EVR	Elastic moduli to Vicious moduli Ratio	URF	Ultimate Recovery Factor
FD	Forced Displacement	USBM	U.S. Bureau of Mines
FI	Forced Imbibition	VDW	Van der Walls
GCTS	Glass covered thin section	WBM	Water Based Mud
GCTS	Glass covered thin section	TWF	Water Thin Film
HC	Hydrocarbons	WW	Water Wet
HSE	Health, Safety, and Environment		
HSW	High Salinity Water		
HSWI	High Salinity Water Injection		
IEC	Ion Exchange Capacity		
IFT	Interfacial Tension		
ILSW	Injected Low Water Salinity		
IOR	Improved Oil Recovery		
L-L	Liquid-liquid		
L-S	Liquid-Solid		
LSW	Low Salinity Water		
LSWI	Low Salinity Water Injection		
MICP	Mercury Injection Capillary Pressure		
MIE	Multi Ion exchange		
MW	Mixed Wet		
NW	Neutral Wet		
OIIP	Oil Initially In Place		
OW	Oil Wet		



# Chapter 1

## Introduction

### 1.1 Background and Context

The increased demand for energy during the last century forced the energy companies to search for unique methods that increase the hydrocarbon production and to reduce the harmful effects of these methods on the underground geology and the environment. Low salinity water (LSW) is an eco-friendly improved oil recovery (IOR) and enhanced oil recovery (EOR) method to increase the recovery factor (RF) from the mature oil fields. Determining the mechanism(s) behind the LSW effect is still ambiguous. Great efforts have been made to discover the primary mechanism(s), but all the works still confusing since there are many hypotheses and theories, and there are a lot of contradictory results. This problem needs to be solved. By solving this problem, lots of money and great efforts will be saved by determining the criterion of LSWI applicability. In this work, we are trying to shed light on this area to provide a better view of these hypothesized mechanisms.

Many analytical tests are being done on reservoir rocks plugs retrieved from the wells or cut from the outcrops to characterize them and to provide quantitative values and qualitative evaluation of them, these tests are divided mainly into two categories, routine core analysis tests (RCA) and special core analysis tests (SCAL). RCA includes Core photography (natural and ultraviolet light), Core-gamma, Grain density, Directional permeability, Grain size distribution, CEC, Fracture orientation and log, Pyrochromatography, and Calcimetry. On the other hand, SCAL includes Capillary pressure, Electrical properties, Petrographic studies (Thin section analysis, SEM, X-ray diffraction, Cathodoluminescence), Micropaleontology and palynology, Trace element identification, and Insoluble residues. Moreover, other tests that are done on non-reservoir rocks ([Keelan 1982](#)).

## 1.2 Scope and Objectives

The project aims to study the behaviour of LSW during spontaneous imbibition and link the results to the different parameters. Moreover, the determination of the required time to reach the final wettability state in Bernheimer Sandston outcrops plugs and the effect of LSW as an IOR agent.

## 1.3 Overview of Thesis

The present work follows the following sequence:

The first milestone, preparation stage: The work started with preparing the plugs starting from drilling the plugs using synthetic water-based mud (WBM) with a salinity of 250g/l TDS, and preserving them until the restoration process starts. During this time, plug characterization was done determining the lithological composition of the rock and the petrophysical parameters using different methods, for example, XRD and thin-sections.

The second milestone, restoration stage: Restoration process contains a cleaning process using the Soxhlet extraction method with chloroform ( $\text{CHCl}_3$ )/methanol ( $\text{CH}_3\text{OH}$ ) Azeotrope solvent, drying process using simple drying method under room temperature and ambient pressure, saturating with brine using two salinities (H1 [180 g/l TDS] or L1 [3.6 g/l TDS]), draining with crude oil (8TH), and finally aging under ambient pressure and at reservoir temperature for 4 different times (15, 34, 46, or 84 days) to create different wettability states. The reached final wettability states varied from weak water wet (WWW) to weak oil-wet (WOW)

Third milestone, Amott Test stage: The test was conducted by placing the plugs in Amott cells and immersing them with imbibed water with different concentrations (H1 [180 g/l TDS] or L1 [3.6 g/l TDS]) for sufficient time, until the capillary forces and the viscous forces become equal. The experiments were set up to determine the minimum required time to reach the final wettability state and to examine the effect of low salinity as an improved oil recovery (IOR) agent on the recovery factor (RF). The result will be obtained regularly by reading the cumulative oil production.

## 1.4 Achievements

The fourth milestone, the analysis of the results: The results have been analysed by studying the cumulative oil production behaviour for both the low salinity cases and high salinity cases. The hematite film showed a tendency to change the wettability toward more OW state. Although the positive surface charge, the wettability alteration refers to the discrete adsorption

regardless of the net surface charge at a specific pH value. The time showed an effect on the final wettability state too. The results showed that 34 days period is sufficient aging time using H1 as a brine under ambient pressure and at 49°C and 8TH crude oil in Bernheimer Sandstone plug. On the other hand, using L1 as brine showed more water wet (WW) state even if the aging time was extended with respect all the other parameters and conditions. L1, as an IOR agent, showed increment of the RF about 2.5% over the H1 when they both used as imbibed water with respect of all the other parameters and the conditions. The increment could be a result of the MIE reactions, EDL, and pH effect. However, many mechanisms could contribute to this increment at different weighting factors. The salinity of the brine plays the most critical role in the URF since it determines the reactions that lead to the wettability alteration at the restoration stage. The cumulative oil production curves analysis supports the claim that counter-current flow regime dominates the early time SI production, whereas the co-current dominates the late time SI production. More another regime, the Mixed regime, appears in the transition time between the early and late time, especially in the WW plugs. On the other hand, the increase of  $D_c$  reduces the capillary forces that lead to less residual oil saturation.

Figure 1 shows the program of the experiment.

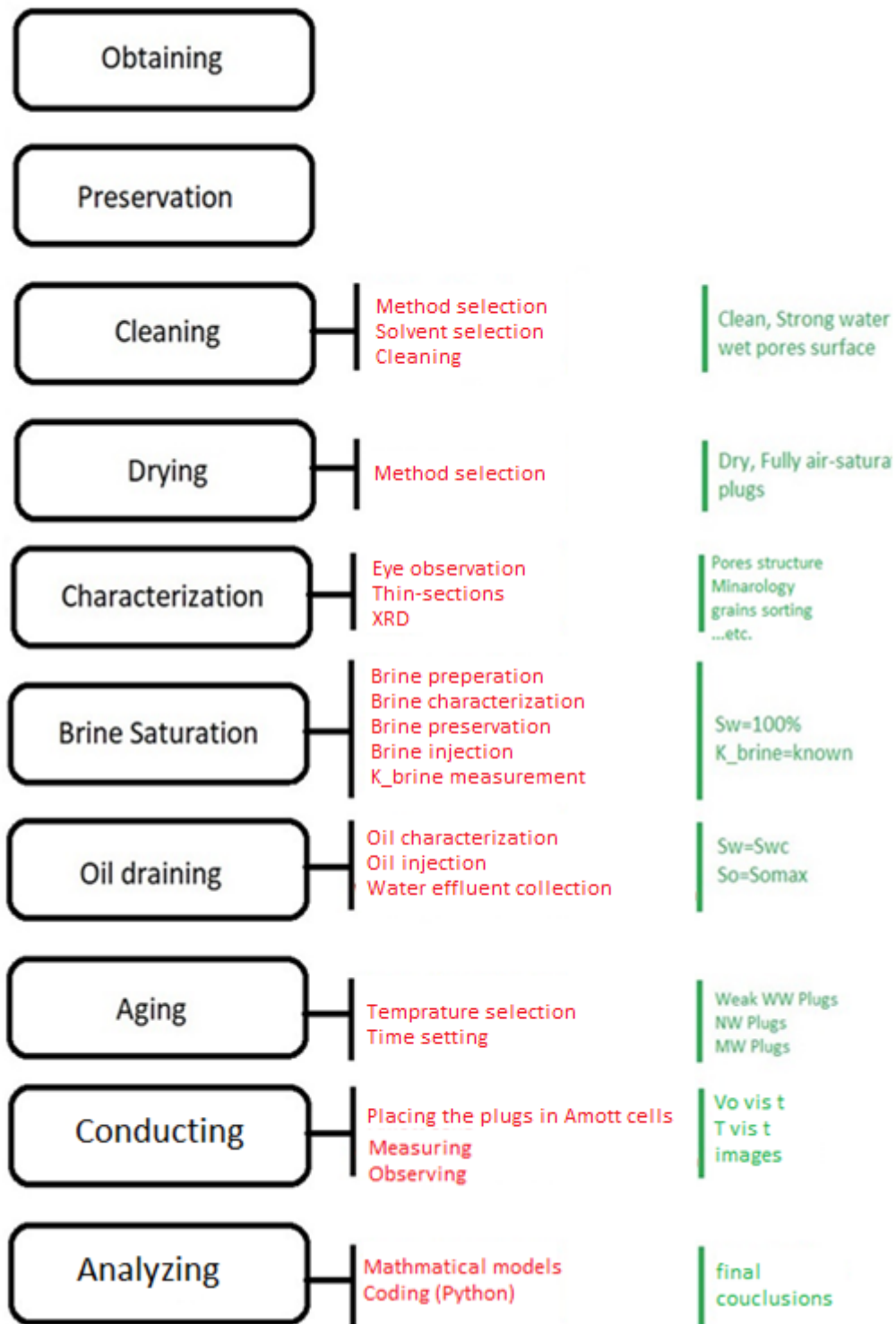


Figure 1: The program of the experiment





# Chapter 2

## Literature Review

### 2.1 Low Salinity Water Effect

Low salinity water injection (LSWI) is the process that includes the injection of water with low concentration of the total dissolved solids in the reservoir as a chemical EOR process (McGuire, et al. 2005) or as an IOR or by modifying the injected water composition (Bartels, Mahani, et al. 2019). Some experiments showed that the total salinity plays less role than the hardness of the brine in increasing RF (Gupta, et al. 2011). LSWI is considered an inexpensive method that does not involve using toxic chemical agents. However, some economic issues like the cost of designing injecting water and disposing of produced water still in the frame, but they are covered by the increment of the RF (Vledder, et al. 2010).

Insufficient provided information by researchers about the system and the focus on one particular side of the problem makes it very difficult to explain many obtained results. On the other hand, the absence of a standard preparation methodology stands as another stone on the way to explain the results accurately.

Nevertheless, the effect of the LSWI started from the smallest length scale, the sub-pores scale, demonstrated by the R/B, B/CO, and CO/B/R interactions. For example, the changes in the TWF thickness, the changes of contact angle, and chemical reactions, especially MIE reactions. At this length scale, the detachment of the CO components is the direct result, and the wettability alteration on the sub-pore scale is the second level result. On the pore-scale many mechanisms are responsible for assisting the sub-pore scale effect; for example, the L-L interaction in general especially viscoelastic, fluid distribution, mixing, and mobility control. Add to that the fine migration and clay hydration. The last two interactions are more critical on

the field-scale than in pore-scale or even on core-scale. On the core scale, the wettability alteration is the result of the sub-pore and the pore-scale effects. From the core scale, it is essential to obtain the main models of relative permeability and capillary pressure. These models are supposed to be used in the simulation works to validate the field data. Wettability alteration, reflected by relative permeability shift and capillary pressure changes, with fine migration and clay hydration play the role of changing the  $E_v$  and  $E_s$  on the field scale. The changes of  $E_v$  and  $E_s$  change the flow paths and hence make it possible for passed region to be swept. Moreover, the formation of oil bank encourages the viscose drag forces to dominate over the capillary forces and hence move oil in front of the waterfront and therefore accelerate the oil production. The acceleration of oil production with the effect of the wettability alteration and the detachment of oil, and hence change the fluids distribution, cause the change of the RF finally.

Many **LSWI pilots** and projects have shown optimistic results supporting the experimental works. Increment of 10-50% OIIP using Log-Injection-Log measuring method by [Webb, Black, & Al-Ajeel \(2004\)](#), 6-12% OIIP using SWCTT in the Prudhoe Bay and Endicott fields, Alaska ([McGuire, et al. 2005](#)), 10-15% STOIIP in Alomar field, Syria ([Vledder, et al. 2010](#)), and many other projects.

LSWI could be applied in the **IOR or EOR** stage<sup>1</sup>. Many experiments showed that the LSWI affects the IOR stage but no effect in EOR stage was observed ([Nasralla, Alotaibi, & Nasr-El-Din 2011](#)). Some other experiments showed increase of the RF in both phases ([Agbalaka, Dandekar, Patil, Khataniar, & Hemsath 2009](#)). However, the increment in RF due to the application of LSWI in the secondary mode is higher than it in the tertiary mode, this may be due to the more mobile oleic phase in the media in the secondary mode ([Bartels, Mahani, et al. 2019](#)). Some experiments showed insensitivity at all for salinity reduction ([Tang and Morrow 1999](#)) ([Zhang and Morrow 2006](#)) whereas others showed insensitivity to the injected water salinity but remarkable sensitivity to brine salinity ([Filoco and Sharma 1998](#)) ([Sharma and](#)

---

<sup>1</sup> Using LSWI in the secondary stage means to start flooding the reservoir at initial water saturation or after the primary depletion of the reservoir by the primary energy of the reservoir, in this case, LSWI is considered as IOR method. On the other hand, flooding the reservoir with LSW when the reservoir was already flooded with HSW until  $S_{or}$  is considered as EOR method (tertiary stage) (Morrow and Buckley 2011)

Filoco 2000). Jiang, Chopping, Forsman, & Xie (2014) presented a case where LSWI was unsuccessful in carbonate plugs neither as EOR agent nor IOR agent.

### 2.1.1 PROPOSED WATERFLOODING MECHANISMS

Many mechanisms were proposed to explain the reason behind the effect of LSWI. There is no concrete statement about the primary mechanism(s). This situation may be due to the variations in procedures, using different systems, and complexity of the systems (Morrow and Buckley 2011) and the contradict observations and results (Al-Shalabi and Sepehrnoori 2017). Nevertheless, the proposed mechanisms are based on indirect observations or inferred from the results; some of them are, actually, contradictory (Bartels, Rücker and Berg, et al. 2016). This methodology of explanation (inverse problem) can provide a somehow partial understanding of the problem and can explain particular observation(s), but it cannot explain why one or more observation(s) is (are) different or even absence (Bartels, Mahani, et al. 2019). The proposed mechanisms cover a wide range of concepts. Some of them depend on the microscopic explanations, for example, fine migration and clay hydration; others depend on the physicochemical explanations, for instance, pH changes, MIE, double layer expansion, and others related proposed mechanisms (Suijkerbuijk, et al. 2012). Moreover, they can also be categorized into L-L or L-S interactions, or they can be classified according to the length or time scale (Bartels, Mahani, et al. 2019).

#### I. EFFICIENCY ENHANCEMENT

##### 1. CLAY HYDRATION:

Clay hydration, due to the reduction of water salinity, causes clay swelling and fluctuation. Clay swelling causes the reduction of the space available for the fluids in the porous media. The reduction forces the fluids to flow toward the low-pressure area which means enhancing  $E_v$  and  $E_s$ . This process reduces the residual oil saturation trapped physically by passing out (Bernard 1967). When the salinity reduces too much to hydration range, clay hydration reduces  $K$  in great values (Johnston and Beeson 1945) due to clay volume expansion and pore throats plugging. Bernard (1967) believed that clay hydration cannot cause increase RF without increasing pressure drop (fine migration and pores plugging).

##### 2. FINES MIGRATION:

Fine migration can be due to the compensation of MIE and the change of local pH and is considered a mechanical interaction that causes changes in rock quality due to blockage and dispersion (Law, Sutcliffe and Fellows 2014). According to the DLVO theory, the stripping-

out of the particles happens when the ionic strength becomes equals or less than CTIS, which depends on the relative concentration of positive divalent ions (Khilar, Vaidya and Fogler 1990). The increase of divalent cations concentration decrease zeta potential, in this case, the repulsive forces are weakened, and attraction forces are strengthened, and clay is stabilized (Khilar, Vaidya and Fogler 1990) (A. Lager, K. Webb and C. Black, et al. 2008). In this case, the decrease the total dissolved solids concentration causes the increase of the repulsive forces between the clay particles and the pore wall which, consequently, increases the probability of clay stripping out (Khilar, Vaidya and Fogler 1990). In case of fine release from the walls of the pores, they flow with the stream, the water paths, and they plug them when they accumulate in sufficient amount at the pore throat or when they have bigger diameter than the pore throat. This process forces the stream to follow another path where the oil fills the path. However, this mechanism can not be noticed in the experiment length scale.

## II. WETTABILITY ALTERATION:

Wettability is defined according to Craig (1971) as “the tendency of one fluid to spread on or adhere to a solid surface in the presence of other immiscible fluid”. The rock is WW when water imbibes spontaneously in the pores spaces displacing oil, and vice versa for OW state (Anderson 1986a). However, in flooding experiments, strong water-wet state is determined by the clean breakthrough (Jadhunandan and Morrow 1995). The concept of wettability is related to the L-S interfacial energy, the higher the L-S interfacial energy, the less wetting affinity, hence the less difficult to remove the wetting film (Sharma and Filoco 2000). Tang & Morrow (1997) stated that the final wettability state of the aged plugs depends on the fluid’s distribution and saturation and the contact time.

The alteration of the wettability state toward a specific stated depends on the rock properties, for example, rock composition and pores geometries (Salathiel 1973). Different methods are used to **measure the wettability quantitatively**, for instance, the Contact Angle Method, Amott Method, and USBM Method, and **qualitatively**, for example Imbibition Method, Microscope examination Method, and many others.

Wettability alteration affects a lot of the reservoir fundamental parameters, for example, **P<sub>c</sub>**, kr. The entry pressure during the drainage increases with the tendency forward the wetting by the entering phase (Tiab and Donaldson 2015). LSWI leads to change the **relative permeability** curves toward more oil relative permeability and less water permeability at certain water saturation, as well as to decrease the residual oil saturation and to increase the connate water saturation. Moreover, it leads to lower the water relative permeability endpoint and increase the oil relative permeability endpoint (Rivet, Lake and Pope 2010).

During LSWI, many researchers (for example (Rivet, Lake and Pope 2010)) noticed alteration of the wettability toward more WW. This alteration is local and happens in the pore after the pore itself is flooded with LSW. This alteration on the pore-scale leads to increment in RF in Darcy-scale (Bartels, Rücker and Berg, et al. 2016).

Many mechanisms work separately or even together to alter the wettability. The presence of water layer between oil and rock, where the electrostatic repulsion between O/W and W/R, and divalent cations works as bridges to bond them together (Brady and Krumhansl 2012), is essential to obtain the wettability alteration toward WW state during flooding (Dubey and Doe 1993). Ion exchange, mineral dissolution salting in, surfactant flooding effect, and others, all of them are responsible for wettability alteration.

### 3. MULTI ION EXCHANGE:

MIE reaction describes the competence between different cations to be exchanged on the mineral sites (Valocchi, Street and Roberts 1981). In this theory, the ionic organometallic complexes are replaced with simple metallic ions for example  $\text{Ca}^{+2}$  and  $\text{Mg}^{+2}$  (A. Lager, K. Webb und C. Black, et al. 2008) causing wettability alteration toward WW (Seccombe, et al. 2010) and hence increase RF. This mechanism was proposed by Lager A., Webb, Black, Singleton, & Sorbie (2006) when they noticed the decrease of the  $\text{Mg}^{+2}$  concentration in the effluent. This mechanism is supported by Lager, Webb, Black, Singleton, & Sorbie (2008)'s observations. They found that the effluent samples are sharply less  $\text{Ca}^{+2}$  and  $\text{Mg}^{+2}$  concentrations than the injected water which implies the desorption of these cations on the minerals surfaces. Wickramathilaka, Morrow, & Howard (2010) measured a decrease in the brine conductivity after their seawater SI experiments finished and increment after their LSW SI finished. MIE theory can explain the insensitivity of the stabilized core to LSWI. The reason behind that is that the ion exchangers on the clay surfaces were destroyed (A. Lager, K. Webb and C. Black, et al. 2008). Ligthelm, et al. (2009) stated that ion exchange could contribute to the RF increment, but for sure it is not the main reason of this increment and the wettability alteration.

### 4. DOUBLE LAYER EXPANSION:

This mechanism describes the force competition between Van der Waals forces and electrostatic forces between two layers of counter ions (Sheng 2014), namely O/W and W/R interfaces (Buckley and Liu 1998). In 2014, Nasralla & Nasr-El-Din (2014) conducted many LSWI experiments on sandstone plugs. They stated that EDL is affected by the pH value, where at lower levels of pH, thin water film (TWF) thickness is reduced, and attraction between rock

and heavy oil components increase altering the rock to more OW. In contrast, increasing pH value causes thicker TWF and the Van der Waals attraction is mitigated altering the surface to more WW. Finally, they concluded that the double layer expansion is the dominated mechanism in LSWI in the secondary stage of the production. Moreover, [Lee, et al. \(2010\)](#) found that the reduction of salinity leads to increase in the thin water layer thickness which means expanding the double layer. This expansion gives more likelihood to oil detachment and hence movement. The expansion value on clay minerals is more significant than it is on quartz minerals.

Finally, the double-layer theory requires to show effect during LSWI a reactive geochemical surface with similar charges of the O/B interface and the presence of counterally charged ions.

### **5. SATING IN:**

This mechanism was proposed by [\(Austad, Strand, et al. 2008\)](#). It hypothesizes that decreasing the water salinity increases the DOM solubility in water due to the initiation of the hydrogen-bonded structure around the DOM, and hence increases the RF [\(RezaeiDoust, et al. 2009\)](#). The amount of oil dissolved in the aqueous phase equals the amount of oil detached from the pore surface, due to the detachment of oil, rock surface is turned into more WW [\(Sheng 2014\)](#). However, [\(Austad, RezaeiDoust and Puntervold 2010\)](#) noticed a small difference in desorption of quinoline from kaolinite surfaces due to decreasing brine salinity.

### **6. MINERAL DISSOLUTION:**

This reaction is a chemical [\(Law, Sutcliffe and Fellows 2014\)](#) heterogeneous reaction. The dissolution/precipitation reaction is measured using the solubility of a product, and it can be kinetically or locally equilibrated according to the reaction speed [\(Al-Shalabi and Sepehrmoori 2017\)](#). Rock dissolution is characterized as a slow reaction, and it is difficult to describe its effect on the laboratory time scale, whereas ions exchange reaction is a fast reaction [\(Jensen and Radke 1988\)](#). it is promoted by increasing the pH, which produces more OH<sup>-</sup> ions increase the local pH [\(Jensen and Radke 1988\)](#). The dissolution reaction depends on the minerals type, brine composition, temperature, and pH. It is related to the aqueous reactions since some of the ions react, or are produced from D/P reaction, are consumed or produced during, or from, the aqueous reactions [\(Lee and Lee 2018\)](#).

Dissolution/presentation reactions seem to be more important in carbonate than in sandstone. Some cases showed the presence of carbonate minerals in the sandstone composition and contributed RF increment to this reaction.

## 7. OSMOTICITY:

Osmoticity mechanism proposes that the attached oil plays the role of semi-permeable membrane that allows water molecules, but not the ions (Sandengen, et al. 2016), to transport from the higher osmotic potential site (LSW) to the lower potential site (HSW) (Fredriksen, Rognum and Fernø 2016) the transported molecules forms a water pockets, called micro-dispersions with nano-size, surrounded by the polar components came from the phase interfaces (Mahzari and Sohrabi 2014) when the pocket transport to the brine film it causes its expansion and reduces its salinity and hence the salinity shock, or it causes its contraction depending on the direction of salinity concentration gradient (Sandengen, et al. 2016) and associated with compositional changes of the detached oil (Mahzari and Sohrabi 2014). Mahzari & Sohrabi (2014) pointed that the formation of the micro-dispersion is associated with a salinity threshold, and some types of the CO have higher tendency to form micro-dispersions, especially with high aromatics, Sulphur, cyanide, and nitrile basis content. Moreover, ARR affects the formation of micro-dispersion positively.

As soon as the micro-dispersions are initiated, they migrate through the CO bulk surrounded by the surface-active components, coming from the O/R interface, until they reach the TWF and then disappear as soon as they diffuse in the brine (Sandengen, et al. 2016). Due to the expansion of the TWF and the release of the surface-active components, that surround the micro-dispersion pockets, from the rock surface to the CO bulk, the energy of the bond between rock and oil is reduced (Mahzari, Sohrabi and Cooke, et al. 2018) and the attraction forces between the CO/R is reduced and the repulsion forces are increased. Once the repulsion forces are stronger than the attraction forces, oil detaches from the surface and becomes free to be transported by other force in the porous medium. This detachment is followed by the relocation of the oil in the porous media and the increase of  $S_{or}$  that sometimes leads to the movement of the oil in the NW to weak OW porous media (Sandengen, et al. 2016) (Emadi and Sohrabi 2013).

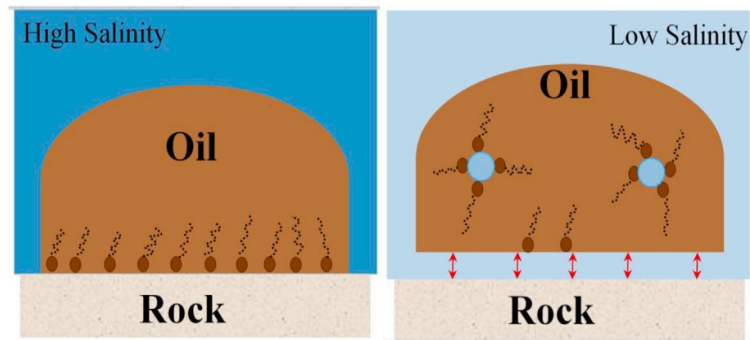


Figure 2: A sketch represents micro-dispersion formation

Osmoticity is supposed to be inefficient in WW systems where the water is the continuous phase, and the oil is the discontinuous phase. In this case, mixing happens directly between LSW and brine. On the other hand, OW systems appear to be more favorable conditions for it since oil is the continuous phase and it separates the injected LSW and brine (Sandengen, et al. 2016).

### III. RHEOLOGY ENHANCEMENT.

#### 8. pH INCREMENT

This mechanism was proposed by (McGuire, et al. 2005). due to the ion exchange between LSW and rock minerals (Austad, RezaeiDoust and Puntervold, Chemical mechanism of Low Salinity Water Flooding in Sandstone Reservoirs 2010) and/or mineral dissolution, like carbonate, hydroxyl ions are produced, these reactions are coupled with increasing of pH locally (A. Lager, K. Webb and C. Black, et al. 2008) and hence decreasing zeta potential, LSW in special case works like Alkaline agent. However, the recorded IFT values in literature are not low enough to cause the positive effect of LSWI (Zhang and Morrow 2006) (Buckley and Fan 2007) and no ultra-low IFT was recorded (Al-Shalabi and Sepehrnoori 2017).

If  $\text{pH} > 11$  (Jensen and Radke 1988), as a special case, and when acidic oil present in the media, hydroxyl ions react with it and produce in-situ **surfactants** and in this case, LSWI works like surfactant flooding (McGuire, et al. 2005). if the TAN of the CO is low, the probability to generate surfactants turned to be small or even ignored (Jensen and Radke 1988). However, it is difficult or even impossible to maintain the  $\text{pH} > 11$  in a real reservoir (A. Lager, K. Webb and C. Black, et al. 2008) due to buffering effect especially when  $\text{CO}_2$  presents and due to  $\text{H}^+$  buffering that result from acidic components and minerals oxides (A. Lager, K. Webb and C. Black, et al. 2006).  $\text{CO}_2$  and  $\text{H}_2\text{S}$  can reduce the pH in the reservoir conditions to even less than 5 (Austad, RezaeiDoust and Puntervold 2010).

Nevertheless, [Suijkerbuijk, et al. \(2012\)](#) stated that the pH changes during the LSWI experiments are side effects, and they are not the main mechanism, and it is not even a mechanism of LSWI. On the other hand, the increment RF in alkaline flooding is in general low (RF=1-2% generally) ([Mayer, et al. 1983](#)), the RF increment in LSWI should be lower, but this is not the case. pH increase is supposed to reduce IFT and form oil-in-water emulsification that improves the water sweep efficiency and cause the detachment of oil from the minerals due to capillary desorption ([Boussour, et al. 2009](#)).

## 9. VISCOELASTIC BEHAVIOR:

This mechanism depends on the hypothesis that the interface between CO/B is affected by the interaction happens between the two phases. This interaction causes the suppression of the snapped-off portion of the oil and leads to sweep it and hence decrease  $S_{or}$  ([Alvarado, et al. 2014](#)). This mechanism hypothesizes that LSW can show incremental in RF without any wettability alteration and the main reason of the incremental is the increase of the viscosity of the interface between CO and B which hinder the snap-off of the non-wetting phase and hence increase the RF and decreases  $S_{or}$ . Moreover, they proved their experiments that LSW can suppress the capillary hysteresis ([Wang and Alvarado 2016](#)).

The formation of the viscoelastic interface depends on the asphaltenes content, the organic acids, temperature, and salinity of the injected water ([Alvarado, et al. 2014](#)) ([Moradi and Alvarado 2016](#)). [Alvarado, Bidhendi, Garcia-Olvera, Morin, & Oakey \(2014\)](#) observed that the increase of asphaltenes content causes larger elastic modulus and the more viscous modulus. However, non-asphaltic components soften the interface ([Moradi, Topchiy, et al. 2013](#)). The decrease of injected water salinity increases both moduli values and reduce the building up rate (reach the steady-state of the moduli value faster) ([Moradi and Alvarado 2016](#)). The presence of the dissociated acids promotes the formation of different complexes according to the reacted ion. These complexes show different interfacial effects ([Alvarado, et al. 2014](#)). Increase T causes a decrease in both modules.

### 2.1.2 LSW EFFECTS CONDITIONS

Due to the contradictory results of the experiments and the pilots, many researchers tried to summaries the main conditions that cause the LSWI effect. From these conditions:

1. Proper wettability state (MW or NW) at the proper length scale ([Law, Sutcliffe and Fellows 2014](#)).

2. Crude oil with polar components (Tang and Morrow 1999) (Suijkerbuijk, et al. 2012) (Zhang, Xie and Morrow 2007)
3. Primary oil saturation more than the critical value (Tang and Morrow 1999).
4. Presence of clay minerals: (Zhang, Xie and Morrow 2007).
5. Initial water saturation (Tang and Morrow 1999) (Sharma and Filoco 2000) (Zhang, Xie and Morrow 2007).
6. Presence of divalent cations in the initial water (A. Lager, K. Webb and C. Black, et al. 2008).
7. Salinity shock (Mohan, et al. 1993) (Law, Sutcliffe and Fellows 2014).
8. The pH of water less than 7 (Law, Sutcliffe and Fellows 2014)
9. Presence of dissolvable components in rock, for example, Ca and Mg (Law, Sutcliffe and Fellows 2014)
10. Temperature: (Law, Sutcliffe and Fellows 2014).
11. Timing: (Nasralla, Alotaibi and Nasr-El-Din 2011) found that using LSWI as an IOR is the best, whereas using it as an EOR method is useless. However, the time scale was discussed in more details previously in this chapter.

It is worth to mention here that all of the aforementioned conditions are collected from different experiments and field pilots and tests. This fact indicates that the influence of one of them is separated from the others, and the magnitude that was mentioned here is not representative of one whole case. Moreover, not all of the previous conditions are required to observe an effect of LSWI; certain of them are necessary to explain the effect that appears due to a particular mechanism. From this side, the necessity of performing a systematic work to study the influence of each parameter on one, or many identical, system(s) is from the important to be done. Such work makes screening the applicability of LSWI criterion more straightforward and doable.

## 2.2 Oil Recovery by SI

Spontaneous imbibition is the process of flowing the wetting phase under the capillary forces in the porous media (Morrow and Mason 2001) with small but not constant  $N_c$  (Sahimi 2011). By convention, SI means the wetting phase displaces the non-wetting phase causing it to be produced. SI gets its importance in the fractured reservoirs in general and particularly in low permeable fractured reservoirs, where oil saturates the matrix (Morrow and Mason 2001), and it has an even more descriptive role in the production mechanism in NFR (Li and Horne 2005). SI is an unsteady state flow (Nooruddin and Blunt 2016) and many experiments confirmed that the displacement of spontaneous imbibition in porous media is a piston-like displacement

(Mason, et al. 2012) (Wickramathilaka, et al. 2011). Moreover, the total flow rate ( $q_t$ ) is believed to be inversely proportional to the square root of the imbibition time, equation 1.

$$q_t(t) = A t^{-0.5} \quad 1$$

A: imbibition rate

t: the time

Many researchers indicated that equation 1 is not always valid. The exponent was estimated to be -0.62 by (Blair 1964) and -0.45 by (Bourbiaux and Kalaydjian 1990).

## 2.2.1 SI FLOW REGIMES

### 1. Counter-current flow

Counter-current flow is defined by the flow of the two phases (imbibed water and produced oil) in opposite directions. Some of the essential properties of counter-current imbibition are the lower oil and water mobilities lead to lower imbibition rates (Pooladi-Darvish and Firoozabadi 2000), less mobile saturations lead to lower URF (Karimaie, et al. 2006), higher viscous interaction between the wetting and nonwetting phases, and smoother water/oil front (Bourbiaux and Kalaydjian 1990). However, the pressure gradients in this regime are different, and the displacement of one phase will hinder the displacement of the other; hence the viscous forces have a negative effect on the counter-current flow (Bourbiaux and Kalaydjian 1990).

The 1D counter-current flow can be described by equation 2 for incompressible fluids with neglecting the gravity effect (Pooladi-Darvish and Firoozabadi 2000). Equation 2 misses the advection term since the total flow rate in counter-current is zero; equation 3 (Nooruddin and Blunt 2016).

$$\frac{\partial}{\partial x} \left( D(S_w) \frac{\partial S_w}{\partial x} \right) = \frac{\partial S_w}{\partial t} \quad 2$$

$$q_o = -q_w \Rightarrow q_t = 0 \quad 3$$

Counter-current flow is modeled by one open face to imbibed water, Figure 3-A.

### 2. Co-current flow

The flow is termed as “co-current flow” when the wetting and nonwetting phases are flowing in the same direction. In other words, when the wetting phase is imbibing from one face and the non-wetting phase is produced from the opposite face. This regime is believed to be the dominant regime after the wetting phase front travels a certain distance (Haugen, et al. 2014), or even when the matrix is partially in contact with the imbibing water (Pooladi-Darvish and Firoozabadi 2000). However, Bourbiaux & Kalaydjian (1990) noticed oil production from the upper face of the plug with less production from the downside face of the plug, indicating the

counter-current was less effective than the co-current flow regime. On the other hand, the flow of one phase co-currently encourages the flow of the other phase since the pressure gradients are in the same direction, and hence the role of the viscous forces has positive effect in this case. Co-current flow is encouraged by gravity segregation in the fracture (outside the plug), and oil will prefer to flow in the plug toward the faces saturated or in contact with oil (Morrow and Mason 2001). Some essential properties of co-current imbibition are the high displacement efficiency, and it happens faster than the counter-current imbibition (Pooladi-Darvish and Firoozabadi 2000) (Unsal, et al. 2007) (Karimaie, et al. 2006). Moreover, the relative permeabilities are higher in the case of co-current than in the case of the counter-current (Bourbiaux and Kalaydjian 1990).

The 1D co-current flow can be described by equation 4 for incompressible fluids with neglecting the gravity effect (Pooladi-Darvish and Firoozabadi 2000).

$$\frac{\partial}{\partial x} \left( D(S_w) \frac{\partial S_w}{\partial x} - q_{tf}(S_w) \right) = \phi \frac{\partial S_w}{\partial t} \quad 4$$

The equation 23 is composed of two terms, the diffusion term, and the advection term.

Co-current flow is modeled by SI through two open faces to imbibed water, Figure 3-B, and Figure 3-C. Comparing the two equations 2 And 4, it can be seen that the water flow in co-current is greater than it in case of counter-current due to the presence of the positive term of advection or what is called “viscus-coupling term” (Schmid, et al. 2016).

The previous two types may be happening simultaneously depending on the capillary back pressure<sup>2</sup> in case of static experiments (Haugen, et al. 2014) and the injection rate in case of dynamic displacement (Karimaie, et al. 2006). In our experiment and from the analysis of the picture taken daily and regularly, we can notice the behavior of the simultaneously co- and counter-current flow regimes. The counter-current happened in the early time of the SI. During this time oil was produced from all the faces of the freely immersed-in-water plugs. However, the production from the lower part of the plugs reduced over time, and the production occurred

---

<sup>2</sup> Capillary backpressure, or bubble pressure, is defined as the differential pressure between the wetting and the nonwetting phase at the open face of the plug (Haugen, et al. 2014).

only from the upper face and upper part of the plugs in the late time of SI, indicating the co-current type aided by the gravity effect. This observation challenges the prevalent idea that the counter-current dominance when the core is immersed from all the directions in the wetting face, whereas the co-current flow is dominant when one of the faces of the matrix is in contact with the nonwetting phase (Bourbiaux and Kalaydjian 1990).

Taking the next two cases, Figure 3-A, in the first case the counter-current will happen along time of the imbibition if the oil pressure is higher than the capillary back pressure added to the pressure required for the counter-current flow of oil. In the second case, Figure 3-B, which is a two open faces case, counter-current flow happens simultaneously with the co-current flow to a certain time at which the nonwetting capillary pressure at the front is equal or less than the capillary backpressure. Thus, the longer the distance between the open face to water and/or the more viscous the oil, the more likely of the counter-current flow to dominate (Haugen, et al. 2014). The velocity of the front is determined in single tube model according to Washburn equation, that implies that in case of two fluids with same viscosities, the front will advance linearly with the time, but in case of two different viscosities with the displaced phase is more viscous, the front will speed with time.

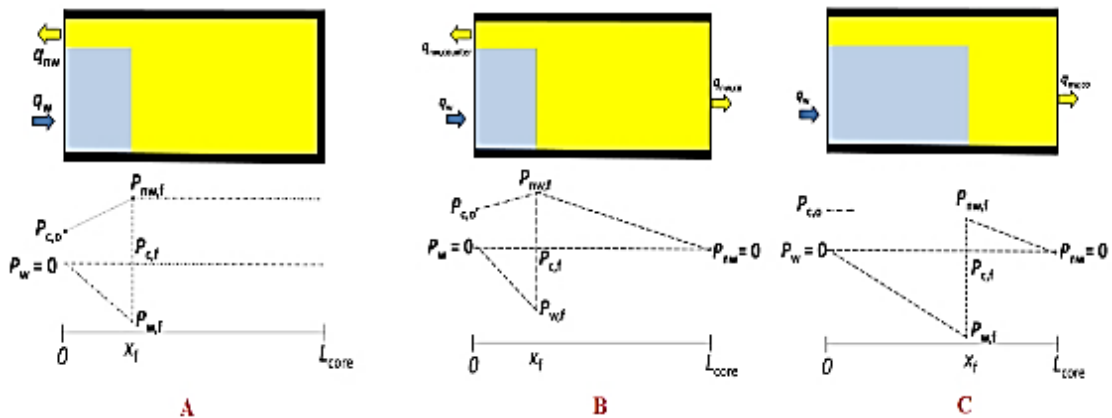


Figure 3: Boundary conditions and pressure gradient for (A) counter-current flow, (B) mixed flow, and (C) co-current flow (after (Morrow and Mason 2001))

Saturation profiles for the three situations obtained by Bourbiaux & Kalaydjian (1990) using the X-ray absorption method are depicted in Figure 4.

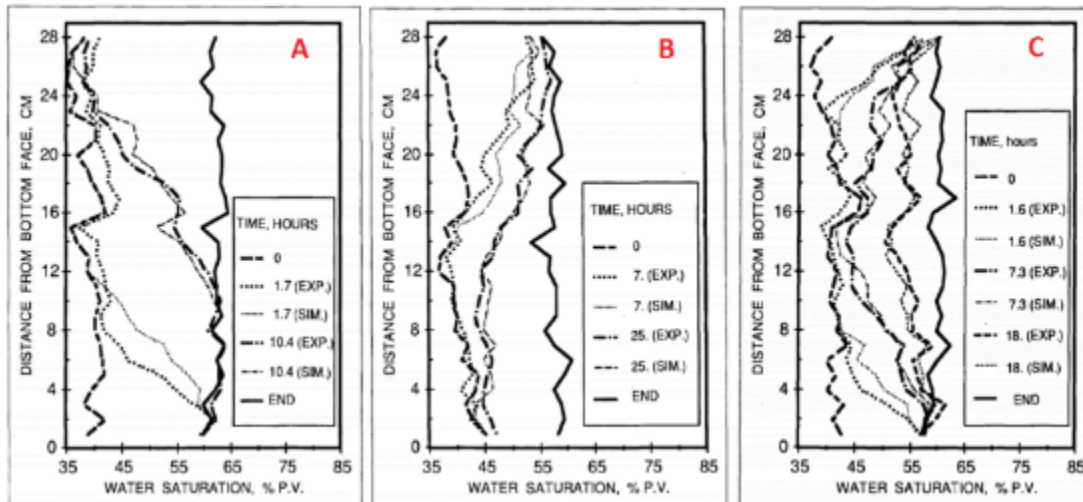


Figure 4: Saturation profiles for (A) co-current, (B) counter-current, and (C) mixed imbibition (after Bourbiaux & Kalaydjian (1990))

At the end of the imbibition process, the oil will be trapped as clusters or blobs, and in this case, the oil mobilization needs to be studied under constant influx-constant capillary number imbibition, Quasi-static imbibition<sup>3</sup>, or Dynamic invasion with a constant flow rate of the displacing fluid<sup>4</sup> (Sahimi 2011). The nonwetting phase at high wetting phase saturation loses its mobility (Ahmed 2010) due to the snapping off effect where the ganglion length is less than the critical length where the viscous forces are more significant than the capillary forces.

## 2.2.2 RESULT SCALING

Scaling SI data is crucial to compare data sets and to predict the application of SI in the real reservoir; in other words, it predicts field-scale production using SI by using plug-scale data. Scaling is done using dimensionless times. The scaling step aims to ignore the difference in the plug's shapes, boundary conditions, differences in rock, and fluids properties. The dimensionless time was discussed by many researchers for a long time. The relation of

<sup>3</sup> This mechanism is considered when the backpressure is reduced regularly and the pores with certain diameter is invaded (Sahimi, 2011).

<sup>4</sup> This mechanism is considered when the backpressure is adjusted to keep imbibition rate constant (Sahimi, 2011).

dimensionless time ( $t_D$ ) is derived based on Poiseuille equation as in (Morrow and Mason 2001). The final equation of  $t_D$  is presented in equation 5:

$$t_D = \frac{\sqrt{2}}{L_{\max}^2} \sqrt{\frac{K}{\phi}} \frac{\sigma}{f(\mu_w, \mu_{nw})} t \quad 5$$

Different attempts were done to define the dimensionless time for real porous media. In the counter-current flow regime, Ma, Zhang, & Morrow (1999b) found that  $L_{\max}$  is better replaced by  $L_c$ , which is defined as the distance between the no-flow boundary and all the other open faces of the plug. In this sense  $L_c$  is a function of the boundary conditions Figure 5.

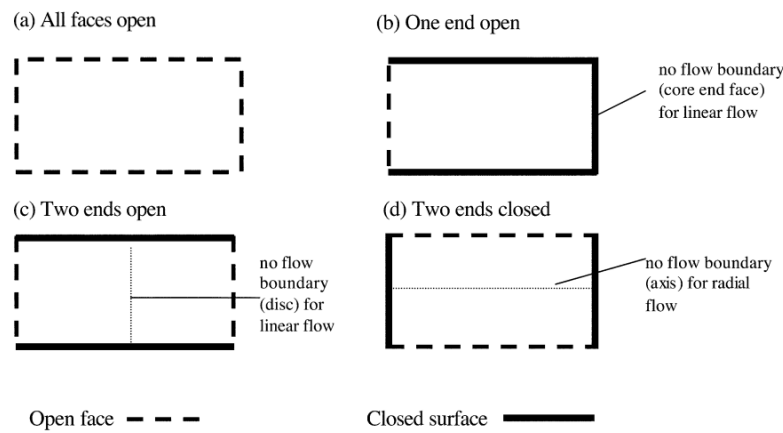


Figure 5: Boundary conditions for core samples summarized by (Morrow and Mason 2001)

Ma, Morrow and Zhang (1997) defined the  $t_D$  of strong water-wet plugs, equation 6. They found that dimensionless time is inversely proportional with the geometric mean of the viscosities of the wetting and nonwetting phases

$$t_D^{\text{MMZ}} = \frac{C}{L_c^2} \sqrt{\frac{k}{\phi}} \frac{\sigma}{\sqrt{\mu_w \mu_{nw}}} t \quad 6$$

Where:

$t_D^{\text{MMZ}}$ : Ma et al.'s dimensionless time.

$L_c$ : the characterization length [cm]. In the case of cylindrical plugs with all faces are opened to the wetting phase imbibed in the media, the characterization length is given by the following equation 7 (Zhang et al. 1996):

$$L_c = \frac{l * d}{2\sqrt{d^2 + 2l^2}} \quad 7$$

$k$ : Absolute **gas** permeability [mD].

$\phi$ : Porosity [Fraction].

$\mu_w, \mu_{nw}$ : the viscosities of the wetting and nonwetting phases, respectively [cP].

$\sigma$ : interfacial tension between the wetting and nonwetting phases [dyne/cm].

t: real-time [hours]

C: Conversion units constant  $C = 0.018849$

# Chapter 3

## Experiment preparation, setup, and conduction

### 3.1 Samples characterization

The sample description aims to characterize rock mineralogy, sedimentary environments, mineral structure, and diagenetic features. This description is the first step in laboratory tests when the experiment is executed on real CBR systems.

The selected rock type in the presented work is an outcrop sandstone from the Bentheim Formation. There are two varieties of the Bentheim sandstone, the first one is pale yellow from the Gildehaus region, and the second one is darker and sometimes reddish because of the hematite minerals from the Bad Bentheim region (Dubelaar and Nijland 2014). These cores are characterized with high permeability, low clay content (Loahardjo, Winoto and Morrow 2013) and good interconnected porous network that contains in general large pores and less meso- to micro-pores (Halisch, et al. 2013)

Established procedure frameworks already exist to provide a common comparison base for data interpretation, even if the same experiment is executed in different infrastructures. Among those, the one used in the frame of this work is described in (API 1998). To study the mineralogical and geological features of the studied plugs, Figure 6, then-sections analysis on a polished uncovered thin-section (PUTS) were conducted. Moreover, the sample geometries were measured carefully using Vernier caliper. Table 1 present the dimensions of the plug. The mineralogical composition also further studied by XRD analysis.



Figure 6: Core plug drilled from outcrop Bentheim Sandstone

Table 1: Samples' geometry

sample ID	Dimension	
	Diameter	Length
	mm	mm
B3	37.8	74.9
B4	37.8	74.8
B5	37.7	71.9
B7	37.5	73.5
B8	37.7	68.7

A synthetic brine was used to drill the plugs from the main block. The main concern was the presence of clay minerals that can swell and disperse. To avoid clay swelling drastic effects, 250 g/l (about 4.277 mole/l) of NaCl synthetic brine was used.

The plugs were preserved after the drilling step by simple preservation. Since they were drilled from outcrops blocks, the plugs were warped with plastic bags with the drilling mud in the pores and minimum air amount outside the plugs. The preservation conditions were at ambient conditions. After some days, salt precipitation was observed on the outer side of the plugs because of the water evaporation at the ambient conditions.

### 3.1.1 MINERALOGY

The Bentheim Sandstone is a marine rock from lower Cretaceous. It forms a very good oil reservoir (Dubelaar and Nijland 2014) due to its high porosity and permeability, and the lateral continuity and homogeneity. The rock is composed of a small number of minerals and is thermally stable. The main mineral component of the rock was well studied in many kinds of literature, for example but not only Peksa, Wolf and Zitha (2015) and Dubelaar and Nijland (2014), in the present thesis the most dominant minerals are listed:

1. **Quartz:** the main component with the highest percentage. The grains are rounded or sub-rounded. They show self-overgrowth (Peksa, Wolf and Zitha 2015, Dubelaar and Nijland 2014) causing the reduction of intergranular porosity (Peksa, Wolf und Zitha 2015). The newly deposited silica may be a result of feldspar weathering during the diagenesis and quartz dissolution in the grain contact points and reprecipitation in other places (Dubelaar and Nijland 2014). Quartz can be noticed in the then section images (Figure 8) and in the XRD analysis (Figure 7).
2. **Feldspar:** with brown to brownish color showing cleavages due to the weathering processes. The feldspar weathering and dissolution cause irregular porosity (Peksa, Wolf und Zitha 2015). The weathering of the feldspar influences the pore structure where clay minerals are located near the dissolved feldspar. The products of the feldspar weathering appear in two types (Halisch, et al. 2013): full or partial coating over the quartz grains and fillings of the interstitial porosity.
3. **Clay minerals:** two possible sources according to Peksa, Wolf, & Zitha (2015): local sources as a result of the feldspar weathering, e.g. Illite (Halisch, et al. 2013), kaolinite and smectite; and original sources due to the original deposition processes such as montmorillonite. Clay minerals appear as booklets on the quartz surfaces and form thin covers that determine the original quartz surfaces (Dubelaar and Nijland 2014). Nevertheless, the source of clay is not yet well known, and it is difficult to state a concrete conclusion about it (Dubelaar and Nijland 2014).
4. **Iron (hydr) oxide:** affects the rock color and appears as a thin layer covering the grains. The main minerals are pyrite transforming to brownish hematite, and goethite indicating the marine origin of the rock (Peksa, Wolf and Zitha 2015). Iron deposits appear along the fault-planes and fractures due to the iron-rich groundwater flowing through them (Dubelaar and Nijland 2014).
5. **Heavy metals:** such as zircon and rutile (Dubelaar and Nijland 2014).

The mineral composition in our experiment was determined using the XRD and thin sections analysis. As shown in Figure 7 and Figure 8 the dominant mineral in the Bentheimer Sandstone is Quartz. In the tested sample, XRD did not capture any measurable quantity of clay minerals.

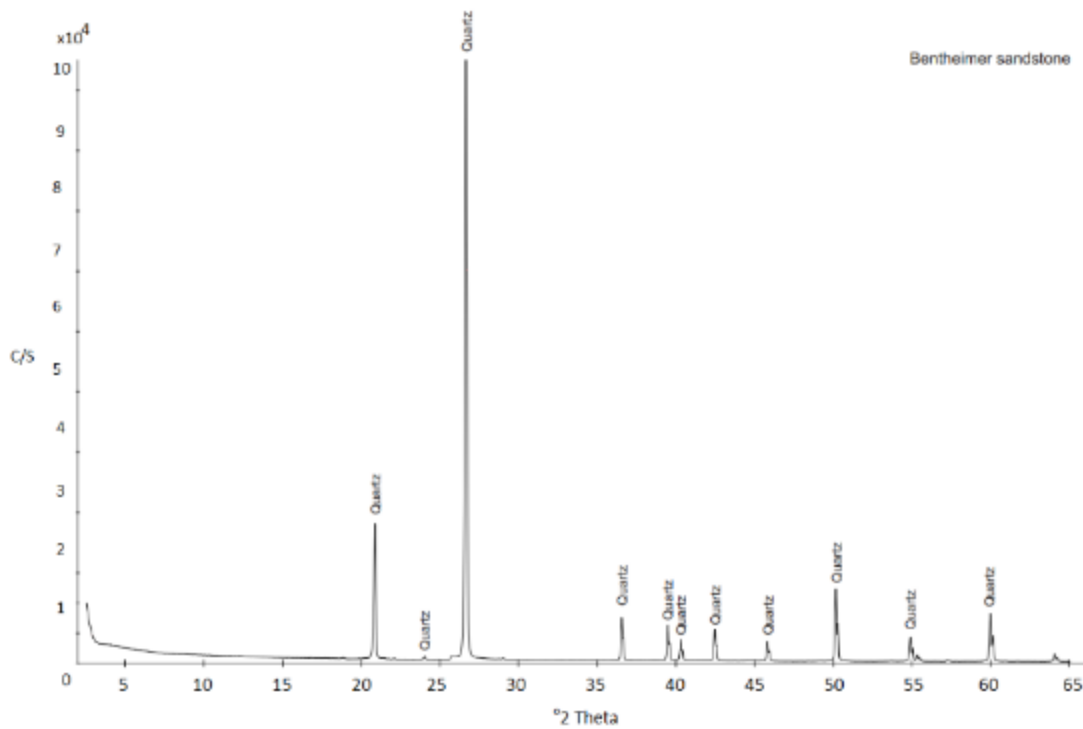


Figure 7: Bentheim Sandstone XRD analysis

Quartz grains show the self-growth (Figure 9-A) and are covered with hematite minerals (Figure 9-B) during the reprecipitation process. However, the self-growth process happened after the hematite precipitation as it is indicated by Figure 9-C, where a thin film of the hematite deposited after then the silica deposited. Another interesting phenomenon is observed in the quartz grains, fluid inclusion is shown in Figure 9-D. This water was included in the quartz grains during the quartz minerals formation. Moreover, traces of heavy metals are observed in Figure 9-E. Figure 9-F shows a rock fragment, which is composed mainly of smaller quartz grains.

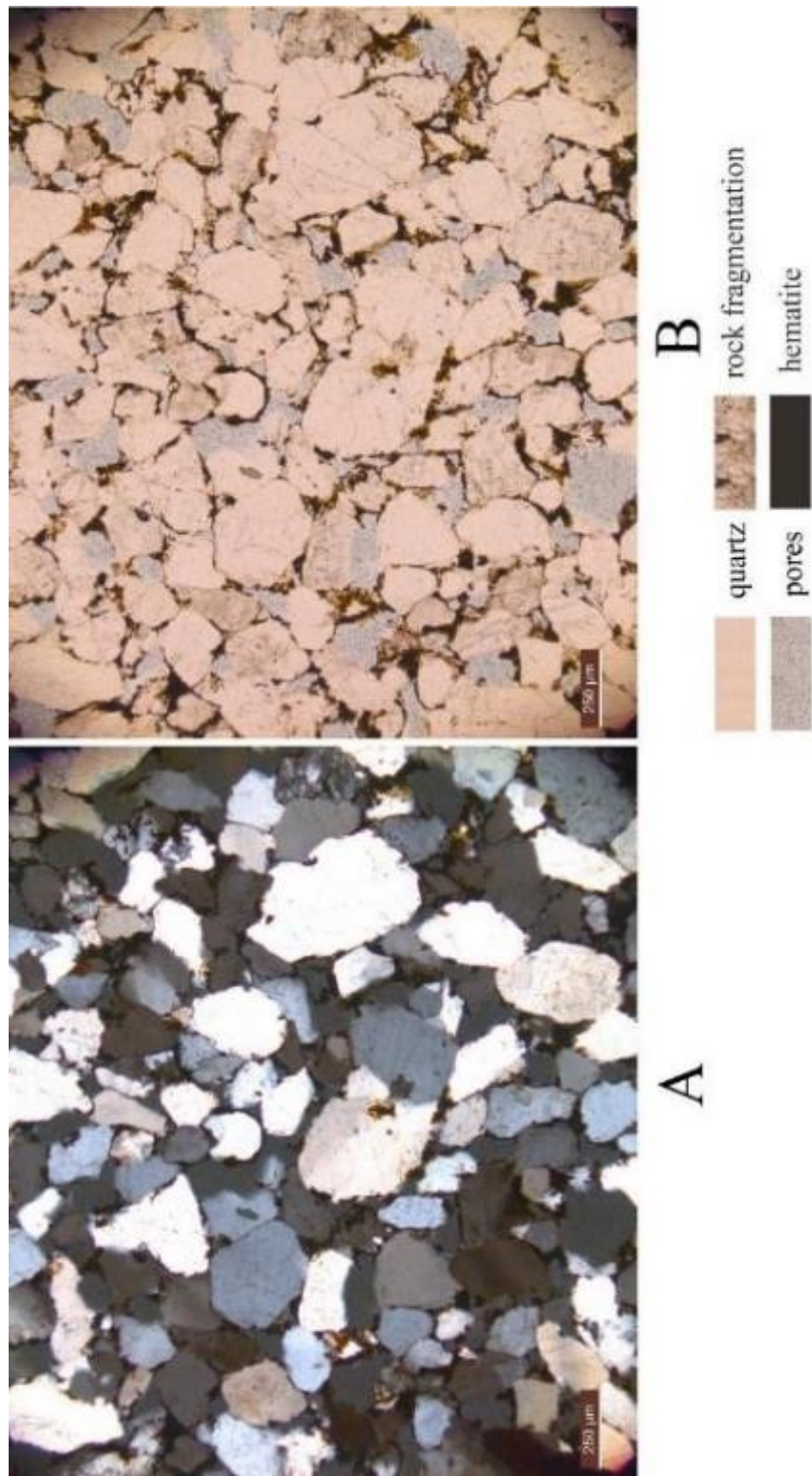
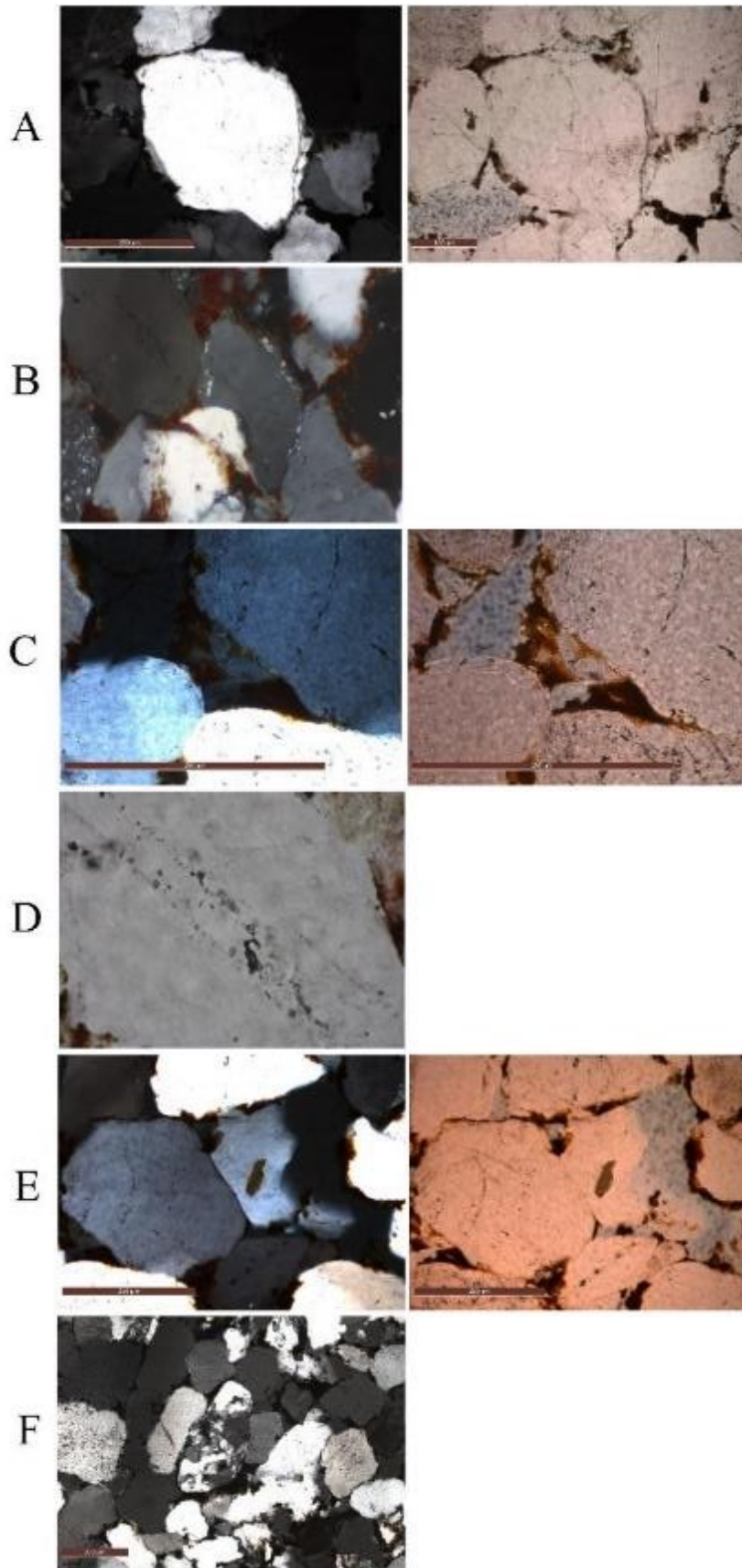


Figure 8: Bentheim thin section under optical microscopy



*Figure 9: Geological features in the Bentheim Sandstone – studied under polarized and non-polarized lenses*

### 3.1.2 GRAIN ORIENTATION

Based on thin-section images (Figure 8) no specific direction can be observed for the grain orientation neither in the Bentheim type. The same conclusion was driven by the different researcher as in (Peksa, Wolf and Zitha 2015). The random orientation is a result of the low energy sedimentary environment resulting in the absence of any favorable permeability direction. (Normally, it should be in the direction of the main axis of the grains (Dubelaar and Nijland 2014)). However, the asymmetric dissolution and precipitation of silica, in other words self-growth, caused less rounded grains but with arbitrary orientation.

### 3.1.3 POROSITY AND PERMEABILITY

The Bentheim block, which the plugs were drilled from, is quite homogeneous: the measured porosity values are summarized in Table 2, show little variance (median: 16.68%, standard deviation: 0.16). The porosity was measured using both Mercury Porosimeter and Helium Porosimeter, and both of them showed an excellent match.

Table 2: Measured porosity values for the Bentheim Sandstone plugs

sample Code	Phi [%]
B3	16.56
B4	16.59
B5	16.65
B7	16.72
B8	16.81

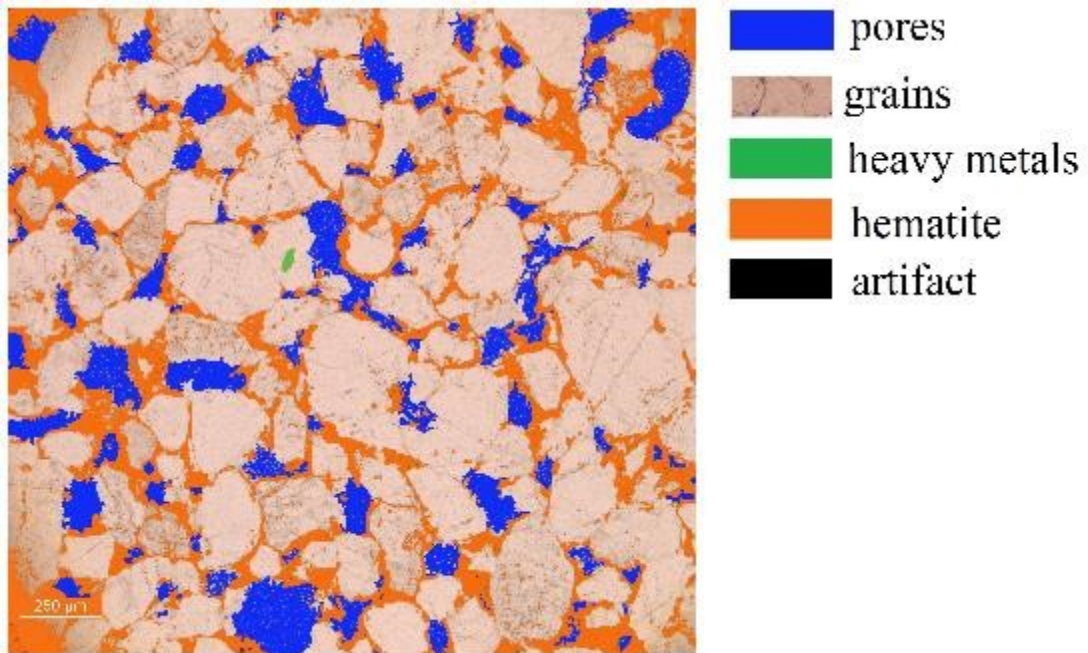


Figure 10: Unpolarized thin-section images of Bentheim sandstones

Gas permeability using inert nitrogen as a flowing fluid and brine permeability (180 g/l TDS) were measured. Table 3 shows the gas and brine permeabilities values.

Table 3: Gas and brine permeability of Bentheim Sandstone plugs used in our experiments

sample ID	K N2	K brine	K N2/K brine
	mD	mD	
B3	271.8	219	0.81
B4	268.2	182.01	0.68
B5	267.3	187.1	0.70
B7	301.5	NA	NA
B8	278.4	212	0.762

A positive linear relationship is observed between permeability and porosity as it is shown in. Permeability affects the SI rate and extension, and the URF. Increase permeability is coupled with an increase in the URF and the time of SI recovery. On the other hand, increase K lead to an increase in the SI rate. However, this relation is not a function of the IFT (Li and Horne 2002).

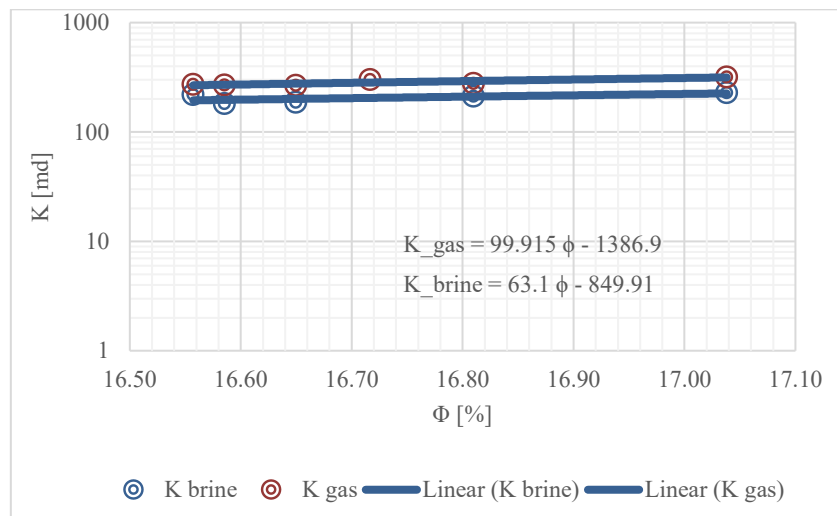


Figure 11: Permeability-Porosity relationship

### 3.1.4 GRAIN DISTRIBUTION AND SORTING

The grain distribution and sorting are functions of the depositional environment energy and sediment transportation (Dutton and Willis 1998). Because of the well-sorted grains (Halisch, et al. 2013) and the same mid-sizes in the range of 180-300 microns (Dubelaar and Nijland 2014), it can be concluded that Bentheim sandstone was deposited in an environment with low and constant wave energy with and slow waves that were not able to transport large grains (Peksa, Wolf and Zitha 2015).

The pore size distribution (Figure 12) shows that the dominated radius for our plugs is between 8-10.5  $\mu\text{m}$  with more than 50% probability. The pore sizes were measured using Mercury Injection Capillary Pressure (MICP) measurement.

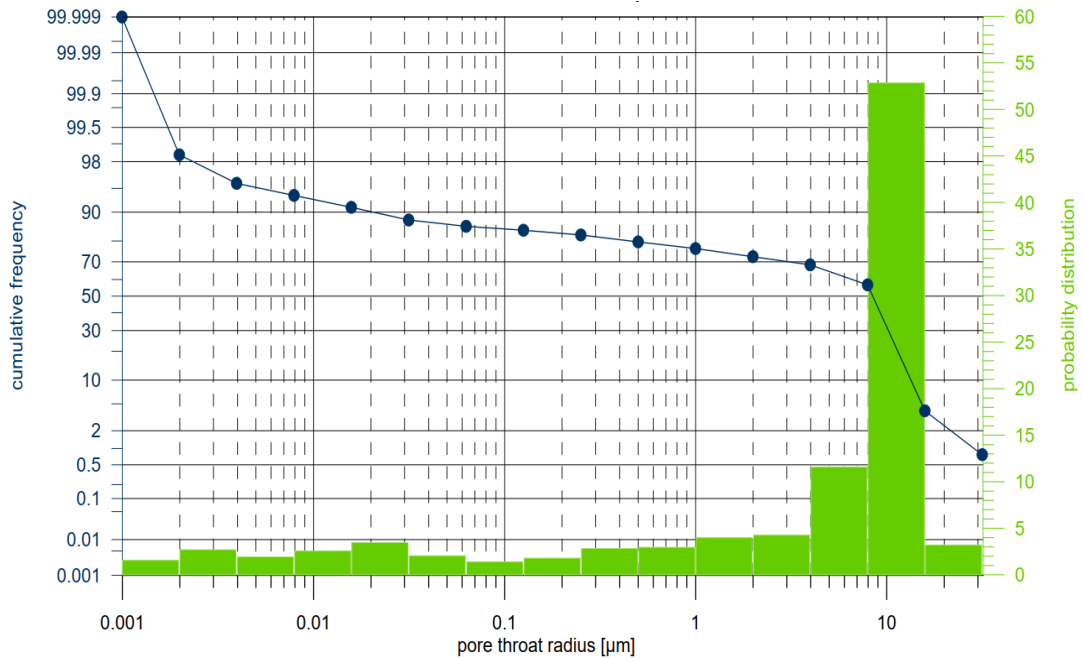


Figure 12: Pore size distribution of Bentheim Sandstone

### 3.1.5 DENSITY

Rock density can be divided into two categories, grain density and bulk density. Grain density varies vertically and horizontally according to the mineral composition especially in the presence of heavy metals (Keelan 1982). Table 4 shows the density values of our plugs.

Table 4: Grains and Bulk densities

sample ID	Grain Density	Bulk Density
	$\text{g/cm}^3$	$\text{g/cm}^3$
B3	2.648	2.209
B4	2.651	2.211
B5	2.649	2.208
B7	2.648	2.206
B8	2.654	2.208

### 3.1.6 COLOR

The Bentheim sandstone appears in different colors: the reddish color is due to the presence of hematite  $\text{Fe}_2\text{O}_3$  (Dubelaar and Nijland 2014). Maloney, Honarpour, & Brinkmeyer (1990) stated that in the fired Bentheim sandstone, other iron oxides converted into hematite and caused the red color of the plugs. In the blocks that our laboratory obtained, precipitation of hematite was observed as small lenses or as sub-layering forms both by the naked eye and under the optical microscope.

## 3.2 Restoration

A successful restoration process consists of three main phases (Gant and Anderson 1988): the first phase is **cleaning** the plug from all of the invading fluids, even those that attach to the surface and getting completely clean pore surfaces with a strong water-wet state. The second phase is to **re-saturate the plugs** with the brine first and then with oil until the water saturation reaches the initial water saturation of the reservoir. This process represents the fluid drainage sequence in the reservoir. Finally, **aging** under reservoir temperature is performed for sufficient time which ensures the adsorption equilibrium and the establishment of the final wettability state. That is important because the wetting state affects the capillary pressure, the residual fluid saturation and relative permeability in addition to many other petrophysical parameters of the rock (L. Cuiec 1965).

### 3.2.1 CLEANING METHODS

The first step of the restoration process is the cleaning step. Cleaning aims to get a clean, strong water-wet pore surface (Cuiec, Longeron and Pacsirszky 1979), according to the fact that all the rocks had formed in aqueous environments and all the clean surfaces of the minerals are water wet.

The selection of the cleaning and drying methods depends on different factors, from them: the mineralogy of the plug, clay content, effects on wettability state, and the aim of the cleaning process (whether RCA or SCAL) (McPhee, Reed and Zubizarreta 2015). The most suitable method for cleaning plugs and cores is determined by the trial-and-error method, and this depends, in addition to the rock mineralogy, for example, the presence of carbonate minerals (Wendell, Anderson and Meyers 1987), on physical, chemical, and petrophysical properties of the COBR system components. Gant & Anderson (1988) stated that two cleaning methods are used for SCAL tests:

1. **Extraction and distillation methods:** for example, Soxhlet extraction method and Dean-Stark extraction. Distillation/extraction methods are cheaper than other methods, relatively fast and can be used to clean many plugs at the same time. Moreover, it does not require intensive work and supervision (McPhee, Reed and Zubizarreta 2015).
2. **Flow-through method:** it is considered as better than distillation and extraction methods because it depends on the pressure difference between the two faces of the plug, which ensures the reaching of the solvent to more pores in the plug. It is

faster and more efficient than the distillation and extraction methods, especially when back-pressure is applied.

Extraction and distillation methods have some disadvantages that affect the results of the cleaning process:

- The solvent cannot reach all the pores especially the capillary pores since these methods depend on gravity forces.
- Depending on the selected solvent, they may turn the core from water-wet to oil-wet. Due to the direct contact with the solvent at high temperature for a long time.
- They can cause the vaporization of initial water, and this encourages the transition to oil-wet state due to the elimination of the thin water film covering the wall of the pore. This effect is influenced by the physical and chemical properties of the solvent, for example, boiling temperature and the content of polar components as well as the salinity and composition of the brine.
- They may cause a wrong measurement of the permeability and other rock properties.
- Introduce the plugs to high temperatures and repeated cycles of liquid and vapor immersion (cyclic drying). Hence it is considered a harsh cleaning method ([McPhee, Reed and Zubizarreta 2015](#)).
- The Long extraction time and the large amount of solvent wasted, as well as the disposal procedure and distillation of the extractant ([Castro and Priego-Capote 2010](#)).

In our experiment, we used the Soxhlet extraction method with chloroform/methanol azeotrope as a solvent. We cleaned the outcrops to dissolve any salt scales precipitated during the preservation step as well as to eliminate the drilling fluid filtration. During the preservation step, traces of salt precipitations were observed on the outside wall of the plug. These salts came from the synthetic drilling fluid. Usually, in outcrop plugs no or only traces of organic matter are expected. In addition, the plugs are consolidated and maintain the boiling temperature of the azeotrope. Bentheim sandstone mineralogy shows no reactivity with the solvent. The chosen method and solvent are based on previous works to avoid the time-consuming trying different methods and solvent. The needed time to complete this step was one week. This time was required because this method depends on the gravity forces. However, the cleaning time depends also on petrophysical quality, which is considered suitable for Bentheim sandstone, plug size, the physical and chemical COBR system components, and the solvent properties. Add to that the cheap costs and good cleaning efficiency.

After finishing the cleaning procedure, it was noticed that the solvent in the flask was discolored with a reddish color. This discoloration is due to the dissolution of the iron oxide. Furthermore,

a white precipitate was also observed. The precipitant is NaCl salt that was used in the synthetic drilling fluid, which was dissolved with methanol (Loahardjo, Xie, et al. 2012).

### 3.2.2 SOLVENTS

Choosing the solvent must be based on the main purpose of the cleaning process, which is obtaining a strong water-wet pore surface in our case additional to clean the salt precipitant. The solvent selection is a trial-and-error matter (API 1998). The primary choice depends on several factors that determine the efficiency and types of solvents in addition to their number in the mixture and number of cleaning cycles and cleaning duration. Among others, these factors are:

1. The type of oil (L. Cuiec 1965).
2. The compatibility with the COBR system: (API 1998)
3. The aim of the cleaning process: (McPhee, Reed and Zubizarreta 2015).
4. compatibility with the equipment (API 1998)
5. The boiling temperature of the solvents (API 1998).
6. During the distillation, solvent drops must not cause any erosion or corrosion to the plug (API 1998).
7. The solvent must preserve the reference state of the surface (Culec 1977).
8. The chosen solvent must preserve the mechanical state of the plug and does not destroy it (API 1998).

Solvents can be divided into two broad categories (API 1998):

1. **Non-polar solvent:** like Alkanes and Halogenic alkenes. They help to dissolve the light components of the oil and water under high temperatures.
2. **Polar solvents:** like alcohols, ketone, and halogenic alcohols. They dissolve heavy oil components and water under low temperatures and salts that precipitate from the connate water or drilling fluid filtration.

For our experiment we used chloroform ( $\text{CHCl}_3$ )/methanol ( $\text{CH}_3\text{OH}$ ) azeotrope. The advantages of using chloroform in the azeotrope are that it is not explosive and does not alter the initial wettability properties of the surfaces it contacts them (Conley and Burrows 1956). Also, using chloroform ensures the surface wettability alteration toward strong water wet (Grist, Langley and Neustadter 1975). Both of the solvents used in the azeotrope are acidic type solvents (Cuiec, Longeron and Pacsirszky 1979). Hence they are compatible with cleaning sandstone plugs. Using each of them individually showed poor efficiency to clean sandstone

outcrops saturated with oil (L. Cuiec 1965). Chloroform is partially miscible with water, while methanol is completely miscible with water. The boiling temperatures of both of them are 61.25°C for chloroform and 64.75°C for methanol, whereas the azeotrope boiling temperature is 53.8°C. The azeotrope is composed of 0.647781 mole chloroform per mole azeotrope and 0.352219 mole methanol per mole azeotrope. Because of the lower boiling temperature, the azeotrope cannot evaporate connate water and ensure avoiding salt precipitation (Yuan and Schipper 1995). Chloroform/methanol azeotrope is believed to preserve the surface properties related to wettability restoration to the initial state after the cleaning step (Holbrook and Bernard 1958). McPhee, Reed, & Zubizarreta (2015) stated that Methanol is used for gas samples to dissolve water and salt precipitations.

### 3.2.3 DRYING THE PLUGS

As soon as the cleaning process is completed, samples are dried before the tests are done on them or they are saturated with the desired fluid to start the aging step of the restoration process. Drying is done, in general, by introducing the cores to temperatures equal or higher than the solvents boiling temperatures and leaving them in this environment for many days until their weight becomes constant (with some acceptance range) (API 1998). The drying time is a function of different factors, such as sample quality and cleaning solvent properties, but, in general, it takes several days. However, choosing the drying method depends on several factors from them the mineral composition of the plugs (API 1998).

Our plugs were dried at ambient conditions for more than two months by placing them in contact with the air.

### 3.2.4 FLUID RESATURATION

The next step is to (re-)saturate the plugs with the brine first and then with oil until the water saturation reaches  $S_{wc}$ . This process stimulates the fluid drainage sequence in the reservoir. It is important in this stage to be sure that the saturation profiles of the fluids are homogenous and the plugs are air-free (Gant and Anderson 1988). The saturation methods involve the porous plate method, centrifuge flooding, core flooding, and the evacuation method.

In our experiments, we used the core flooding method combined with a porous disk to ensure homogeneous fluid distribution in some of our tests (B8-H1-8TH-H1, B5-H1-8TH-L1, and B4-H1-8TH-H1). Figure 13 shows a schematic sketch of the single-phase unit used to saturate the plugs with fluids.

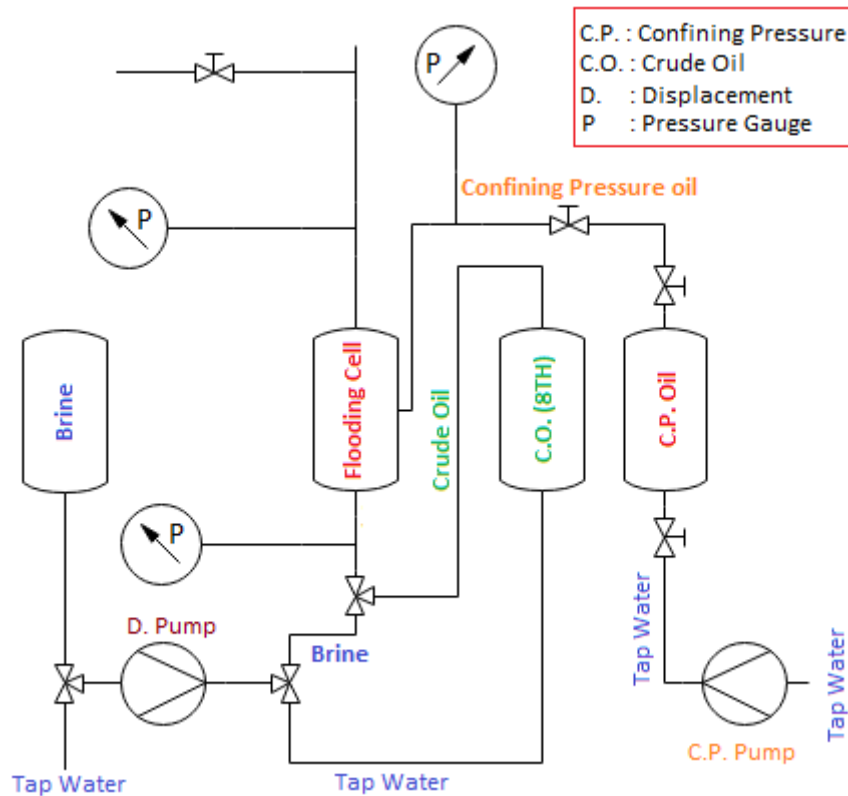


Figure 13: Saturation platform sketch

Before saturation is started, the platform is cleaned. Cleaning the components of the platform is done under the room temperature and using different solvents according to the contaminants:

- Oil contaminated parts with:
  - a. Benzene: to dissolve the oil (Crude oil and the hydraulic oil)
  - b. Flush it with Acetone
  - c. Dry with compressed air
- Brine contaminated parts with:
  - a. methanol: to dissolve salts
  - b. distilled water
  - c. dry with compressed air

The plug was placed into the flooding cell, then confined by the Viton rubber sleeve. The cell was flooded by  $\text{CO}_2$  for 30 min to displace air from the pores. This step is done to ensure the absence of air from the plug, since  $\text{CO}_2$  is better displaced and dissolved in water than air. The flooding cell was mounted to the platform and the confining pressure is applied (35 bar). The confining pressure was applied using a hydraulic oil by the confining pressure pump (C.P. Pump). The hydraulic oil was pumped in the annulus between the flooding cell and the Viton rubber sleeve. It is important to ensure that there is no air in the confining pressure parts since

air will show unreliable pressure readings. After mounting the platform, water saturation was started.

### 3.2.4.1 Saturating with brine:

The first brine saturation demonstrates the sedimentation environment, this is the reason that all pores are filled with water, even the capillary pores. In our preparation, water is saturated using core-flood method. After mounting the platform, brine is injected from the bottom of the flooding cell, to ensure piston-like displacement, displacing CO<sub>2</sub>. The flow rate is set to 0.5 ml/min. The pressure difference ( $\Delta P$ ) is measured using an OMEGA pressure transducer (PXM409-050BAUS) with maximum pressure readings = 50 bar.  $\Delta P$  increases with increasing the PV injected until it becomes constants after the breakthrough (BT). As soon as  $\Delta P$  is stable for enough time, the injection rate is changed to  $Q = 1$  ml/min and  $Q = 1.5$  ml/min to calculate the brine permeability ( $K_{\text{brine}}$ ).  $K_{\text{brine}}$  is calculated after stabilizing  $\Delta P$  for enough time using Darcy's equation for three flow rates (0.5, 1, 1.5 ml/min), and the average is considered the brine permeability. Table 3 shows  $K_{\text{brine}}$  results.

Many steps have been taken before brine was injected into the plugs:

1. Two synthetic brines were prepared:
  - H1: by adding 150 g of NaCl and 30 g of CaCl<sub>2</sub> to 1 liter of distilled water.
  - L1: by adding 3 g of NaCl and 0.6 g of CaCl<sub>2</sub> to 1 liter of distilled water.
2. Water was filtered with a Sartorius filter with 0.45  $\mu\text{m}$  diameter pores, from the solid particles.
3. Water characterization: the conductivity was measured by Cond7110 manufactured by ionLab, the viscosity was measured by Physica MCR 301 manufactured by TruGap<sup>TM</sup> READY at 25°C and 50°C. pH was measured by 827 pH lab manufactured by  $\Omega$  Metrohm. The density was measured by DENSITY METER DMA 35N manufactured by Anton Paar.
4. Water is vacuumed to be degassed

Table 5 shows the brine characterization results.

Table 5: The two brines characteristics

Sample		Density [Kg/m <sup>3</sup> ]		Viscosity [cP]		pH		conductivity [mS/cm]		Composition				
ID	#	T [C]	Value	T [C]	Value	T [C]	Value	T [C]	Value	NaCl [g/L]	CaCl <sub>2</sub> [g/L]	TDS [g/L]		
1	H1	1	22.8 ±0.1	1.113	25	1.22	22.8 ±0.1	5.96	5.997	24.1	177.5	150	30	180
		2	22.8 ±0.1	1.1129	50	0.987	22.8 ±0.1	5.99		24.2	178			
		3	22.8 ±0.1	1.1131			22.8 ±0.1	6.04		24.1	177.6			
2	L1	1	22.8 ±0.1	0.9993	25	0.885	22.8 ±0.1	6.55	6.570	23.4	6.31	3	0.6	3.6
		2	22.8 ±0.1	0.9992	50	0.574	22.8 ±0.1	6.59		23.3	6.29			
		3	22.8 ±0.1	0.9993			22.8 ±0.1	6.57		23.4	6.29			

### 3.2.4.2 Saturation with oil:

The oil first saturation demonstrates the primary drainage, where the first imbibition is demonstrated by the LSWI process. In the presence of the initial water, a force at least equals to the entry force is required to force the oil to enter the pores where the water is present. It is crucial to preserve the oil used away from contamination with chemicals such as materials injected into the reservoir or used during the drilling of samples. After the plugs were saturated with brine, crude oil (CO), 8TH, is injected. Oil saturation was executed with a water-wet porous disk mounted above the plug for three plugs, whereas three other plugs were saturated without a porous disk. The usage of the porous disk aims to reach the maximum, homogenous oil saturation profile. After the porous desk was mounted, brine was injected to saturate the porous disk with water and to initiate a continuous aqueous phase between the plug and the porous disk. After this initiation, CO<sub>2</sub> was injected with an injection rate of Q = 0.1 ml/min. When the porous disk is used, the oil saturation was stopped when the  $\Delta P > 2$  bar. On the other hand, oil saturation of the plugs saturated without the porous disk was stopped after enough time of oil breakthrough.

In the literatures, many steps should be taken before the oil is injected into the plug:

1. The oil is filtered to eliminate solid particles (Loahardjo, Winoto and Morrow 2013). Or it can be centrifuged after being heated to 40C (Suijkerbuijk, et al. 2012).
2. The oil is vacuumed for many hours to reduce any possible gas volumes (ambient conditions) (Loahardjo, Winoto and Morrow 2013).
3. The oil should be water-free (Suijkerbuijk, et al. 2012).
4. Polar components are removed using a packed column of alumina and silica gel (Loahardjo, Winoto and Morrow 2013).

5. Minimizing oil-air contact using argon blanket to minimize oxidation reactions.

Finally, the plugs were saturated with brine then with oil as it is shown in Table 6.

Table 6: Plugs' state after renaturation with brine and crude oil

System	B3H18THH1L1	B4H18THH1	B5H18THL1	B7H18THH2	B8H18THH1
Plug	B3	B4	B5	B7	B8
Brine	H1	H1	H1	L1	H1
Crude oil	8TH	8TH	8TH	8TH	8TH
Swi [%]	29.58	30.69	32.28	29.63	37.17
With porous disk?	No	Yes	Yes	No	Yes

### 3.2.5 AGING

Gant & Anderson (1988) defined the plugs or cores with **native state** as any plug or core that has been preserved using any method that preserves its reservoir wettability regardless the drilling method or the used drilling fluid except that the drilling fluid should not contain any chemicals that cause wettability alteration, for this reason, it is better to use a water-based mud with the minimal chemical additives (Wendell, Anderson and Meyers 1987). Treiber et al (1972) defined the **native state** as the state of the cores that are drilled using an oil-based fluid and the **fresh state** as the state of the cores that are drilled using water-based drilling fluid and their wettability has not changed. Anderson (1986a) defined the **clean state** as the state of the cores after the cleaning process is completed, as a result of it, the plug becomes fluids free and strongly WW. He defined the **restored state** as the state of the core after cleaning, saturation with fluids, and aging to restore the wettability state of the reservoir.

Many factors determine the success of the aging step. From them:

1. The saturation of the sample with brine until  $S_{wc}$  is reached (Cuiec, Longeron and Pacsirszky 1979). This is important for the following reasons:
  - It simulates reality in the reservoir.
  - The importance of the chemical composition of connate water and the importance of its pH.
  - It is vital to restore samples to a mixed wetting state.

Jia, Buckley, & Morrow (1991) found that the relationship between the initial water saturation and the final wettability state takes an “S” shape, Figure 14, they found that for low initial water saturation the final wettability state tend to be MW, on the other hand, with high initial water saturation the final wettability state tends to be SWW, the range between them shows sharp variation in the final wettability state.

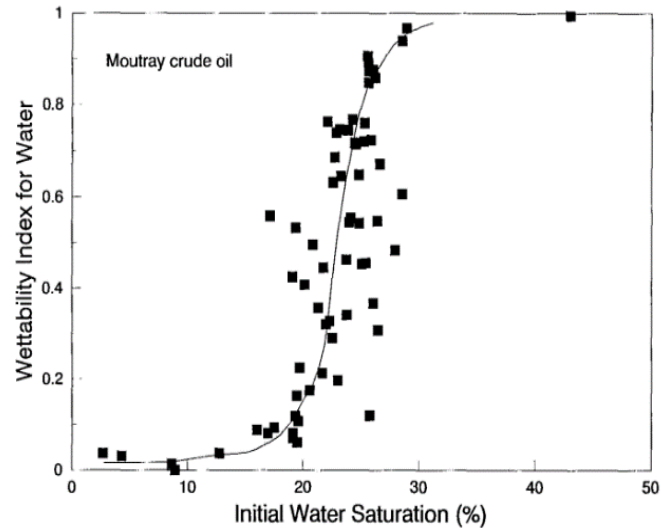


Figure 14: Wettability index as a function of the initial water saturation for different aging times, temperatures, and injected pore volumes. (after Jia, Buckley, & Morrow (1991))

2. Connate water composition: Jadhunandan & Morrow (1995) stated that the oil wetness increases with the increase of the concentration of the divalent cation, namely  $\text{Ca}^{+2}$ , but the wettability sensitivity to brine composition reduces due to aging temperature increase and the presence of monovalent cations, namely  $\text{Na}^{+}$ .

3. Type of oil: The restoration process can be done using dead oil at ambient pressure or live oil. The combination of live oil, reservoir brine, and native state plugs under the reservoir condition is preferred since it simulates the studied case better (Anderson 1986a), but the use of live oil is associated with some risks.

4. The composition of the oil: Just a small portion of the CO involves in wettability alteration toward OW state (Suijkerbuijk, et al. 2012). Aromatics or naphtheno-aromatics, Polar, basic or acidic, compounds, and Asphaltene are responsible for the wettability alteration during the aging step. Moreover, when the CO is a poor solvent of its heavy components, his ability to alter the wettability will increase, and vice versa (Al-Maamari and Buckley 2003).

5. Rock surfaces: The different **rock surfaces** are characterized by different chemical coatings in sandy rocks showing acid properties, while carbon rocks have basic properties (L. Cuiec 1965). Wang & Gupta (1995) found that the contact angle for calcite and quartz are different at the same conditions and other parameters

being constant. They found that calcite shows weak WW state at ambient conditions and the contact angle decreased with increasing temperature. The contrasting case was observed with quartz, which shows strong WW state at ambient conditions.

6. Conditions of the reservoir: Cuiec (1965) stated that the process of restoration is done by exposing the samples to the conditions of the reservoir of pressure and temperature for a sufficient time to ensure adsorption balance. Later he concluded with other researchers that the restoration process should be done using reservoir fluids and respecting the reservoir condition (Cuiec, Longeron and Pacsirszky 1979). To simulate the reservoir conditions, Bentheim Sandstone outcrops plugs were aged at 49°C and ambient pressure. Ignoring the reservoir pressure was based on the fact that the used CO is a dead oil, and the effect of pressure on HC adsorption, in this case, is neglected. The used T was selected based on the reservoir temperature where the CO was taken from.

Table 7: 8TH Crude Oil characteristics

Number	1	
Sample ID	8TH	
density [g/cm3]	T1 [°C]	0.9339 @ 15
	T2 [°C]	0.9306 @ 20
	T3 [°C]	
viscosity [cP]	T1 [°C]	266 @ 22
	T2 [°C]	54.3 @ 49
	T3 [°C]	
IFT mN/m at --C	intial	
	Equilibrium	
API	19.88	
TAN [mg KOH/g]	1.7	
TBN [mg KOH/g]		
VOA [mg TEGO®trant A100 / g]	3.2	
VOA [mmol Surfactant / g]	0.008	
Ali. [%]	29	
Aro. [%]	19	
NSO. [%]	50	
Asph. [%]	3	
Pr/Phy [-]	na	
C27 [%]	54	
C28 [%]	30	
C29 [%]	16	
C29 [S/S+R]	0.67	
C29 [I/I+R]	0.58	
C31 [S/S+R]	0.61	
C32 [S/S+R]	0.59	
C33 [S/S+R]	0.6	
MN [-]	3	
DMN [-]	46	
TMN [-]	51	

7. The time required to restore the reservoir state is related to the COBR system. Different experiments showed different time to establish the equilibrium and get the same wettability state of the reservoir. [Wendell, Anderson, & Meyers \(1987\)](#) mentioned that 1000 hours of aging is required for the following reasons:

- Many experiments have proved that.
- This period is the required period for the stability of the value of the angle of wetting on the surface of satin and flat.

Hence to ensure the success of wettability state recovery, two conditions are necessary. They are ([Wendell, Anderson and Meyers 1987](#)):

- Achieving the maximum time requirement of 1000 hours
- Methods of wettability measuring are used where the measurements are stopped frequently, and measurements are made until the equilibrium is reached. This work needs a great effort as it constantly disturbs the samples.

We divided the plugs into four groups according to aging time. The most important three groups from the aging time point of view are 1,2, and 3. According to this division, our plugs were aged at short, medium, and extended times. Table 8 shows the aging groups.

*Table 8: Aging groups, times, and conditions*

Group	Time		P[bar]	T[C]	System ID
	[days]	[hours]			
1	34	816	Amb.	49	B5-H1-8TH-L1
	34	816	Amb.	49	B3-H1-8TH-H1
2	15	360	Amb.	49	B8-H1-8TH-H1
3	46	1104	Amb.	49	B4-H1-8TH-H1
4	84	2016	Amb.	49	B7-L1-8TH-L1

Finally, using restored plugs is combined with many disadvantages. The main disadvantages of using recovered plugs:

- High costs ([Wendell, Anderson and Meyers 1987](#))
- Losses resulting from investigating the proper cleaning method using the trial and error method, which can cause damage to the clay or other minerals compose the rock ([Wendell, Anderson and Meyers 1987](#)).
- Time-consuming to prepare enough number of plugs.
- The representation of the reservoir state is limited and depends highly on COBR system components and the aging conditions.

### 3.3 Amott SI Test

To evaluate the wettability after the restoration process, different methods are used. From those methods, the centrifuge, USBM and Amott indices, Capillary pressure curves analysis, and Residual oil saturation analysis (Hirasaki, et al. 1990). Spontaneous imbibition test is a part of Amott test, which includes four steps (Amott 1959), SI by free imbibition using Amott cell, FI using centrifuge (Amott 1959) or waterflooding (L. Cuiec 1984), SD and FD. The test depends on the fact that the wetting phase will imbibe spontaneously displacing the nonwetting phase (McPhee, Reed and Zubizarreta 2015) under the capillary force (Bartels, Rücker and Boone, et al. 2017) which may dominant in fractured reservoir as a recovery mechanism (Zhou, et al. 1995). This test is more reliable than the contact angle measurements since this test is done on real rocks sample whereas the contact angle tests are done on the single-mineral-composed surface (Shehata and Nasr-El-Din 2014) and contact angle measurement does not take in account the effect of  $S_{wi}$  (Morrow and Mason 2001) and other reservoir conditions, that affect the wettability state. However, this test provides a qualitative estimation of the wettability and wettability alteration, whereas contact angle measurement provides quantitative values (Anderson 1986b). Moreover, Amott test and even USBM cannot provide a reasonable estimation of the wettability state in some ranges when there is no oil recovery (Ma, et al. 1999). The rate of SI is the most direct indicator of the wettability state of the rock (Morrow and Buckley 2011) and cheaper than flooding tests (Wickramathilaka, Morrow and Howard 2010). The criteria of determining the end of each SI test is reaching the zero-capillary condition, which is a function of different parameters, for example (Shehata and Nasr-El-Din 2014),

- The size of the plug.
- The quality of the media ( $\phi$ ,  $k$ ). Amott (1959) noticed that imbibition rates in sandstone plugs depend on  $K$ .
- Wettability state: Skrettingland, Torleif Holt, & Skjevrak (2011) stated that the wettability plays an essential role in determining the efficiency of LSWI
- Liquids properties.

- Pore geometry: [Amott \(1959\)](#) considered it as a real problem in vugular limestone but not in sandstone and sandstone-type limestone.

### 3.3.1 THE EXPERIMENT SETUP

The experiment is done using Amott cells, Figure 15. Amott cell is a glass cell with a graduated tube at the top (1) to measure the produced oil volume and reservoir at the bottom (2), where the plug and core holder are placed. After taking the plug from the aging vessel, it was warped with a fully saturated tissue to avoid any extra attached oil to the outer surface and to avoid oil soaking into a clean tissue. Any direct contact with the glass of the cell was avoided. This process was followed for all the experiments. Furthermore, air/brine/rock contact angle was measured for two of the plugs show more affinity of the rock to be covered by water in case of B8-8TH-H1 than in case of B7-8TH-L1 system, Figure 16. This observation was translated to less oil produced in case of higher air/brine/rock contact angle.

Figure 15: Amott cell

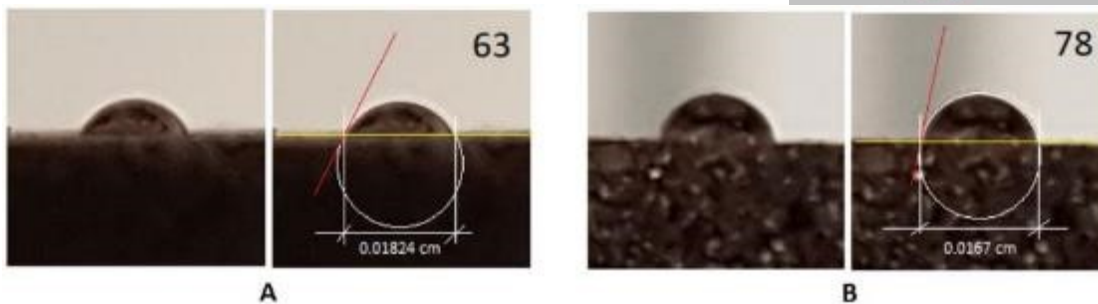


Figure 16: Air/brine/rock system contact angle of (A) B8-8TH-H1 and (B) B7-8TH-L1 systems

### 3.3.2 BOUNDARY AND INITIAL CONDITIONS

The plugs were cooled gradually to room temperature and were waited until it equilibrated with the environment. By the cooling step, the error due to the shrinkage of the fluids and the grains, and hence the bulk volume, was avoided. However, the recovery by gas diffusion is neglected due to the experiment is conducted with dead oil; therefore no gases are liberated or flow in the system ([Karimaie, et al. 2006](#)). However, the gravity forces were neglected in the analytical solutions, but they showed effect experimentally in our experiment and even in ([Karimaie, et al. 2006](#))'s experiments on carbonate plugs. The plug was immersed in the imbibed water to

allow it imbibe from all the sides. In this case, the imbibition cannot be considered as linear (Ma, et al. 1999).

To avoid any error of the produced oil volume, the cells were mounted and stabilized in a place where no-touch, move or shaking were possible. However, this was not effective since in some cases the plugs were moved little bit that caused a sudden increase in production depicted in the  $V_o$  vs.  $t$  curves. On the other hand, the experiments were done in a place where great changes in the temperature were avoided, Figure 17.

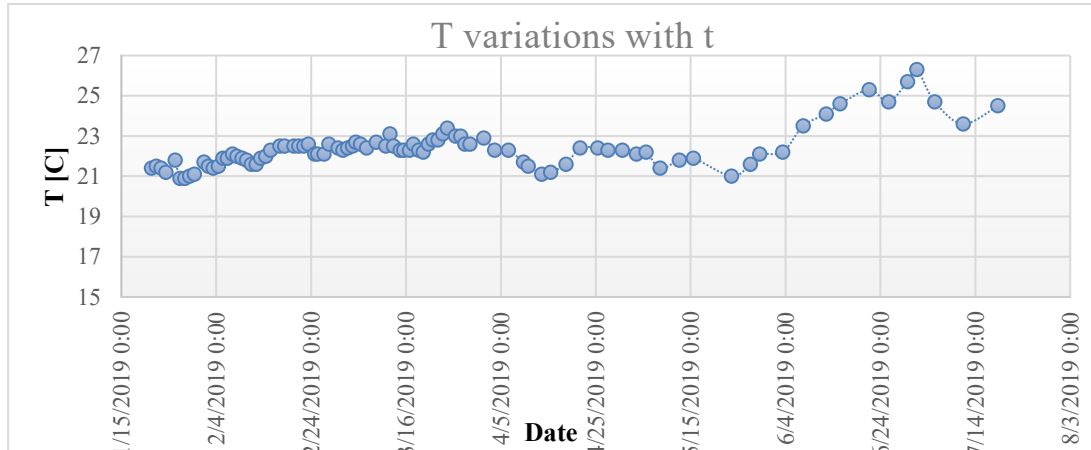


Figure 17: Temperature variation during the experiment period

### 3.3.3 TESTS SETUP

In this part, the results obtained from the experiments are presented. The result will be separated according to the code of the experiment, which is written as the following:

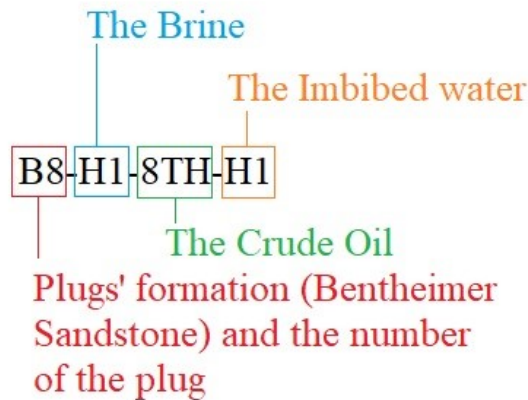


Table 9: A summary of the different tests set up

<b>System</b>	<b>Brine</b>	<b>Crude Oil</b>	<b>Aging time[days]</b>	<b>Aging conditions</b>	<b>Imbibing water</b>	<b>Aim of the test</b>
<b>B8-H1-8TH-H1</b>	H1	8TH	15	T=49°C P= ambient	H1	Determining the optimum aging time
<b>B3-H1-8TH-H1</b>	H1	8TH	34	T=49°C P= ambient	H1	Determining the optimum aging time
<b>B4-H1-8TH-H1</b>	H1	8TH	46	T=49°C P= ambient	H1	Determining the optimum aging time
<b>B5-H1-8TH-L1</b>	H1	8TH	34	T=49°C P= ambient	L1	Comparing the role of the low salinity imbibed water in enhancing the RF compared with the high salinity imbibed water
<b>B7-L1-8TH-L1</b>	L1	8TH	84	T=49°C P= ambient	L1	studying the role of the brine's salinity in altering the wettability state

# Chapter 4

## Results and Discussion

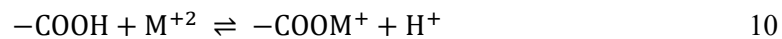
### 4.1 Restoration Process

Wettability alteration from the SWW state (clean plugs) to the NW, MW, or OW state (restored state) is the result of the oil components interactions with the pore surfaces. The restoration process includes many processes and interactions, such as direct bonding or electrostatic interactions. Oil components adsorption on the rock surface is a complex subject since it depends on many factors. The understanding of the adsorption mechanism is from the impotence to understand the possible mechanism behind the LSW effect on the pore and sub-pore scale. Pore surface in Bentheim sandstone is covered mainly by hematite, which exhibits a positive charge in environments with pH less than  $8.68 \pm 0.12$  (Zero-point of charge) (Smith and Salman 1966). On the other hand, quartz exhibits a negative surface charge in the environments with a pH more than 2. In this range of pH between 2-8.68, the interaction between the interfaces is more complex than the case of sandstone covered with clay minerals since rock surfaces exhibit two different charges. Even though quartz is believed to not contribute to the adsorption. On the other interface, CO is composed of differently-charged components. The overall charge of the CO/B surface plays an important role in the wettability alteration, but the differently charged components can accumulate on this interface too. In this manner, the alteration process could be understood with positively and negatively mixed areas regardless of the total net interfaces charges. This conclusion highlights the importance of the presence of the polar CO components regardless of their charge and regardless of the total net TAN or TBN.

The used CO in the experiment contains asphaltene that can be adsorbed on the surface of the hematite. On the other hand, asphaltene may interact with hematite according to the double-layer theory where the electrostatic interaction between the two CO/R and B/R interfaces causes

the precipitation of the asphaltene on the rock surfaces causing the wettability alteration. The direct interaction between the polar organic components (such as NOS components) and the rock sites depends on the thickness of the layer at the CO/B interface. In the case of the diffuse layer is thicker than the thin water film, the interaction is possible. Otherwise, the possibility is expected just for the highly dissolved organic components in water. The polar components' content is high in the used CO. On the other hand, the solubility of these heavy components depends on the temperature where the increase in the temperature causes an increase in the heavy components' solubility. Increase the solubility makes direct interaction possible. However, the salinity plays a reverse role, since the increase of the divalent cations in the brine film are attracted to the negatively charged sites of both CO and R. Cation bridges, in this case, bond the negatively charged sites of the quartz and the negative groups in the CO. However, the monovalent cations play the screening role on both of the two interfaces (CO/B and B/R). On the other hand, the ion present in the brine is Cl. It plays the screening role of the positively charged sites on both of the interfaces.

According to surface complexation model, the reactions at the CO/B interface are (Brady and Krumhansl 2012) equations 8, 9, and 10:



Based on the complexation models and the oil properties, the ligand exchange, water bridges, hydrogen bonding, protonation, Van der Waals attraction, and the hydrophobic effects are possible mechanisms of organic components adsorption on the lattice of hematite.

From analyzing COBR system components and their interactions, the contact angle related to the plugs saturated with L1 as a brine should show less contact angle than those which were saturated with H1 for many reasons. First,  $\text{pH}^{\text{L1}} > \text{pH}^{\text{H1}}$ . Second L1 salinity is less than H1 in great magnitude, especially the monovalent cations, which assumes the reduction of contact angle with L1 and thicker, more stable TWF and exhibiting more WW characteristics than plugs saturated with H1. On the other hand, the great difference in the salinity, especially the divalent cations, assumes that, in the presence of the oleic phase, IFT will be lower in case of L1 than it is in case of H1. Moreover, the result exhibits the importance of aging time to obtain OW characteristics, and they indicate higher contact angle related to the plugs aged for longer time. However, the effect of salinity appears to be more important in altering wettability state. However, the role of hematite in determining the contact angle is seen from two angles. The first is the roughness of the hematite films, which is a possible reason for the contact angle

hysteresis, whereas the second is the surface charge that affects the contact angle value deeply. In either case, these statements need to be proved through further works.

The chemical reactions, that are expected to happen in the system due to the LSW SI, are neglected since the chemical composition of the brine and the imbibed water are the same. The ions in these two water types are  $\text{Ca}^{+2}$ ,  $\text{Na}^{+}$ , and  $\text{Cl}^{-}$ , and hence no aqueous phase reactions and oleic acid species reactions are expected. On the other hand, the dissolution reaction could happen at the saturation stage due to the weak acidic environment. Because the aqueous chemical reactions are quick, they are not expected during the SI experiments. Moreover, MIE could happen in the case of the direct interaction between Fe and polar organic matter. In this case  $\text{Ca}^{+2}$  and/or  $\text{Na}^{+}$  ions could replace the metal-organic complex according to the selectivity coefficient.

Figure 18 shows the production curves of all the systems.

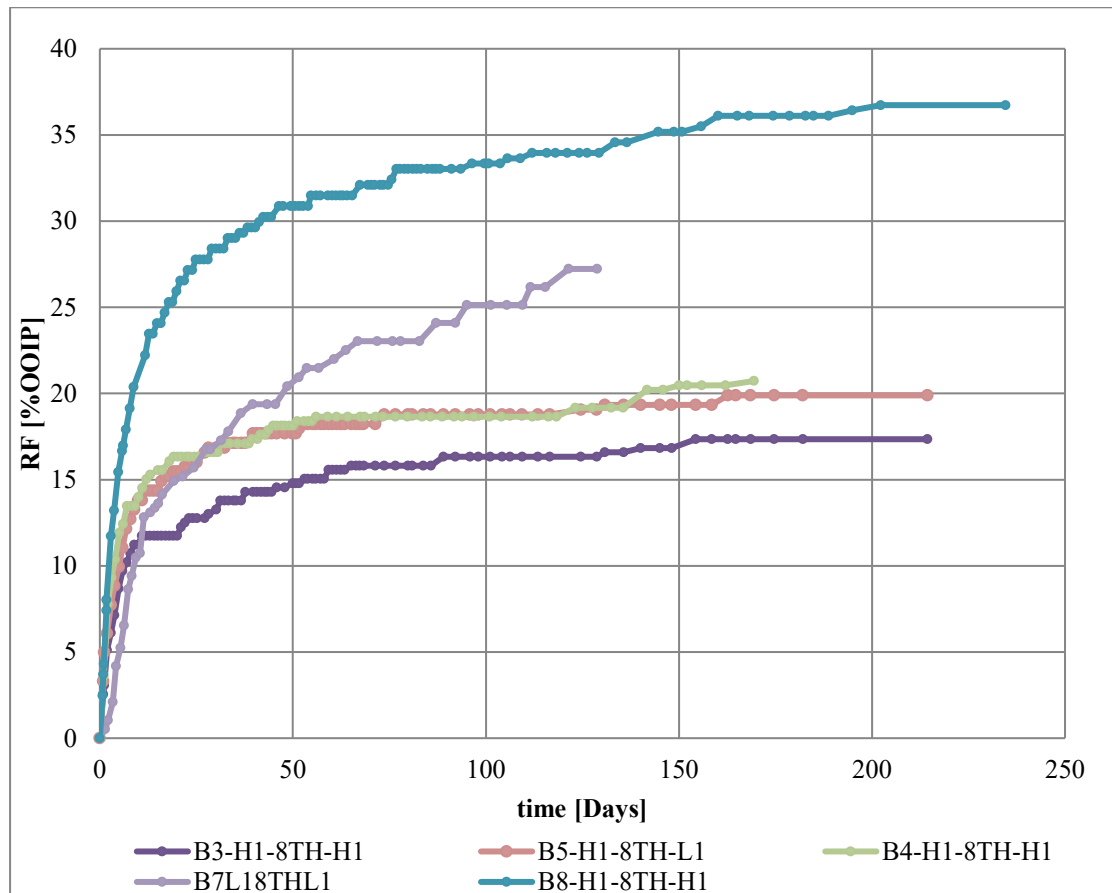


Figure 18: Produced oil during the experiment for all of the systems

## 4.2 Aging time effect

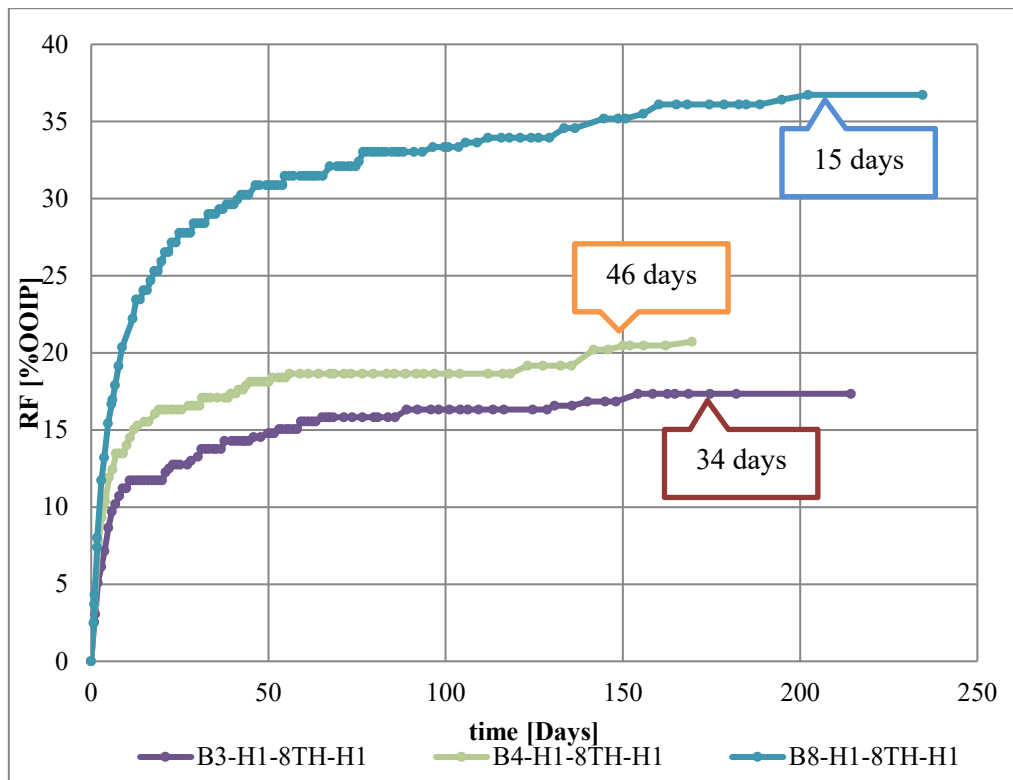


Figure 19: RF of three plugs with different aging time with respect of other parameters

Analyzing the relationship between the cumulative oil production with time, the data reveals that the aging time has an effect on altering the wettability state of the plugs from the SWW state (clean state) to MW state. Systems B8-H1-8TH-H1, B3-H1-8TH-H1 and B4-H1-8TH-H1 were designed to find the optimum time at which the equilibrium is reached. Figure 19 shows that the system B8-H1-8TH-H1 is more WW than B4-H1-8TH-H1 since B4-H1-8TH-H1 was aged for a longer time. However, system B3-H1-8TH-H1 was aged for 34 days but showed less production rate which indicates less WW even than the longest aged system (B4-H1-8TH-H1) but little bit longer SI time. The difference in the extension comes from the co-current flow regime. The co-current flow regime in B3-H1-8TH-H1 needed longer time to be initiated and the mixed regime was absent. However, the counter-current regime was shorter. The previous statement refers to stronger capillary forces in the case of B3-H1-8TH-H1 than it is in case of B4-H1-8TH-H1. However, there is another difference between the two systems besides the aging time. The difference is the preparation method. Systems B8-H1-8TH-H1 and B4-H1-8TH-H1 were oil-saturated with porous disk, whereas the system B3-H1-8TH-H1 was oil-saturated without porous disk but for very long time of oil saturation step. This preparation difference caused difference in the initial water saturation. The initial water saturation difference may be one of the reasons behind the unexpected behavior. As it was reviewed in

chapter 3.2.5, increasing  $S_{wi}$  causes increase in water wetness. Regardless the aging time, the increase of  $S_{wi}$  is coupled with increase the water wetness.

Table 10: A comparison between three systems with different aging times with respect of the other parameters

System	B8-H1-8TH-H1	B3-H1-8TH-H1	B4-H1-8TH-H1
Aging time [days]	14	34	46
$S_{wi}$ [%]	37.17	29.58	30.69
Sw @ Pc=0 [%]	63.15	45.03	51.56
Delta Sw [%]	25.99	15.45	20.83
RF @ Pc=0 [% OOIP]	36.73	21.94	30.05
PD	Yes	No	Yes

Wettability affects the RF by SI remarkably. (Karimaie, et al. 2006) noticed the increase of RF with the increase in the water wetness properties.

The previous systems showed wettability alteration toward less WW state. The mineral composition of Bentheim Sandstone plugs does not show any clay presence. The distinctive change in RF between the three cases studied gives a great indication of the role of hematite in change the wettability state. Table 10 shows that the system B8-H1-8TH-H1 shows WW state. However, the other two systems show WOW state.

### 4.3 Low salinity effect

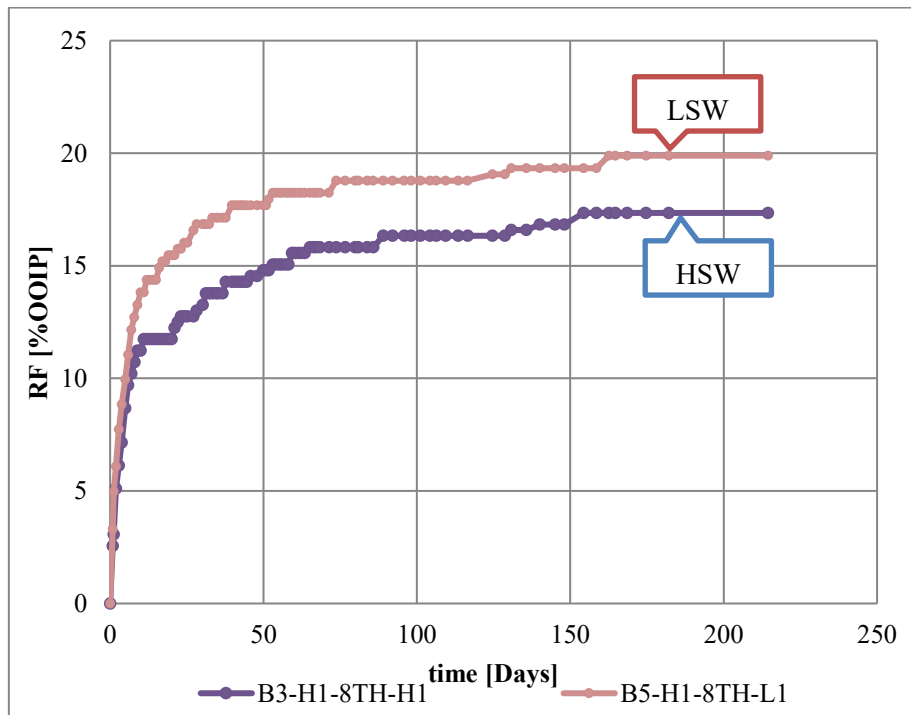


Figure 20: Recovery factor for high salinity SI case and Low salinity SI case.

Comparing the behavior of the systems B3-H1-8TH-H1 and B5-H1-8TH-L1 infers that production showed an increase of the RF ( $\Delta RF = 2.54\% \text{OOIP}$ ) with low salinity imbibed water as an IOR agent.

The increment can be explained by the neither clay flocculation nor the fine migration since the mineralogical analysis indicates that the plugs are clay-free. Moreover, the pressure drop through the plug is composed of just  $P_c$ . thus, these two mechanisms are not expected to show effects on plug-scale. Furthermore, they cannot explain the chemical and physical observations that happen during LSWI.

The RF increment could be attributed to the wettability alteration process toward more WW. The imbibed water in the system B5-H1-8TH-L1 is expected to **increase the thickness of the TWF** and hence decrease the electrostatic attraction and Van der Waals forces between the O/B and CO/R interfaces. Moreover, as the Stern layer expands, the immobile water saturation is increased, and the water pass-way around the oil droplet decreases; that exerts a dragging force on the outer face of the oil droplet. However, this process takes place in case of waterflooding.

On the other hand, the salting-in mechanism is a possibility, but the decrease in the salinity causes increasing the solubility of the dissolved organic matter (DOM). In the IOR process, the bulk DOM comes from the oil bulk since the concentration of the dissolvable organic matter is higher from this on the B/R interface. In this case, the wettability of the plugs aged with L1 brine is expected to show wettability alteration toward OW by direct adsorption and MIE more than those that were aged with H1. In the EOR process, the DOM comes from the oil film or/and from the trapped oil in the large pores. The first case indicates an alteration of the wettability state to more WW. However, the second case is linked to viscoelastic behavior. The increase of the DOM solubility will lead to reduce the non-asphaltic components that soften the B/O interface and hence increase the content of the asphaltic component that increases the viscoelastic behavior effect. Even if the salting-in process does not contribute to the RF increment remarkably, it affects the other interactions.

However, MIE is expected to happen in case of the direct interaction between the polar components and the ions that are adsorbed on the rock surface forming a metallic-organic complex. The increase of pH supports this mechanism, but the increase of pH is marginal (1 magnitude), indicating that this reaction is not very active in this system.

The other possibility is mineral dissolution. Although the dissolution of Bentheim sandstone shows dependency on pH and salinity (Peksa, Wolf and Zitha 2015). In the range of pH and salinities that are used in the experiments, the dissolution rate is negligible and the effect of the injected  $\text{CO}_2$  in the preparation stage makes it less likely to contribute to the RF increment.

The formation of micro-dispersions is possible in case of a continuous film of oil separating two aqueous phases with different salinities. This condition is suitable in case of oil-wet state or MW state with some pores completely OW, or in the case of full oil-saturated and strong OW dead ends. This condition is not fulfilled in the case of our experiments.

Because there is no dissolution process expected, increase pH is expected just due to the mixing process between H1 and L1, and MIE process. The pH increment is not great, nevertheless it is about 0.5 magnitude and hence the condition of forming in-situ surfactants is not fulfilled. Moreover, no emulsions formation was noticed and the CO/B interface is clear.

The wettability state obtained after the aging process appears to be suitable for LSWI. However, the SWW state is not suitable since the mixing process will be dominated and the salinity shock will smear out and the LSWI effect will minimum. on the other hand, the SOW state is not suitable since the oil plays the role of the membrane between the brine and the injected water. The effect in this case maybe appear just in case of the salting in and if the osmoticity takes place.

The presence of clay minerals, as a condition of the LSW effect, is not generally correct. The correct condition is the presence of the active-geochemical surfaces. if this condition is fulfilled the presence of the active surface components in CO is another condition that must be fulfilled. The interaction between the two active ingredients is the most important link in this series. If the two conditions are fulfilled, but there is no interaction between the active surface and the active oleic components, the wettability alteration to MW during the aging step will fail, and hence the effect will depend on other mechanisms than the wettability alteration. This conclusion can explain the outcomes of many experiments, that showed insensitivity to LSWI in spite of the presence of the two components. However, in the cases of the absence of the active-geochemically surfaces, the LSW effect is contributed to the L-L interactions and efficiency enhancement.

The interaction in some of its forms, demands the presence of the divalent cations. However, other mechanisms cause wettability alteration toward MW state that does not require the fulfillment of this condition, for example, the asphaltene adhesion by Van der Waals forces.

The absent of the salinity shock in SI experiments, due to the great diffusion process, and in the EOR stage, due to the more significant fraction of the brine volume to injected water volume ratio, maybe the explanation of the small increment of the RF of both of the two process compared to the higher RF increment in the IOR stage. On this basis the condition of the salinity shock could be arranged another way, for example the brine volume to the injected water volume in the region of the dilution or mixing. Then the parameters of this region could be obtained to study the effect of these parameters on the system. In another way, the most

important parameters are not the injected water parameters, instead the parameters of the water in the mixing region. Another explanation of the better results in the IOR stage than in the EOR stage could be the domination of the vicious dragging on the capillary forces.

Finally, the expected active mechanism is DLE. Depending on the EDL mechanism, the RF is linked to the initial wettability state by the thickness of the TWF. According to this linkage, OW surfaces have unstable, or even no, TWF, this means the opportunity to stabilize TWF and increase its thickness is more than any other initial wettability state and hence the recovered oil due to overcoming the attraction forces. In the same since NW state surfaces are less affected, and the very low effect is related to WW state. This is a simple understanding of the more complex system but a base case. In case of MW plugs, the portion of oil attracted to the pore surfaces due to attraction forces is accessible by LSW, hence it is recovered by EDL. More oil portion in homogenous OW plugs is not accessible hence, the RF in case of OW plugs depending on EDL mechanism is less. On the other hand, the increase in stable (static) TWF thickness decreases the pore space for oil and hence work likewise the fluctuated clay.

#### 4.4 Water wet state by H1 and L1, and aging time

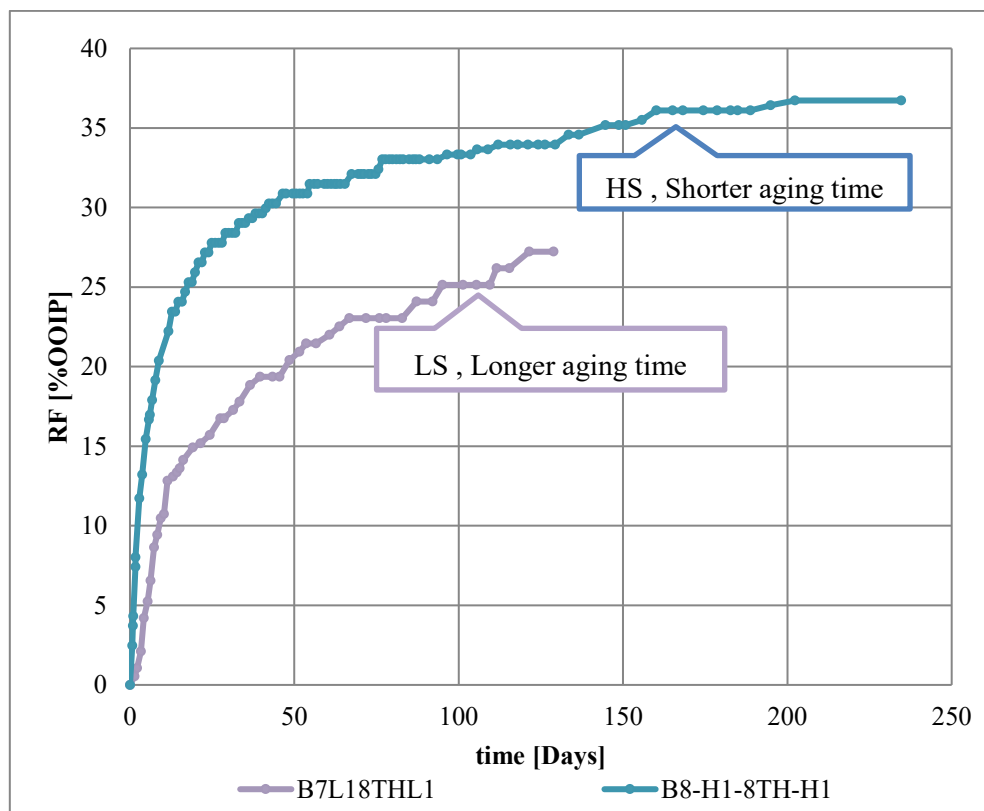


Figure 21: The compensation between brine composition and salinity and the time to determine the final wettability state

Comparing the behavior of the systems B3-H1-8TH-H1 and B7-L1-8TH-L1 infers the role of the brine composition. H1 brine composed of higher TDS and  $M^{+2}$  components, namely  $Ca^{+2}$ , than L1. The effect of the brine composition was clear in spite of the difference in the aging time. System B3-H1-8TH-H1 showed less RF than the RF of the system B7-L1-8TH-L1 and the imbibition time was longer. The increase of the RF and the behavior of the system B7-L1-8TH-L1 refers to a stronger WW state. On the other hand, the lower pH value of H1 makes the thickness of the water film less in B3-H1-8TH-H1 than it is in case of B7-L1-8TH-L1 leading to less water film stability and hence more oil components precipitation and hence more OW state. Moreover, the ions bonding interaction is less in case of B7-L1-8TH-L1 than in case B3-H1-8TH-H1 due to the less  $M^{+2}$  concentration of the brine in the first system compared to the second one. Moreover, pH of L1 in the first system is higher than the pH of H1 in the second system ( $pH^{L1} = 6.57 > pH^{H1} = 5.99$ ) leading to more negatively charged CO/B surface and hence increase the repulsion between the CO/B and B/R interfaces leading to thicker, stable water film. In the system B3-H1-8TH-H1, DLVO theory is limited, and due to the high brine salinity.

At the pH values of the brine for both cases L1 and H1, pH value is less than 7, and the hematite is expected to show a positive surface charge. Comparing the values of the pH and the salinity of both cases, hematite film is expected to show a more positive surface charge in the case of H1 than it is in the case of L1. These positive surface charges promote the transition toward more OW in case of the presence of the anions in the brine. In this case TAN plays minor role, and TBN plays the major role in the transition toward more OW.

It is also observed that the oil wetness increases with the increase of the salinity. However, more experiments need to be designed to explore the effect of the divalent and monovalent ions changes on the wettability changes in the presence of hematite film.

## 4.5 Curvature

At the early time of the experiments, no curvature of the imbibed water and oil in the graduated pipe was noticed for the system H1/8TH/glass. However, the curvature was developed at the late time in the systems: B8-H1-8TH-H1, Figure 22 On the other hand, the curvature was developed starting from the early time to the end of the experiment for the system L1/8TH/glass. The curvature is to be related to the pH changes and alkalinity. The curvature also was noticed starting from the early time in case of the system B5-H1-8TH-L1. The contact angle variation is less in magnitude in case of the system B5-H1-8TH-L1 than it is in case of the system B8-H1-8TH-H1. However, the system B3-H1-8TH-H1 does not show any changes in the curvature.

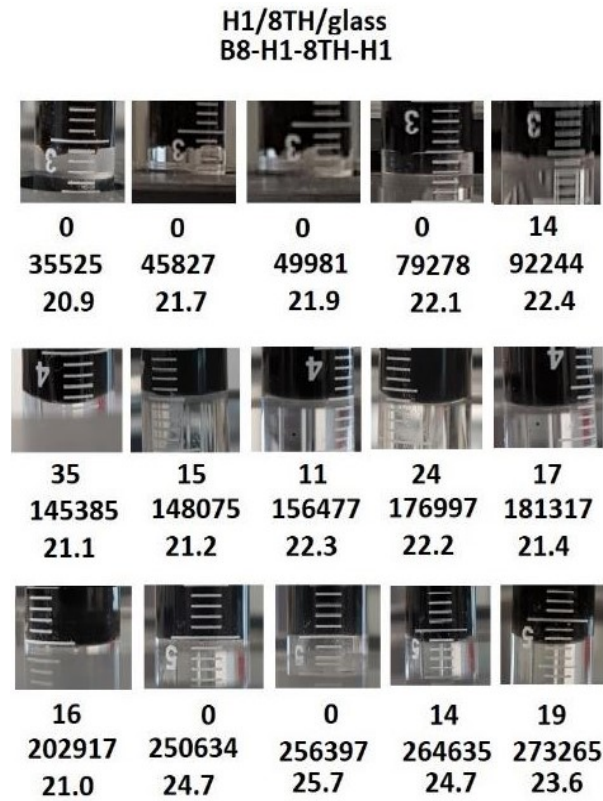


Figure 22: H1/8TH/glass contact angle changes during the experiment

Moreover, the size of the droplets, attached to the plug surface, was reducing with time, indicating the increase of the pH and decreasing IFT. Figure 23 shows the changes in the size of the droplets during the experiment.

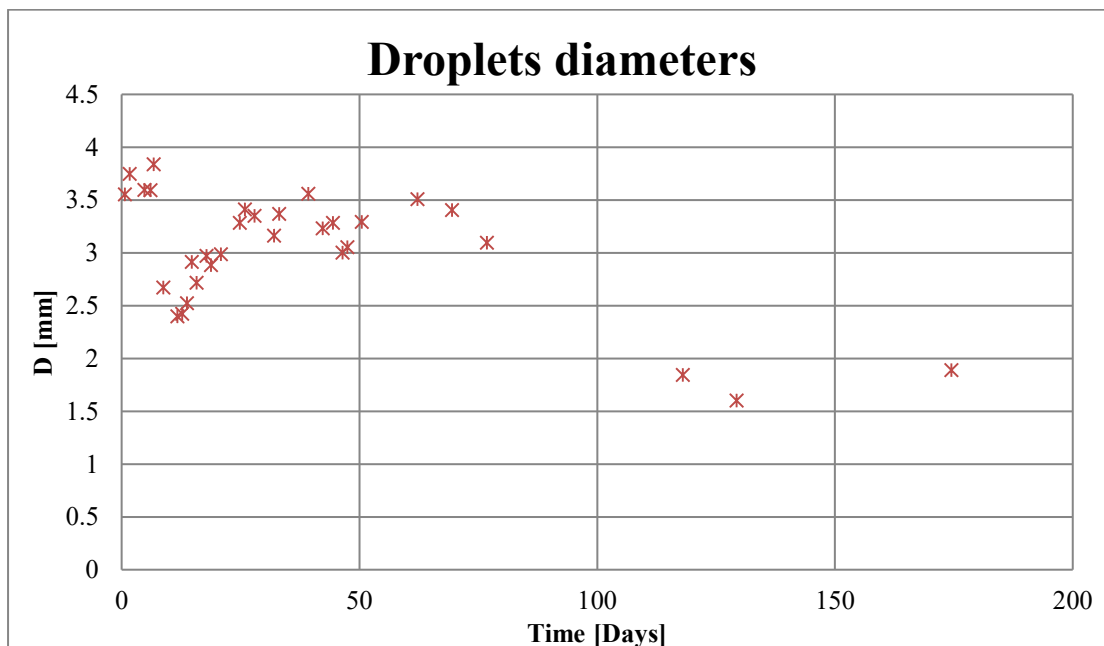


Figure 23: Droplets size changes of the system B8-H1-8TH-H1

As it is shown in Figure 18, all the systems except B7-L1-8TH-L1 have no induction time<sup>5</sup>. However, system B7-L1-8TH-L1 shows induction time. Many explanations were proposed for the induction time including the time needed to build the interface curvature at the interring point (Morrow and McCaffery 1978), low relative permeability of water at high oil saturation (Behbahani and Blunt 2005) local heterogeneities (Mason et al., 2012) or the time needed for water to create a path and the slow changes toward WW state at the entry of the pores (Morrow and Mason 2001).

## 4.6 Imbibition

Two types of flow happen during the SI of the wetting phase in the porous media, the co-current imbibition, where the wetting and the non-wetting phases are flowing in the same direction, and the counter-current imbibition, where the non-wetting phase and the imbibing phase flow in counter directions (Føyen 2016). Image analysis revealed that the density of the oil droplets on the upper surface was higher than it is on the bottom surface of the more OW plugs. However, in the case of less OW plugs, Image analysis showed that at the early time of the imbibition, all the faces of the plug were covered with oil droplets. Later with time, the downside part of the plugs maintained the same droplets, but the upper side lost the majority of the droplets. The side walls maintained the droplet after a certain time until the end of the experiment. After this time, the production continued from the upper face of the plug. Figure 24 shows the change in droplets density from the walls during time.

---

<sup>5</sup> is a period of the spontaneous imbibition process where the imbibition does not start immediately after the sample is exposed to the wetting fluid, or the initial imbibition rate is extremely low (Føyen 2016)



Figure 24: Droplets distribution on the plug's wall during the time for the system B8-H1-8TH-H1

In the case of stronger WW plugs, such B7-L1-8TH-L1, the production was initiated from all the sides of the plugs at the early time. Later the downside plugs started to be clean, and the upper side maintained its oil droplets density. The production at the later time was noticed to be from the upper face.

Table 11: Droplets relative density and size on the plugs sidewalls

		Early time	Late time	Droplets size at early time/ late time
Strong WW	Upside	production	maintained	Big / Big
	Downside	production	clean	Big / no droplets
Less OW	Upside	production	Maintained/ less dense	Middle / middle (less dense)
	Downside	production	maintained	Middle-small/small
More OW	Upside	production	maintained	Small-tiny / Small-tiny
	Downside	production	Maintained/ less dense	tiny /tiny

From Table 11, it could be inferred that the size of the droplets plays a role on the distribution of the droplets vertically. The strong WW plugs showed big droplets. In this case the gravitational force is bigger than the adhesion forces, the droplets will release, and the rock surface becomes clean. On the other hand, the less OW plugs showed middle size droplets on

the top and middle to small size droplets at the bottom. The weak adhesion forces cannot maintain the middle size droplets. Thus, at the late time the walls showed less dense middle size droplets. On the other hand, the adhesion force, in the more OW plugs, is stronger, and hence it maintained the density of the droplets.

The oil was produced from the whole height of the plugs at the early time of the experiment. This observation supports the claim that the imbibition in situ at the early time is counter-current imbibition (Mason and Morrow, 2013). At the late time of the experiment, it was produced only from the upper part of the plug and the lower part starts to be clean in the plugs with low salinity imbibing water (System B7-L1-8TH-L1), or maintained the same oil droplets density in the plugs with high salinity imbibing water, Figure 25 (System B4-H1-8TH-H1). The change in both cases was propagating from the bottom to the top with time. The change is believed to represent the gravity-aided co-current imbibition waterfront. However, the increase of the oil droplets density on the upper surface promotes the co-current imbibition upward since the back pressure at this surface will decrease with the increase of oil droplets density. Moreover, the viscous drag of the wetting phase increases and the viscous drag of the non-wetting phase decreases with the front advance. The advance of the front is also associated with increase in the wetting phase pressure and decrease in the non-wetting phase pressure; the decrease will last until the non-wetting phase pressure becomes less than the bubble pressure at the wetted face and starting from this time the imbibition is pure co-counter imbibition (Føyen 2016). Fernø, et al. (2013) imaged the SI front propagation starting from a point in a wetting face in a cylindrical plug. He noticed that the imbibed water formed a hemisphere surface until it reached the cylindrical walls of the plug to propagate in the shape of piston-like front. However, the dominant factor, in this case, is the heterogeneity. In cases where the small pore throats are concentrated on one side of the plug, it is expected the imbibition front to be faster in this part and advances the front in the part where the larger pore throats concentrate.

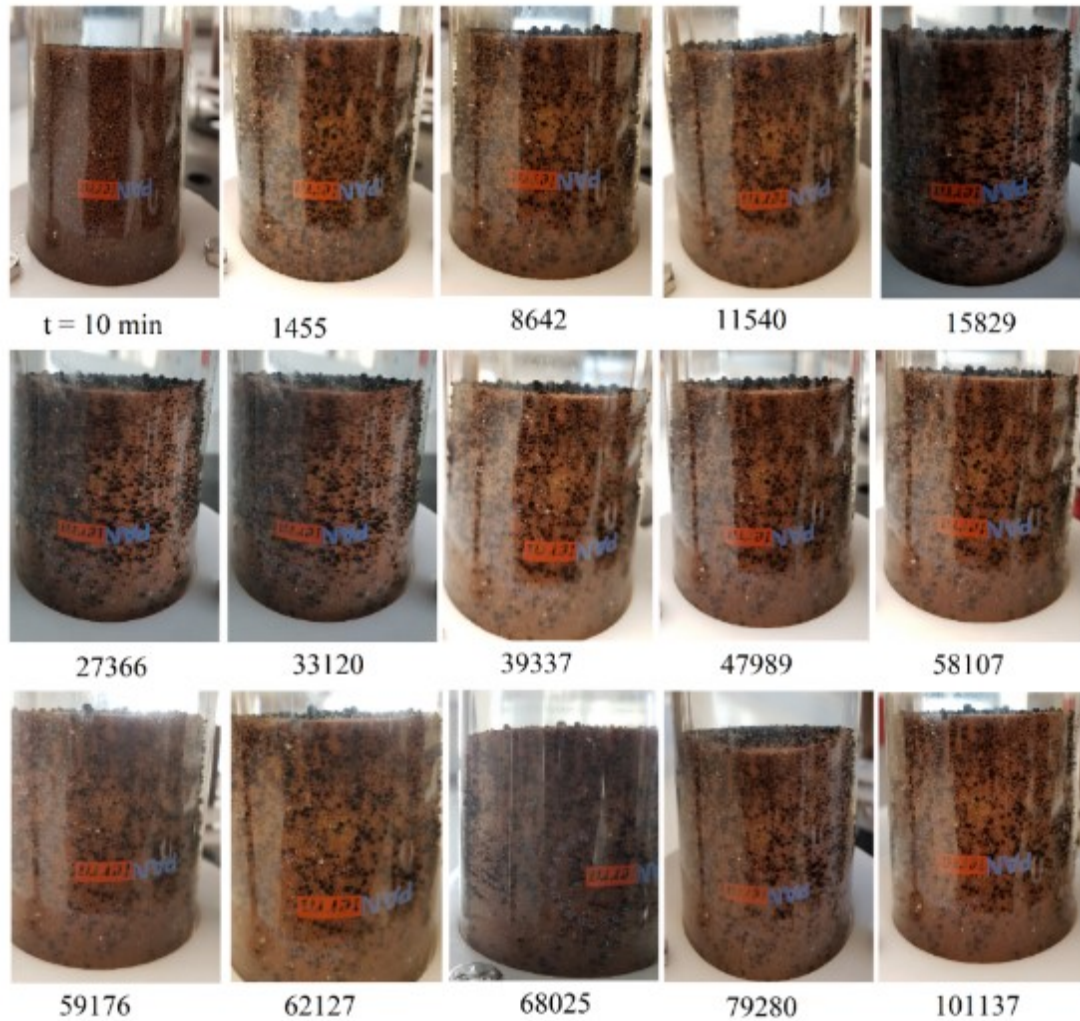


Figure 25: Droplets distribution at the surface of the system B4-H1-8TH-H1

Changes in droplets sizes with time is a method to estimate the wettability, IFT, and surface properties changes of the plug during the time. The images analysis shows a reduction of droplets size with time. The  $P_c$  reduces with increasing water saturation, which is a function of time. Hence  $P_c$  reduces with time. However, the reduction of the droplets' sizes and the reduction of  $P_c$  indicates that the product of IFT and  $\cos(\theta)$  is decreasing with time. The two parts of the product are related to the wettability state and L-L interaction. However, the IFT should decrease to compensate the effect of decrease the droplets sizes. The reduction of IFT indicates the increase of pH to higher values that cause the alteration toward more WW and hence increase  $\theta$  and finally decrease  $\cos(\theta)$ .

In general, both of the two flow types, at the early time, are working together to show higher production rate. However, at the late time, the co-current is the dominant type. Figure 26 shows a schematic water saturation profile at different times. By analyzing the production curve, it can be inferred that in cases of WW state, the curve can be divided into three parts. The first

one is the counter-current -dominated part. In this part the cumulative oil is produced in larger volumes. The second part is a mixed co- and counter-current dominated regime. The third part is the co-current -dominated part. In case of less water-wet state, the second part diminishes and the other two parts dominants. Figure 27 shows the two cases for the systems B8-H1-8TH-H1 (WW) and B3-H1-8TH-H1 (less WW). The slop of the curve is related to the area of the open faces of the plug. When the counter-current regime stops, the area of the flow is reduced, and the equilibrium between the capillary forces and the drainage forces seals the walls and makes boundary condition at this stage like open face to brine, sealed walls, and opened face to oil. In this case the area exposed to brine is very small comparing to the area of the total plug at the beginning of the SI.

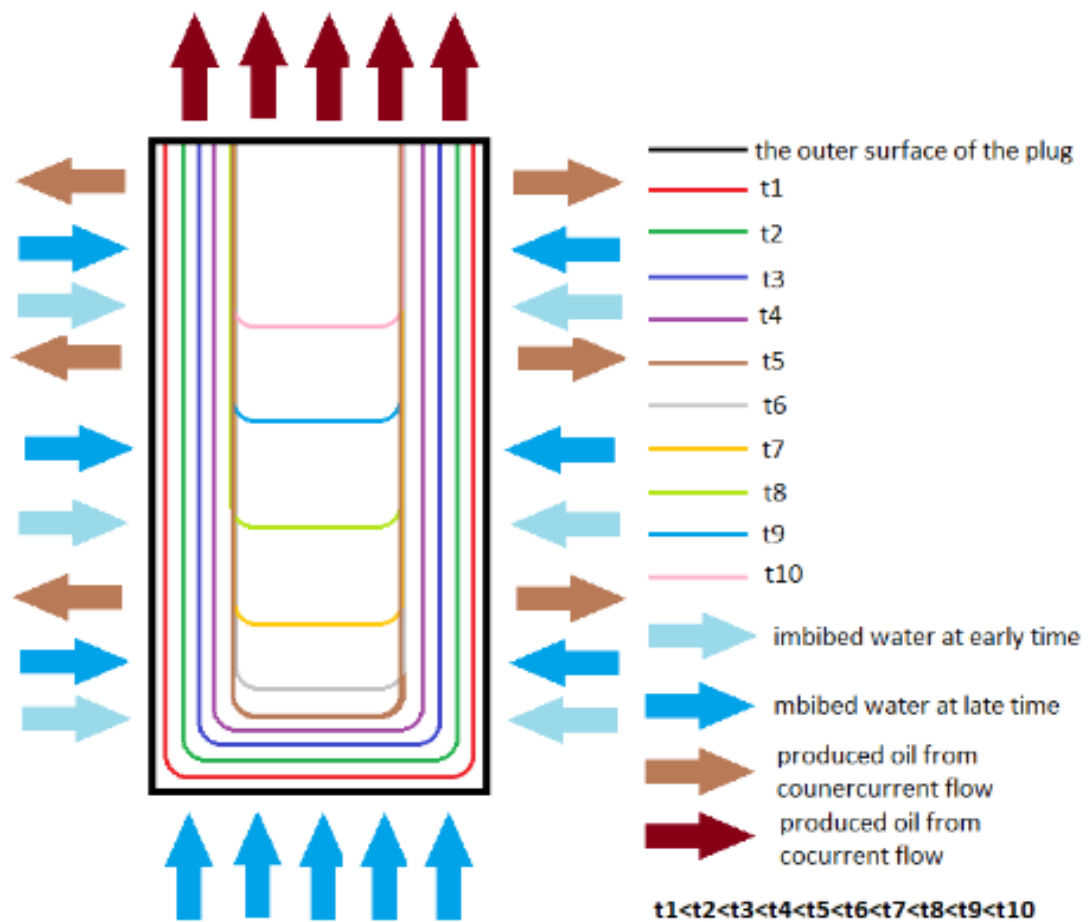


Figure 26: Schematic water profile during the SI experiment

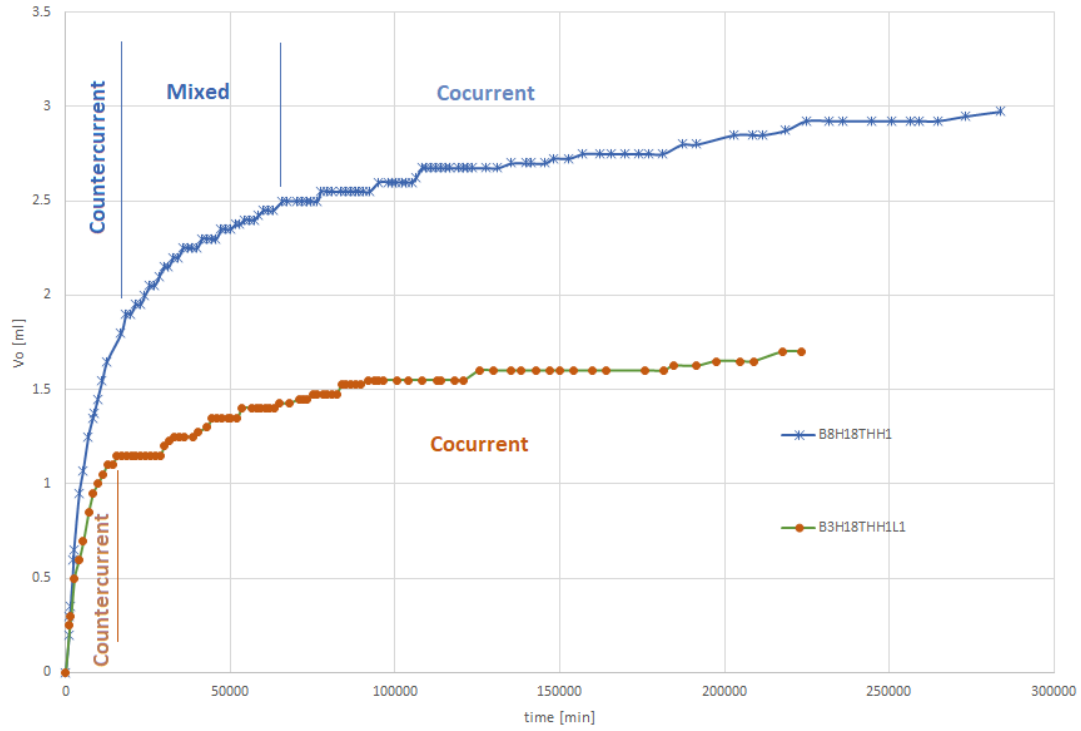


Figure 27: Flow regime dominance during the experiment

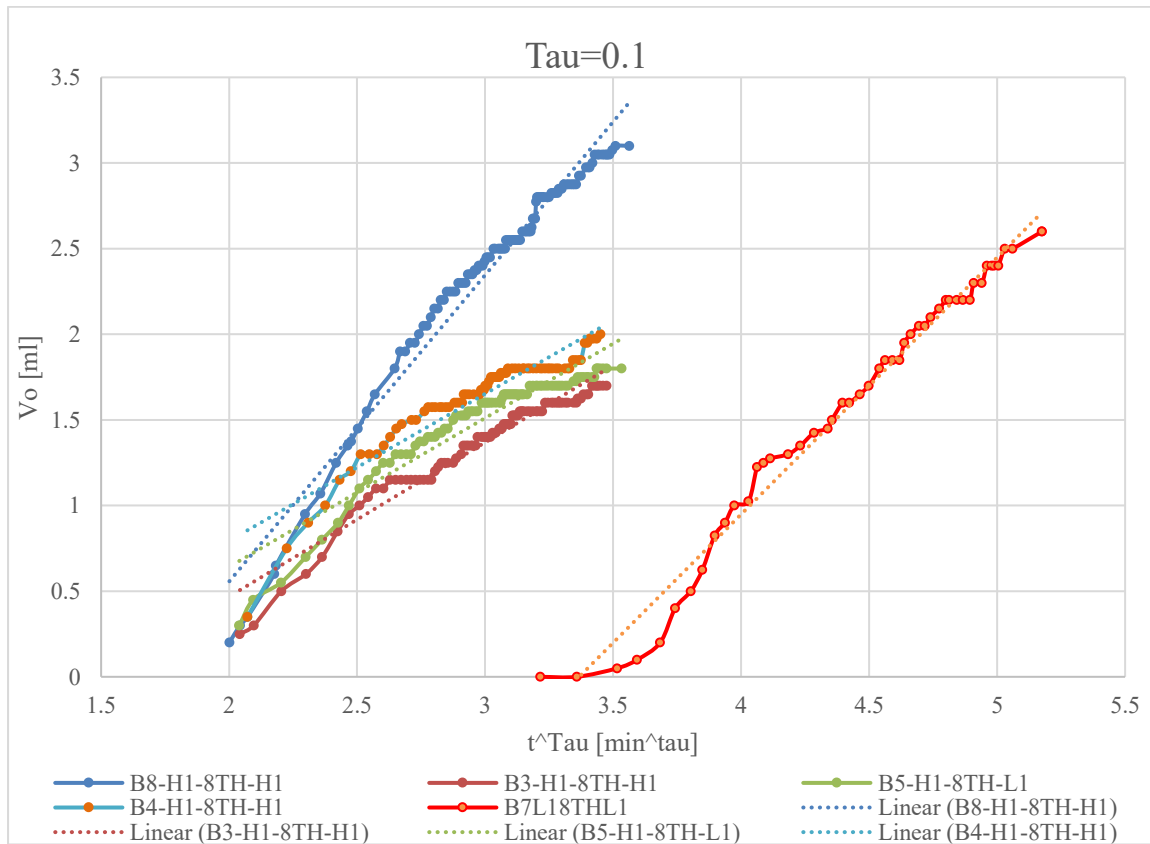


Figure 28: The relationship between the produced oil and the time to the power  $v$

The proposed model, equation 11, is a generalization of the traditional model which is inversely proportional to the square root of the time. It stimulates the oil produced with a good match and better than the traditional model. Figure 29 shows the history match of the system B3-H1-8TH-H1.

$$V_o = \tau t^u \tag{11}$$

And in this case, the oil production rate is calculated by the equation 12:

$$q_o = \tau u t^{u-1} = \beta t^\alpha \tag{12}$$

Where:

$V_o$ : produced oil [m3]

$q_o$ : oil production rate [m3/s]

$t$ : time [s]. Time is recorded during the SI experiment at each reading point.

$\beta$ : imbibition rate [m3/s<sup>alpha</sup>], where  $\beta > 0$

$\alpha$ : imbibition exponent, where  $-1 > \alpha > 0$

$\tau$ : cumulative production rate, where  $\tau > 0$ , and it represents the slope of the measured  $V_o$  vis  $t^u$  curve.

$u$ : cumulative production exponent, where  $0 > u > 1$ .

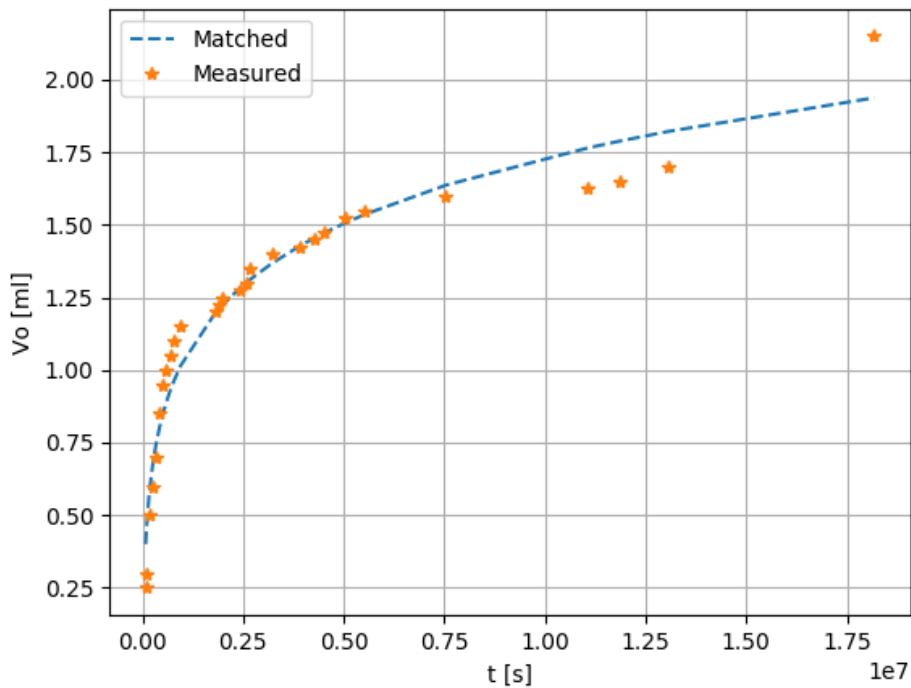


Figure 29: History matching of the produced oil of the system B3-H1-8TH-H1

Analyzing equation 11 reveals that  $\nu = 0.1$  is valid for all the plugs, which indicate that the exponent is related to the rock static characteristics and it is insensitive to L-L or L-S interactions.  $\nu = 0.1$  shows a linear relationship between  $V_o$  and  $t^\nu$ . More restrict linear relationship appears to be between the oil volume produced and the logarithm of the time. However different values of the slop  $\tau$  are obtained. This value is related directly to the wettability state. The more the water-wet state, the higher the value of  $\tau$ .

The imbibition rate is linearly related to the cosine of the static advancing contact angle (Kim and Whitesides 1996), in other words, on the wetting state of the system. On the other hand, the imbibition constant is a function of rock and fluids properties, for example, the wetting state, viscosities, and relative and absolute permeabilities (Schmid, et al. 2016). And it is related to  $D_c$ . The amount of the water imbibed in the sample is a function of the micropores in the plug (Maloney, Honarpour and Brinkmeyer 1990). Jadhunandan and Morrow (1995) found in their HSWF that the maximum recovery was obtained in NW state plugs, with the NW state in the waterside, they contributed this behavior to the minimizing of the capillary forces. However, they stated that the effect of the wettability and the interface stability determine the oil displacement efficiency.

$D_c$  is a strong function of the water saturation and hence a strong function of the oil saturation. At a specific time, global oil saturation is known. Based on calculating the normalized oil saturation,  $D_c$  at this time is calculated. The calculation is based on equation 13, (Chevalier, et al. 2018)

$$S_o^* = C_{ps} C_{cyl} \quad 13$$

Where:

$S_o^*$ : the normalized oil saturation [-]

It is calculated for each oil saturation measurement by equation 14:

$$S_o^* = \frac{S_o - S_{or}}{S_{oi} - S_{or}} \quad 14$$

Where:

$S_o$ : oil saturation [-] (measured)

$S_{oi}$ : initial oil saturation [-] (measured)

$S_{or}$ : residual oil saturation [-] (measured)

$C_{ps}$ : The concentration of the plane sheet solution [-]

It is given by equation 15:

$$C_{ps} = \sum_{n=0}^{\infty} \frac{8}{((2n+1)\pi)^2} \exp\left(-D_c((2n+1)\pi)^2 \frac{t}{(2l)^2}\right) \quad 15$$

Where:

n: The number of the reading.

$D_c$ : Capillary diffusion coefficient [ $m^2/s$ ]

t: Time [s], (is recorded for each reading point during the SI experiment)

2l: The length of the plug [m]

$C_{cyl}$ : The concentration of the cylinder solution [-]

It is calculated for each point applying equation 16:

$$C_{cyl} = \sum_{n=1}^{\infty} \left(\frac{2}{rx_n}\right)^2 \exp(-D_c x_n^2 t) \quad 16$$

Where:

r: The radius of the plug [m]

$x_n$ : The positive root of the first type Bessel function of order zero ( $J_0(rx_n) = 0$ )

The capillary diffusion coefficient is calculated using a code, that was written in Python and presented with its explanation in appendix A. Figure 30 presents the capillary diffusion coefficient curve as a function of the water saturation of the system B8-H1-8TH-H1. The capillary diffusion coefficient shows the bell shape. Comparing the capillary diffusion coefficient curves of different systems shows that B5-H1-8TH-L1 has  $D_c$  values higher than the two other systems, B3-H1-8TH-H1, and B8-H1-8TH-H1. Figure 31 shows that increase  $D_c$  is related to decrease the salinity of imbibed water. More investigations need to be done to determine the dominant factor whether it is TDS or the composition of the imbibed water. Moreover, the brine is the same in the three cases, and it needs to be investigated in more details.

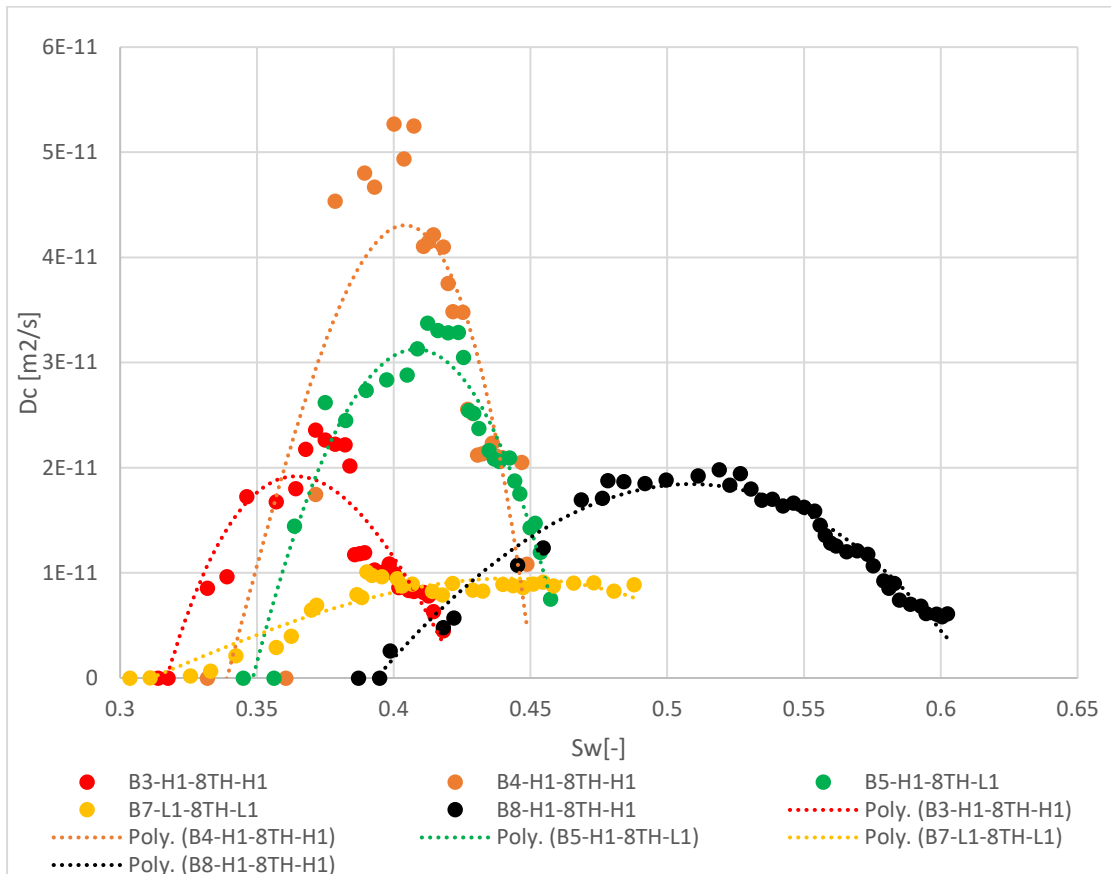


Figure 30: The relationship between Diffusion Capillary Coefficient and the water saturation

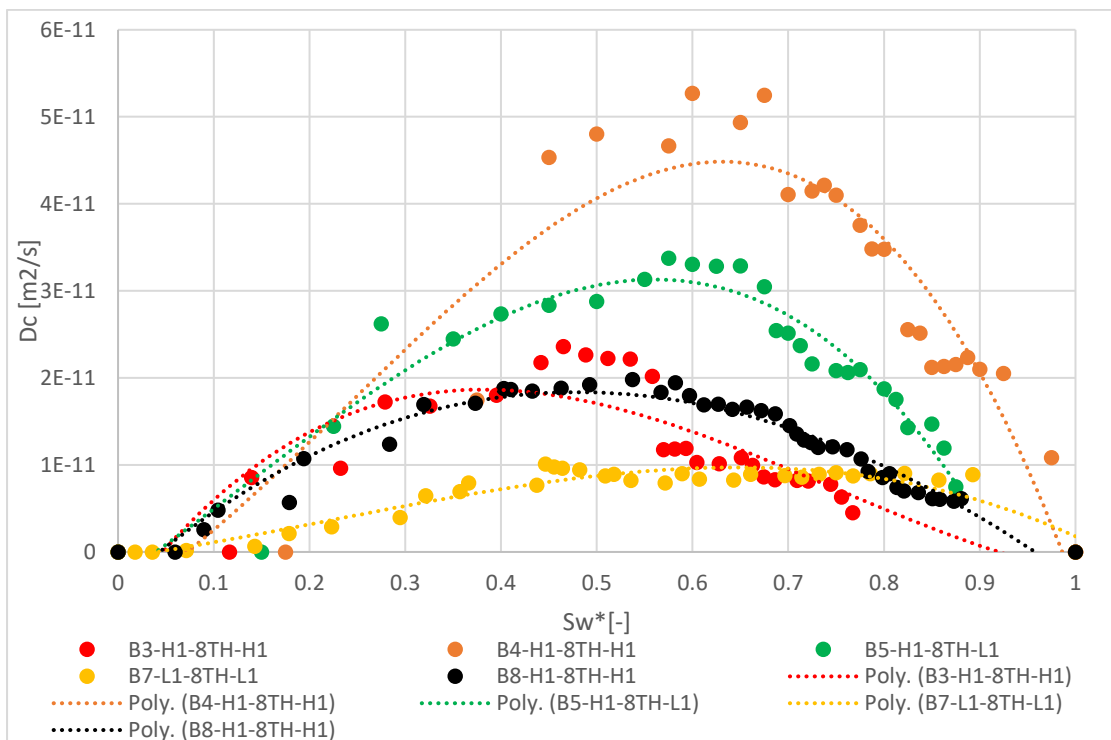


Figure 31: The relationship between Diffusion Capillary Coefficient and the normalized water saturation

It is noticeable that the affected saturation range in the systems B3-H1-8TH-H1 and B5-H1-8TH-L1 is the same (=10%) whereas it is wider (twice) for the system B8-H1-8TH-H1(=20%). However, the value of  $D_c$  in the case of the LSW SI was higher that caused the increase of the recovered oil compared to the HSW SI nevertheless that the water saturation range affected is the same. This indicates the effect of the capillary forces that act on the third system are weaker but affected on a broader range of water saturation. Increase  $D_c$  makes the system reach the equilibrium state faster. This is the reason behind the short SI time in case of LSW SI case but the longer time of HSW SI with shorter aging time case.

The application of dimensionless time could be the estimation of the contact angle in-situ. Comparing the cumulative oil production curve as a function of one of the dimensionless times (for example  $t_D^{MMZ}$ ), considering the formula gives good results of the studied systems, the relationship between the contact angle for each system could be calculated based on a value of the contact angle of the base case (a reference case). Figure 32 shows the match of the curves of the different systems based on the relative values of the product  $\sigma \cos(\theta)$ , that are presented in Table 12.

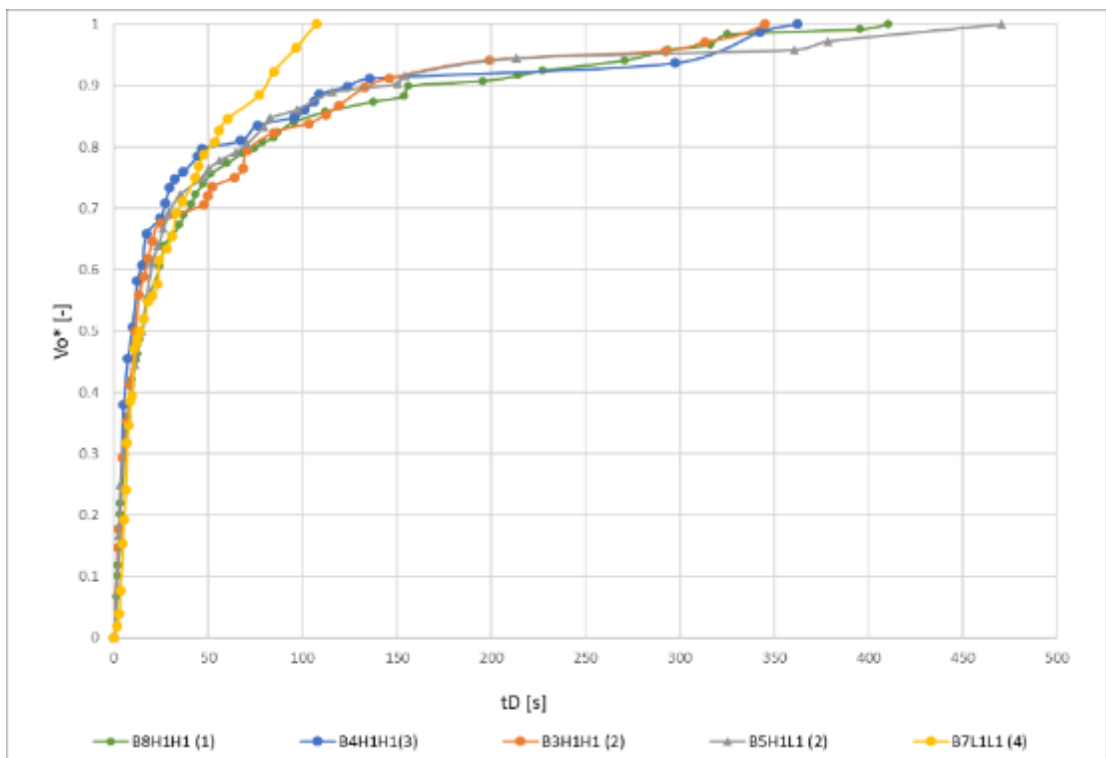


Figure 32: Normalized  $V_o$  as a function of  $tD$

Table 12: Relative values of the product  $\sigma \cos(\theta)$  of the different systems compared to the reference system B8-H1-8TH-H1

System ID	B8-H1-8TH-H1	B3-H1-8TH-H1	B5-H1-8TH-L1	B4-H1-8TH-H1	B7-L1-8TH-L1
$\sigma \cos(\theta)$ [dyne/cm]	1	1.1	1.3	1.3	0.4

## 4.7 Issues related to the results

Many factors can affect the results from different experiments, for example, the standard each experiment follows; technical issues; the accuracy of the taken measurement; and the methodology of the explanation itself (Bartels, Mahani, et al. 2019)

The first flood that was conducted on the plug is the CO<sub>2</sub> flood to displace air from the clean pores as a part of the restoration process but not a part of the experiment itself. CO<sub>2</sub> adsorbs strongly on the surface of moist hematite as carboxylate, bicarbonate, and carbonate species. On the other hand, CO<sub>2</sub> adsorbs as CO<sub>3</sub><sup>2-</sup> on the surface of moist goethite, and CO<sub>3</sub><sup>2-</sup> and HCO<sub>3</sub><sup>-</sup> on the dry goethite. CO<sub>3</sub><sup>2-</sup> complexation is extremely stable (Cornell and Schwertmann 1996). This flood can cause the suppression of the wettability alteration. However, all the plugs were flooded at the beginning with CO<sub>2</sub>, so it is still not clear the magnitude of the effect of this step on the results.

Moreover, the saturation values obtained in the preparation process are not really representative. The water saturation is higher than the connate water saturation estimated by the MICP method. The increase of the initial water saturation and the decrease of the initial oil saturation affect the wettability state in a critical range drastically. This issue was observed with the B4-H1-8TH-H1 system.

The used CO is dead oil. It is more representative to use live oil in the experiments, especially in cases of real reservoir plugs. However, even in case of dead oil more details are needed to determine the role of the CO in wettability alteration such as its solvent properties.



# Chapter 5

## Conclusion

### 5.1 Summary

From the previous work, result, and discussion, the following conclusions can be driven:

1. Bentheim sandstone is a possible play of LSWI. The rock showed an MW wettability state with the previously described system of fluids and an increase of the recovery factor (about 2.54 %IOOP) due to the LSW SI.
2. The L-L interactions between 8TH crude oil and LSW support point 1 since the pH causes increases about one magnitude in case of HSW SI and 1.5 magnitudes in case of LSW SI.
3. The increment of the recovery factor is contributed to the ELD and MIE mechanisms. However, the increase in pH is also a possible mechanism.
4. LSWI shows its effects due to many mechanisms that work together and have a cooperative final result. This collective effect comes from the fact that introducing new components to the system will affect the equilibrium; hence each component will react differently with the new component. Because of the complexity of the system and the components themselves, the reactions will vary in magnitude, time and length scale, complexity, and the final effect on RF. Future works aim to study the weighting factor of each mechanism, and the factors influence its value to determine the criterion that determines LSWI opportunities in certain reservoirs at certain production stages and conditions.
5. The flow regimes in the SI process is a combination of the co- and counter-current regimes. Moreover, based on the initial wettability state a third flow regime can be noticed, which is the mixed flow regime. However, each regime dominants at certain stage of the SI process.
6. The wettability alteration in sandstone is explained better by the surface chemistry, and it is not related only to the clay content but to any geochemically active minerals.

7. Understanding the interactions that lead to the wettability alteration toward OW is the first and most crucial step to understand and determine the mechanisms that lead to wettability alteration toward WW state.
8. To make them comparative, all the plugs must reach the Swc. Otherwise, the Swc will affect the wettability state remarkably.
9. The traditional relation between the imbibition rate and the square root of time is not valid in our case. However, the time to the power -0.9 shows better results.
10. The Dc of the LSW SI experiment shows a higher value of the HSW SI at the same preparation and experiment conditions.

## Chapter 6

### References

- Ahmed, Tarek. *Reservoir Engineering Handbook*. Oxford, UK: Gulf Professional Publishing, 2010.
- Al-Maamari, Rashid S.H., and Jill S. Buckley. "Asphaltene Precipitation and Alteration of Wetting: The Potential for Wettability Changes During Oil Production." *SPE Reservoir Evaluation & Engineering*, 2003: 210 - 214.
- Al-Shalabi, Emad Walid, and Kamy Sepehrnoori. *Low Salinity and Engineered Water Injection for Sandstones and Carbonate Reservoirs*. Gulf Professional Publishing, 2017.
- Alvarado, Vladimir, Mehrnoosh Moradi Bidhendi, Griselda Garcia-Olvera, Brendon Morin, and John S. Oakey. "Interfacial Visco-Elasticity of Crude Oil - Brine: An Alternative EOR Mechanism in Smart Waterflooding." *SPE Improved Oil Recovery Symposium*. Tulsa, Oklahoma, USA : Society of Petroleum Engineers, 2014.
- Amott, Earl. "Observations Relating to the Wettability of Porous Rock ." *Petroleum Transactions, AIME*, 1959: 156-162.
- Anderson, William G. "Wettability Literature Survey- Part 1: Rock/Oil/Brine Interactions and the Effects of Core Handling on Wettability." *Journal of Petroleum Technology*, 1986a: 1,125 - 1,144.
- Anderson, William G. "Wettability Literature Survey- Part 2: Wettability Measurement." *Journal of Petroleum Technology*, 1986b: 1,246 - 1,262.
- API. *Recommended Practices for Core Analysis, RECOMMENDED PRACTICE 40*. Washington, D.C: American Petroleum Institute, 1998.
- Austad, T., A. RezaeiDoust, and T. Puntervold. "Chemical mechanism of Low Salinity Water Flooding in Sandstone Reservoirs." *SPE*, 2010.
- Austad, T., S. Strand, M.V. Madland, T. Puntervold, and R.I. Korsnes. " Seawater in chalk: An EOR and compaction fluid." *SPE Reservoir Eval. & Eng.*, 2008: 648-654.
- Bartels, W.-B., et al. "Micor-CT Study of the Impact of Low Salinity Waterflooding on the Pore-Scale Fluid Distribution During Flow." *the International Symposium of the Society of Core Analysts*. Snow Mass, Colorado, USA, 2016.
- . "Pore-Scale Displacement during Fast Imaging of Spontaneous Imbibition." *Society of Core Analysts Annual Symposium*. Vienna, Austria, 2017.

- Bartels, W.-B., H. Mahani, S. Berg, and S.M. Hassanizadeh. "Literature review of low salinity waterflooding from a length and time scale perspective." *Fuel*, 2019: 338-353.
- Behbahani, Hassan, and Martin J. Blunt. "Analysis of Imbibition in Mixed-Wet Rocks Using Pore-Scale Modeling." *SPE Journal*, 2005: 466-474.
- Bernard, George G. "Effect of Floodwater Salinity on Recovery Of Oil from Cores Containing Clays." *SPE California Regional Meeting*. Los Angeles, California, USA: Society of Petroleum Engineers, 1967.
- Blair, P.M. "Calculation of Oil Displacement by Countercurrent Water Imbibition." *Society of Petroleum Engineers Journal*, 1964: 195 - 202.
- Bourbiaux, Bernard J., and Francois J. Kalaydjian. "Experimental Study of Cocurrent and Countercurrent Flows in Natural Porous Media." *SPE Reservoir Engineering*, 1990: 361 - 368.
- Boussour, Soraya, Cissokho Malick, Cordier Philippe, Henri Jacques Bertin, and Gerald Hamon. "Oil Recovery by Low-Salinity Brine Injection: Laboratory Results on Outcrop and Reservoir Cores." *SPE Annual Technical Conference and Exhibition*. New Orleans, Louisiana, USA: Society of Petroleum Engineers, 2009.
- Brady, Patrick V., and James L. Krumhansl. "A surface complexation model of oil-brine-sandstone interfaces at 100 °C: Low salinity waterflooding." *Journal of Petroleum Science and Engineering*, 2012: 171-176.
- Buckley, J.S., and Y. Liu. "Some mechanisms of crude oil/brine/solid interactions ." *Journal of Petroleum Science and Engineering*, 1998: 155-160.
- Buckley, Jill S., and Tianguang Fan. "Crude Oil/Brine Interfacial Tensions." *Petrophysics*, 2007.
- Castro, M.D.Luque de, and F. Priego-Capote. "Soxhlet extraction: Past and present panacea." *Journal of Chromatography A*, 2010: 2383-2389.
- Chevalier, T., et al. "A novel experimental Approach for studying spontaneous Imbibition process with alkaline solutions." *International Symposium of the Society of Core Analysts*. Trondheim, Norway, 2018.
- Clement, William P. *Writing and Thinking Well*. 2 February 2008.  
<http://cgiss.boisestate.edu/~billc/Writing/writing.html> (accessed July 13, 2016).
- Conley, Francis R., and David B. Burrows. "A Centrifuge Core Cleaner ." *Journal of Petroleum Technology*, 1956: 61 - 62.
- Cornell, R.M., and U. Schwertmann. *The Iron Oxides: Structure, Properties, Reactions, Occurrence and Uses*. Weinheim, New York, Basel, Cambridge, Tokyo: Wiley , 1996.
- Cuiec, L. "Rock/Crude-Oil Interactions and Wettability: An Attempt To Understand Their Interrelation." *SPE Annual Technical Conference and Exhibition*. Houston, Texas, USA: Society of Petroleum Engineers, 1984.
- Cuiec, L., D. Longeron, and J. Pacsirszky. "On The Necessity Of Respecting Reservoir Conditions In Laboratory Displacement Studies." *Middle East Technical Conference and Exhibition*. Bahrain, Bahrain : Society of Petroleum Engineers, 1979.

- Cuiec, L.E. "Restoration of the Natural State of Core Samples." *Fall Meeting of the Society of Petroleum Engineers of AIME, 28 September-1 October, Dallas, Texas*. Dallas, Texas, USA: Society of Petroleum Engineers, 1965.
- Culec, Louis. "Study of Problems Related to the Restoration Of the Natural State of Core Samples." *Journal of Canadian Petroleum Technology*, 1977.
- Dubelaar, C.W., and T.G. Nijland. "The Bentheim Sandstone: Geology, petrophysics, varieties and its use as dimension stone." *Engineering Geology for Society and Territory*, 2014: 557-563.
- Dubey, S.T., and P.H. Doe. "Base Number and Wetting Properties of Crude Oils ." *SPE Reservoir Engineering*, 1993: 195 - 200.
- Dutton, Shirley P., and Brian J. Willis. "Comparison of outcrop and subsurface sandstone permeability distribution, Lower Cretaceous Fall River Formation, South Dakota and Wyoming ." *Journal of Sedimentary Research*, 1998: 890-900.
- Emadi, Alireza, and Mehran Sohrabi. "Visual Investigation of Oil Recovery by Low Salinity Water Injection: Formation of Water Micro-Dispersions and Wettability Alteration." *SPE Annual Technical Conference and Exhibition*. New Orleans, Louisiana, USA: Society of Petroleum Engineers, 2013.
- Filoco, Paulo R., and Mukul M. Sharma. "Effect of Brine Salinity and Crude Oil Properties on Relative Permeabilities and Residual Saturations." *SPE Annual Technical Conference and Exhibition*. New Orleans, Louisiana, USA: Society of Petroleum Engineers, 1998.
- Føyen, Tore Lyngås. "Onset of Spontaneous Imbibition." *A master thesis at Department of Physics and Technology, University of Bergen*, 2016: 1-111.
- Fredriksen, Sunniva B., Arthur Uno Rognmo, and Martin A. Fernø. "Pore-Scale Mechanisms During Low Salinity Waterflooding: Water Diffusion and Osmosis for Oil Mobilization." *SPE Bergen One Day Seminar*. Griegshallen, Bergen, Norway : Society of Petroleum Engineers, 2016.
- Gant, Preston L., and William G. Anderson. "Core Cleaning for Restoration of Native Wettability." *Society of Petroleum Engineers*, 1988: 131-138.
- Grist, D.M., G.O. Langley, and F.L. Neustadter. "The Dependence of Water Permeability On Core Cleaning Methods In the Case of Some Sandstone Samples." *Journal of Canadian Petroleum Technology*, 1975.
- Gupta, Robin, et al. "Enhanced Waterflood for Carbonate Reservoirs - Impact of Injection Water Composition." *SPE Middle East Oil and Gas Show and Conference*. Manama, Bahrain: Society of Petroleum Engineers, 2011.
- Halisch, Matthias, et al. "Capillary Flow Porometry – Assessment of an Alternative Method for the Determination of Flow Relevant Parameters of Porous Rocks." *the International Symposium of the Society of Core Analysts* . Napa Valley, California, USA, 2013.
- Haugen, Å., M.A. Fernø, G. Mason, and N.R. Morrow. "Capillary pressure and relative permeability estimated from a single spontaneous imbibition test." *Journal of Petroleum Science and Engineering*, 2014: 66-77.

- Hirasaki, G.J., J.A. Rohan, S.T. Dubey, and H. Niko. "Wettability Evaluation During Restored-State Core Analysis." *SPE Annual Technical Conference and Exhibition*. New Orleans, Louisiana, USA: Society of Petroleum Engineers, 1990.
- Holbrook, O.C., and George G. Bernard. "Determination of Wettability by Dye Adsorption." *Original copyright American Institute of Mining, Metallurgical, and Petroleum Engineers, Inc. Copyright has expired.* (Society of Petroleum Engineers), 1958.
- Jadhunandan, P.P., and N.R. Morrow. "Effect of Wettability on Waterflood Recovery for Crude-Oil/Brine/Rock Systems." *SPE Reservoir Engineering*, 1995.
- Jensen, J.A., and C.J. Radke. "Chromatographic Transport of Alkaline Buffers Through Reservoir Rock." *SPE Reservoir Engineering*, 1988: 849-856.
- Johnston, Norris, and Carrol M. Beeson. "Water Permeability of Reservoir Sands." *Transactions of the AIME*, 1945: 43 - 55.
- Karimaie, H., O. Torsæter, M. R. Esfahani, M. Dadashpour, and S.M. Hashemi. "Experimental investigation of oil recovery during water imbibition." *Journal of Petroleum Science and Engineering*, 2006: 297-304.
- Keelan, Dare K. "Core Analysis for Aid in Reservoir Description." *Journal of Petroleum Technology*, 1982: 2483 - 2491.
- Khilar, Kartic C., R.N. Vaidya, and H.S. Fogler. "Colloidally induced fines release in porous media." *Journal of Petroleum Science and Engineering*, 1990: 213-221.
- Kim, Enoch, and George M. Whitesides. "Imbibition and Flow of Wetting Liquids in Noncircular Capillaries." *J. Phys. Chem.*, 1996: 855-863.
- Lager, A., K.J. Webb, C.J. Black, M. Singleton, and K.S. Sorbie. "Low salinity oil Recovery – An Experimental Investigation." *International Symposium of the Society of Core Analysts.* , 2006.
- Lager, A., K.J. Webb, C.J.J. Black, M. Singleton, and K.S. Sorbie. "Low salinity oil recovery – an experimental investigation." *Petrophysics* (Petrophysics), 2008.
- Law, Stuart, Philip Graham Sutcliffe, and Susan Alison Fellows. "Secondary Application of Low Salinity Waterflooding to Forties Sandstone Reservoirs." *SPE Annual Technical Conference and Exhibition*. Amsterdam, The Netherlands : Society of Petroleum Engineers, 2014.
- Lee, Ji Ho, and Kun Sang Lee. "Geochemical evaluation of low salinity hot water injection to enhance heavy oil recovery from carbonate reservoirs." *Petroleum Science*, 2018.
- Li, Kewen, and Roland N. Horne. "A Scaling Method for Spontaneous Imbibition in Systems with Different Wettability." *International Symposium of the Society of Core Analysts*. 2002.
- Li, Kewen, and Roland N. Horne. "Extracting Capillary Pressure and Global Mobility from Spontaneous Imbibition Data in Oil-Water-Rock Systems." *SPE Journal*, 2005: 458-465.
- Loahardjo, Nina, Sheena Xina Xie, Winoto Winoto, Jill S. Buckley, and Norman R. Morrow. "Oil Recovery by Sequential Waterflooding: the Effects of Aging at Residual Oil and Initial Water Saturation ." *SPE Improved Oil Recovery Symposium*. Tulsa, Oklahoma, USA : Society of Petroleum Engineers, 2012.

- Loahardjo, Nina, Winoto, and Norman R. Morrow. "Oil Recovery From Bentheim Sandstone by Sequential Waterflooding and Spontaneous Imbibition." *Petrophysics*, 2013: 547 - 553.
- Ma, S.M., N.R. Morrow, X. Zhang, and X. Zhou. "Characterization of Wettability from Spontaneous Imbibition Measurements." *Journal of Canadian Petroleum Technology*, 1999.
- Mahzari, Pedram, and Mehran Sohrabi. "Crude Oil/Brine Interactions and Spontaneous Formation of Micro-Dispersions in Low Salinity Water Injection." *SPE Improved Oil Recovery Symposium*. Tulsa, Oklahoma, USA : Society of Petroleum Engineers, 2014.
- Mahzari, Pedram, Mehran Sohrabi, Alexander J. Cooke, and Andrew Carnegie. "Direct pore-scale visualization of interactions between different crude oils and low salinity brine." *Journal of Petroleum Science and Engineering*, 2018: 73-84.
- Maloney, D. R., M. M. Honarpour, and A. D. Brinkmeyer. *The effects of rock characteristics on relative permeability*. Bartlesville, OK (USA): National Inst. for Petroleum and Energy Research, 1990.
- Mason, G., M.A. Fernø, Å. Haugen, N.R. Morrow, and D.W. Ruth. "Spontaneous counter-current imbibition outwards from a hemi-spherical depression." *Journal of Petroleum Science and Engineering*, 2012: 131-138.
- Mayer, E.H., R.L. Berg, J.D. Carmichael, and R.M. Weinbrandt. "Alkaline Injection for Enhanced Oil Recovery - A Status Report." *Journal of Petroleum Technology*, 1983: 209-221.
- McGuire, P.L., J.R. Chatham, F.K. Paskvan, D.M. Sommer, and F.H. Carini. "Low Salinity Oil Recovery: An Exciting New EOR Opportunity for Alaska's North Slope." *SPE Western Regional Meeting*. Irvine, California: Society of Petroleum Engineers, 2005.
- McPhee, Colin, Jules Reed, and Izaskun Zubizarreta. *Core Analysis: A Best Practice Guide*. Amsterdam, Netherlands: Elsevier , 2015.
- Mohan, K. Krishna, Ravimadhav N. Vaidyab, Marion G. Reed, and H. Scott Fogler. "Water sensitivity of sandstones containing swelling and non-swelling clays." *Colloids and Surfaces A: Physicochemical and Engineering Aspects*, 1993: 231-254 .
- Moradi, Mehrnoosh, and Vladimir Alvarado. "Influence of Aqueous-Phase Ionic Strength and Composition on the Dynamics of Water–Crude Oil Interfacial Film Formation." *Energy Fuels*, 2016: 9170-9180.
- Moradi, Mehrnoosh, Elena Topchiy, Teresa E. Lehmann, and Vladimir Alvarado. "Impact of ionic strength on partitioning of naphthenic acids in water–crude oil systems – Determination through high-field NMR spectroscopy." *Fuel*, 2013: 236-248.
- Morrow, N.R., and F.G. McCaffery. "Displacement Studies in Uniformly Wetted Porous Media." *Wetting, Spreading, and Adhesion*, Academic Press, 1978: 289-319.
- Morrow, N.R., M. Valat, and H. Yidliz. "Effect of Brine Composition On Recovery of an Alaskan Crude Oil By Waterflooding." *Annual Technical Meeting*. Calgary, Alberta, Canada: Petroleum Society of Canada, 1996.

- Morrow, Norman R., and Geoffrey Mason. "Recovery of oil by spontaneous imbibition." *Current Opinion in Colloid & Interface Science*, 2001: 321-337.
- Morrow, Norman, and Jill Buckley. "Improved Oil Recovery by Low-Salinity Waterflooding ." *Journal of Petroleum Technology*, 2011: 106 - 112.
- Nasralla, Ramez A., Mohammed B. Alotaibi, and Hisham A. Nasr-El-Din. "Efficiency of Oil Recovery by Low Salinity Water Flooding in Sandstone Reservoirs." *SPE Western North American Region Meeting*. Anchorage, Alaska, USA: Society of Petroleum Engineers, 2011.
- Nooruddin, H. A., and M. J. Blunt. "Analytical and numerical investigations of spontaneous imbibition in porous media." *Water Resour. Res.*, 2016: 7284–7310.
- Peksa, Anna E., Karl-Heinz A.A. Wolf, and Pacelli L.J. Zitha. "Bentheimer sandstone revisited for experimental purposes." *Marine and Petroleum Geology*, 2015: 701-719.
- Pooladi-Darvish, Mehran, and Abbas Firoozabadi. "Cocurrent and countercurrent imbibition in a water-wet matrix block." *SPE Journal*, 2000: 3 - 11.
- RezaeiDoust, A., T. Puntervold, S. Strand, and T. Austad. "Smart Water as Wettability Modifier in Carbonate and Sandstone: A Discussion of Similarities/Differences in the Chemical Mechanisms." *Energy Fuels*, 2009: 4479–4485.
- Rivet, Scott, Larry W. Lake, and Gary A. Pope. "A Coreflood Investigation of Low-Salinity Enhanced Oil Recovery." *SPE Annual Technical Conference and Exhibition*. Florence, Italy : Society of Petroleum Engineers, 2010.
- Sahimi, Muhammad. *Flow and Transport in Porous Media and Fractured Rock : From Classical Methods to Modern Approaches*. Weinheim, Germany: WILEY-VCH Verlag GmbH & Co. KGaA, 2011.
- Salathiel, R.A. "Oil Recovery by Surface Film Drainage In Mixed-Wettability Rocks." *Journal of Petroleum Technology*, 1973: 1216-1224.
- Sandengen, Kristian, Anders Kristoffersen, Karen Melhuus, and Leif O. Jøsang. "Osmosis as Mechanism for Low-Salinity Enhanced Oil Recovery." *SPE Journal*, 2016: 1227 - 1235.
- Schmid, K. S., N. Alyafei, S. Geiger, and M. J. Blunt. "Analytical solutions for spontaneous imbibition: Fractional-flow theory and experimental analysis." *SPE Journal*, 2016: 2308-2316.
- Secombe, Jim, et al. "Demonstration of Low-Salinity EOR at Interwell Scale, Endicott Field, Alaska." *SPE Improved Oil Recovery Symposium, 24-28 April, Tulsa, Oklahoma, USA*. Tulsa, Oklahoma, USA: Society of Petroleum Engineers, 2010.
- Sharma, M.M., and P.R. Filoco. "Effect of Brine Salinity and Crude-Oil Properties on Oil Recovery and Residual Saturations." *SPE Journal*, 2000: 293-300.
- Shehata, Ahmed Mahmoud, and Hisham A. Nasr-El-Din. "Reservoir Connate Water Chemical Composition Variations Effect on Low-Salinity Waterflooding." *Abu Dhabi International Petroleum Exhibition and Conference*. Abu Dhabi, UAE: Society of Petroleum Engineers, 2014.
- Sheng, James J. "Critical review of low-salinity waterflooding." *Journal of Petroleum Science and Engineering*, 2014: 216-224.

- Smith, G.W., and T. Salman. "Zero-Point-of-Charge of Hematite and Zirconia." *Canadian Metallurgical Quarterly*, 1966: 93-107.
- Suijkerbuijk, Bart, et al. "Fundamental Investigations into Wettability and Low Salinity Flooding by Parameter Isolation." *SPE Improved Oil Recovery Symposium*. Tulsa, Oklahoma, USA: Society of Petroleum Engineers, 2012.
- Swiss Academic Software. *Citavi - Organize your knowledge. Reference management, knowledge organization, and task planning*. n.d. <https://www.citavi.com/> (accessed May 24, 2016).
- Tang, Guo-Qing, and Norman R. Morrow. "Influence of brine composition and fines migration on crude oil/brine/rock interactions and oil recovery." *Journal of Petroleum Science and Engineering* (Journal of Petroleum Science and Engineering), 1999: 99-111.
- Tiab, Djebbar, and Erle C. Donaldson. *Petrophysics: Theory and Practice of Measuring Reservoir Rock and Fluid Transport Properties*. Gulf Professional Publishing, 2015.
- Unsal, E., G. Mason, N. R. Morrow, and D. W. Ruth. "Co-current and counter-current imbibition in independent tubes of non-axisymmetric geometry." *Journal of Colloid and Interface Science*, 2007: 105-117.
- Valocchi, Albert J., Robert L. Street, and Paul V. Roberts. "Transport of ion-exchanging solutes in groundwater: Chromatographic theory and field simulation." *Water Resources Research*, 1981: 1517-1527.
- Vledder, Paul, Ivan Ernesto Gonzalez, Julio Cesar Carrera Fonseca, Terence Wells, and Dick Jacob Ligthelm. "Low Salinity Water Flooding: Proof Of Wettability Alteration On A Field Wide Scale." *SPE Improved Oil Recovery Symposium*. Tulsa, Oklahoma, USA : Society of Petroleum Engineers, 2010.
- Wang, Xiao, and Vladimir Alvarado. "Effects of Low-Salinity Waterflooding on Capillary Pressure Hysteresis." *SPE Improved Oil Recovery Conference*. Tulsa, Oklahoma, USA : Society of Petroleum Engineers, 2016.
- Wendell, D.J., W.G. Anderson, and J.D. Meyers. "Restored-State Core Analysis for the Hutton Reservoir." *SPE Formation Evaluation*, 1987: 509-517.
- Wickramathilaka, S., et al. "Magnetic resonance imaging of oil recovery during spontaneous imbibition from cores with the two ends open boundary condition." *the International Society of Core Analysts Annual Meeting*. Austin, Texas, USA, 2011.
- Wickramathilaka, Siluni, Norman R Morrow, and James J. Howard. "Effect of Salinity on Oil Recovery by Spontaneous Imbibition." *the International Symposium of the Society of Core Analysts*. Halifax, Nova Scotia, Canada, 2010.
- Yuan, H.H., and B.A. Schipper. *Core Analysis Manual*. Shell internationale petroleum maatschappij b.v, 1995.
- Zhang, Yongsheng, and Norman R. Morrow. "Comparison of Secondary and Tertiary Recovery With Change in Injection Brine Composition for Crude-Oil/Sandstone Combinations." *SPE/DOE Symposium on Improved Oil Recovery*. Tulsa, Oklahoma, USA: Society of Petroleum Engineers, 2006.

- Zhang, Yongsheng, Xina Xie, and Norman R. Morrow. "Waterflood Performance By Injection Of Brine With Different Salinity For Reservoir Cores." *SPE Annual Technical Conference and Exhibition*. Anaheim, California, USA: Society of Petroleum Engineers, 2007.
- Zhou, Xiam-min, Ole Torsaeter, Xina Xie, and N.R. Morrow. "The Effect of Crude-Oil Aging Time and Temperature on the Rate of Water Imbibition and Long-Term Recovery by Imbibition." *SPE Formation Evaluation*, 1995: 259 - 266.



# Appendix A

## Python Code

This code is used initially to calculate the capillary diffusion coefficient based on comparing the measured normalized oil saturation (equation 14) and the calculated normalized oil saturation (equation 13).

First of all, the required libraries are imported, and then the necessary data are read from an excel file located in the same directory of the code file. Time,  $V_o$ , and the positive root of Bassel equation are read as lists, and the other input parameters are read as single values. Moreover, the initial lists are initialized, and some necessary calculations are conducted. After the calculation of the measured normalized oil saturation from equation 14, the code supposes an initial  $D_c$  value equals to  $0 \text{ m}^2/\text{s}$ . The code calculates the concentration of the plane sheet solution ( $C_{ps}$ ) and the concentration of the cylinder solution ( $C_{cyl}$ ) based on the initial value of the  $D_c$ . Then the code calculates  $S_o^*$  and compares it with the measured  $S_o^*$ . If the two values are different then the code adds a  $\Delta D_c = 1e-14 \text{ m}^2/\text{s}$  to the initial value and repeats the calculation applying the new value of  $D_c$ . This loop is repeated until the calculated  $S_o^*$  becomes higher than the measured  $S_o^*$  then the code will consider the value of  $D_c$  and add it the  $D_c$  list. The loop of each  $D_c$  value will be repeated for each reading point until the list of  $D_c$  is completed. The code then writes the calculated parameters to an excel file. Finally, the plots of the  $D_c$  vs  $Sw$  and  $Sw^*$ , and the  $V_o$  measured and calculated vs time are plotted and visualized.

```
""" ===== This code was written by Walid HAMAD ===== """
# ===== LIBRARIES =====
import math as m # it is a default library
import matplotlib.pyplot as plt # Download before you run the code using the command: pip3 install matplotlib
import xlrd as xl # Download before you run the code using the command: pip3 install xlrd
import xlswriter as xr # Download before you run the code using the command: pip3 install xlswriter
# ===== INTIALIZATION =====
#Intialyzing the nesserey empty lists
Vo=[]
Sw=[]
T=[]
SwNormMeau=[]
SoNormMeau=[]
Sonorm=[]
Qn=[]
```

```

tt=[]
Sw1=[]
Q=[]
qo=[]
DC=[]
Dcall=[]
mobw=[]
mobnw=[]
dPcoverdSw=[]
YY=[]
TT=[]
VO=[]
krwCorey=[]
krnwCorey=[]

# ===== INPUT =====
# ===== DATA FROM XLSX FILE =====
i=xf.open_workbook('SI_data.xlsx')
sheet = i.sheet_by_name('B8')
l=sheet.cell_value(0,1) # the length of the plug
r=sheet.cell_value(1,1) # the radius of the plug
NoP=int(sheet.cell_value(2,1)) # Number of Points
Pce=sheet.cell_value(3,1) #Entry Capillary Pressure
Pcmax=sheet.cell_value(4,1) # Maximum Capillary pressure
PV=sheet.cell_value(5,1) # Pore Volume
OOIP=sheet.cell_value(6,1) # Original Oil in Place
K=sheet.cell_value(7,1) # Absolute brine permeability
nw=sheet.cell_value(8,1) # Corey water exponent
no=sheet.cell_value(9,1) # Corey oil exponent
krwmax=sheet.cell_value(10,1) # End point water relative permeability
kromax=sheet.cell_value(11,1) # End point oil relative permeability
muw=sheet.cell_value(12,1) # Water viscosity
muo=sheet.cell_value(13,1) # Oil viscosity
Dci=sheet.cell_value(14,1) # Boundary condition of Dc at the Swc (Dc (Swc) = 0)
nau=sheet.cell_value(15,1) # Cumulative production exponent
tau=sheet.cell_value(16,1) # Cumulative production rate
INT=sheet.cell_value(17,1)
Df=sheet.cell_value(18,1) #fractal dimension, which is a representation of the heterogeneity of rock

for ji in range(2,NoP):
    Ji=sheet.cell_value(ji, 6) # reading time
    qoi=beta*(Ji**alpha) # calculating the production rate
    Qi=tau*(Ji**nau)+INT # calculating the cumulative production volume
    Voii=sheet.cell_value(ji, 4) # reading measured cumulative production volume
    qo.append(qoi) #adding the calculated oil production rate value the calculated production oil rate list
    Q.append(Qi) #adding the calculated cumulative oil production the calculated cumulative oil production list
    VO.append(Voii) #adding the measured cumulative oil production value the measured cumulative oil
production list
    TT.append(Ji) #adding the read time value to the time list

for g in range(1,NoP):
    Voi=sheet.cell_value(g, 4) # reading measured Vo
    J=sheet.cell_value(g, 6) # reading the time
    D=sheet.cell_value(g, 8) # reading the value of qn = Bessel positive root / the radius of the plug
    Qn.append(D) # adding the value of qn to Qn list
    T.append(J) #adding the value of time to the time list
    Vo.append(Voi) #adding the measured cumulative oil production value the measured cumulative oil production
list
    Sw1.append(Swi) #adding the measured water saturation value to the water saturation list

Swmin=min(Sw1) #finding the Swmin
Swmax=max(Sw1) #finding the Swmax
Somin=1-Swmax #calculating the Somin
Somax=1-Swmin #calculating the Somax
deltaS=1-Somin-Swmin
mobwmax=krwmax/muw #calculating the maximum mobility of water
mobomax=kromax/muo #calculating the maximum mobility of oil
lamda=3-Df
a=(Pce/Pcmax)**-lamda
b=1-a
c=(2+lamda)/lamda
alpha=nau-1 #calculating imbibition exponent
beta=nau*tau #calculating the imbibition rate
for g in range(2,NoP-1):
    Voi=sheet.cell_value(g, 4)
    Swi=((PV-OOIP+Voi)/PV) # calculating Sw at each Vo value
    Sw.append(Swi) # adding Sw value to Sw list

```

```

# ===== THE SOLVER =====
Dcall.append(Dci)
for ii in range(len(T)):
    for t in [T[ii]:
        for ss in range(20000):
            #calculating Cps
            Cpsi=0
            for ns in range(NoP):
                Cpsii=(8/(((2*ns+1)**2)*(m.pi**2)))*(m.exp(-Dci*((2*ns+1)**2)*(m.pi**2)*(t/((2*1)**2))))
                Cpsi=Cpsi+Cpsii
            #calculating Ccyl
            Ccyl=0
            for qn in Qn:
                Ccyl=(4/((r*qn)**2))*(m.exp(-Dci*t*qn**2))
                Ccyl=Ccyl+Ccyl
            #calculating So*
            Sonormi=Cpsi*Ccyl
            #comparing the calculated and the measured So*
            if Sonormi>SoNormMeau[ii]:
                Dci=Dci+1e-14 # adding ΔDc= 1e-14 m²/s if the condition is fulfilled
            else:
                #adding another Dc value to the list if the condition is not fulfilled
                Dcall.append(Dci)
            break
        Dci=0 # returning the value of Dc to the initial value Dc=0 m²/s
Dcall[NoP-2]=0 # Boundary condition at the last point
# ===== RESULTS =====
# writing to .xlsx file
RE = xr.Workbook('Results')
worksheet = RE.add_worksheet()
"""upper row"""
worksheet.write(0, 0, "Sw")
worksheet.write(0, 1, "krw")
worksheet.write(0, 2, "kro")
worksheet.write(0, 3, "Pc")
worksheet.write(0, 4, "Dc")
worksheet.write(0, 5, "Sw*")
worksheet.write(0, 6, "So*")
worksheet.write(0, 7, "Vo")
worksheet.write(0, 8, "qt")
for e in range(1, NoP - 2):
    worksheet.write(e, 0, Sw[e - 1])
    worksheet.write(e, 1, krwCorey[e - 1])
    worksheet.write(e, 2, krnwCorey[e - 1])
    worksheet.write(e, 4, Dcall[e - 1])
    worksheet.write(e, 5, SwNormMeau[e - 1])
    worksheet.write(e, 6, SoNormMeau[e - 1])
    worksheet.write(e, 7, Q[e - 1])
    worksheet.write(e, 8, qo[e - 1])
RE.close()
#Visualization
fig , ax=plt.subplots(2,2)
fig.subplots_adjust(0.1,0.1,0.9,0.9)
# Dc vs Sw
ifig=0
rfig=0
ax[ifig][rfig].set_title ("Capillary diffusion coefficient")
ax[ifig][rfig].set_xlabel('Sw[-]')
ax[ifig][rfig].xaxis.labelpad = 5
ax[ifig][rfig].set_ylim([0,1])
ax[ifig][rfig].set_ylabel('Dc [$m^2/s$]')
ax[ifig][rfig].yaxis.labelpad = 5
ax[ifig][rfig].plot (Sw1,Dcall,"o", label="Dc")
ax[ifig][rfig].grid(True)
ax[ifig][rfig].axis('tight')
ax[ifig][rfig].legend(loc=0)
#Dc vs Sw*
ifig=0
rfig=1
ax[ifig][rfig].set_title ("Capillary diffusion coefficient")
ax[ifig][rfig].set_xlabel('Sw*[-]')
ax[ifig][rfig].xaxis.labelpad = 5
ax[ifig][rfig].set_ylabel('Dc [$m^2/s$]')
ax[ifig][rfig].yaxis.labelpad = 5
ax[ifig][rfig].plot (SwNormMeau,Dcall,"o", label="Dc")
ax[ifig][rfig].grid(True)
ax[ifig][rfig].axis('tight')
ax[ifig][rfig].legend(loc=0)
#Production History Matching
ifig=1
rfig=0

```

```
ax[ifig][rfig].set_title ("History Matching")
ax[ifig][rfig].set_xlabel('t [s]')
ax[ifig][rfig].xaxis.labelpad = 5
ax[ifig][rfig].set_ylabel('Vo [m]')
ax[ifig][rfig].yaxis.labelpad = 5
ax[ifig][rfig].plot (TT,Q,"--", label='Matched')
ax[ifig][rfig].plot (TT,VO,"*",label='Measured')
ax[ifig][rfig].grid(True)
ax[ifig][rfig].axis('tight')
ax[ifig][rfig].legend(loc=0)
plt.show ()
```

*# End of the code*